

# “Notes of Fluid Mechanics”

Piero Olla

*ISAC-CNR and INFN, Sez. Cagliari, I-09042 Monserrato, Italy*

May 1, 2025

---

## Contents

<b>1</b>	<b>Continuous limit</b>	<b>2</b>
1.1	Suggested reading . . . . .	5
<b>2</b>	<b>Fluid kinematics</b>	<b>6</b>
2.1	Lagrangian and Eulerian description of a flow . . . . .	6
2.2	Lagrangian transport of a vector field . . . . .	8
2.2.1	Parallel transport . . . . .	8
2.2.2	The Lie derivative . . . . .	10
2.3	Vorticity, rate of strain and compression rate . . . . .	11
2.4	Application to Hamiltonian dynamics . . . . .	13
2.5	Suggested reading . . . . .	15
<b>3</b>	<b>Conservation of mass and momentum</b>	<b>16</b>
3.1	Suggested reading . . . . .	18
<b>4</b>	<b>Constitutive laws</b>	<b>19</b>
4.1	Condition of local thermodynamic equilibrium . . . . .	19
4.1.1	Digression into plasma physics . . . . .	20
4.2	Microscopic interpretation of pressure and viscosity . . . . .	21
4.3	Non-Newtonian fluids . . . . .	23
4.4	Suggested reading . . . . .	24
<b>5</b>	<b>The Navier-Stokes equation</b>	<b>25</b>
5.1	Viscous flows . . . . .	26
5.2	Suggested reading . . . . .	28
<b>6</b>	<b>Hydrostatics</b>	<b>29</b>
6.1	Suggested reading . . . . .	30
<b>7</b>	<b>Conservation of energy</b>	<b>31</b>
7.1	Kinetic energy balance . . . . .	31
7.2	Heat transport . . . . .	32

7.2.1	The enthalpy of a fluid . . . . .	34
7.2.2	The entropy of a fluid . . . . .	34
7.3	An equation for the total energy . . . . .	35
7.4	Isoentropic flow . . . . .	35
7.5	Bernoulli's equation . . . . .	36
7.6	Suggested reading . . . . .	39
<b>8</b>	<b>Ideal hydrodynamics</b>	<b>40</b>
8.1	Potential flows . . . . .	41
8.2	Fluid inertia . . . . .	42
8.3	Gravity waves . . . . .	45
8.3.1	Viscous corrections . . . . .	46
8.4	Suggested reading . . . . .	47
<b>9</b>	<b>Vorticity dynamics</b>	<b>48</b>
9.1	Kelvin's theorem . . . . .	48
9.2	Helicity conservation . . . . .	51
9.3	Two-dimensional flows . . . . .	53
9.4	Invariance under relabeling . . . . .	54
9.5	Suggested reading . . . . .	57
<b>10</b>	<b>Compressible flows</b>	<b>58</b>
10.1	Sound waves . . . . .	59
10.1.1	Nonlinear and non-ideal effects . . . . .	59
10.1.2	Dynamics of the loudspeaker . . . . .	60
10.2	The Burgers equation . . . . .	60
10.2.1	Viscous Burgers equation . . . . .	61
10.2.2	The method of characteristics . . . . .	63
10.3	Shock waves . . . . .	64
10.3.1	Entropy production and shock structure . . . . .	65
10.4	Suggested reading . . . . .	67
<b>11</b>	<b>Thermal convection</b>	<b>68</b>
11.1	Stability under convection . . . . .	68
11.2	The Boussinesq approximation . . . . .	69
<b>12</b>	<b>Turbulence</b>	<b>72</b>
12.1	Homogeneous isotropic turbulence . . . . .	74
12.1.1	Time structure of the inertial range . . . . .	77
12.1.2	Transport of a passive scalar . . . . .	77
12.1.3	Two-dimensional turbulence . . . . .	79
12.2	Suggested reading . . . . .	80

# 1 Continuous limit

We are interested in the description of fluids at scales  $l$  much larger than the typical molecular separation  $a_0$ . The typical number  $N_l$  of molecules in a volume  $V_l$  of linear size  $l$  will thus be very large,

$$N_l \sim (l/a_0)^3 \gg 1, \tag{1.1}$$

and the relative fluctuation  $\delta N_l/N_l$  very small, which means that we can approximate instantaneous quantities with averages,  $N_l \simeq \langle N_l \rangle$ . This is a macroscopic description that will make sense only if the spatial scale of variation of the variables of interest is itself macroscopic. We assume this to be the case, and identify with  $l$  the scale of variation of the macroscopic quantities.

The condition  $l \gg a_0$  allows us to define macroscopic quantities through a process of coarse-graining. Introduce then an intermediate scale  $a$ ,  $a_0 \ll a \ll l$ , such that the variation of macroscopic quantities at that scale is small, and the relative fluctuation magnitude of macroscopic quantities is small as well. Let us carry out the procedure with the density  $n$ . We first define a coarse-grained density

$$n_a(\mathbf{x}, t) = \frac{N_a(\mathbf{x}, t)}{V_a} \simeq \frac{\langle N_a(\mathbf{x}, t) \rangle}{V_a} = \langle n_a(\mathbf{x}, t) \rangle \quad (1.2)$$

and then exploit the condition  $a_0 \ll a \ll l$  to formally carry out the continuum limit

$$n(\mathbf{x}, t) = \lim_{a \rightarrow 0} n_a(\mathbf{x}, t). \quad (1.3)$$

We follow the same procedure with the current density  $\mathbf{J}$  and the fluid velocity  $\mathbf{u}(\mathbf{x}, t)$ . Indicate with  $\mathbf{v}_i(t)$  the instantaneous velocities of the molecules in  $V_a = V_a(\mathbf{x})$  centered around  $\mathbf{x}$  and define

$$n(\mathbf{x}, t)\mathbf{u}(\mathbf{x}, t) = \mathbf{J}(\mathbf{x}, t) = \lim_{a \rightarrow 0} V_a^{-1} \sum_{i \in V_a} \mathbf{v}_i(t), \quad (1.4)$$

We shall focus in this course on systems composed of a single species of molecules. The density  $n$  and the current density  $\mathbf{J}$  will then be proportional through the molecular mass  $m$  to the mass density  $\rho$  and the mass current density  $J_m$ ,

$$\rho = mn, \quad \mathbf{J}_m = m\mathbf{J}. \quad (1.5)$$

Macroscopic quantities such as the density  $n$  and the fluid velocity  $\mathbf{u}$  are sums of microscopic contributions by the individual molecules. If the interaction of the molecules is not too strong, it is then possible to consider the microscopic contributions to the generic macroscopic quantity  $X$  as statistically independent. This allows us to make estimates of its fluctuation amplitude.

Suppose we have  $N$  molecules, and indicate with  $x_i$  the contribution to  $X$  by the  $i$ -th molecule, so that  $X = \sum_i^N x_i$ . We have for the average of  $X$

$$\mu_X = N\mu_x, \quad (1.6)$$

and for its RMS:

$$\sigma_X^2 = \langle (X - \mu_X)^2 \rangle = \sum_{ij} \langle (x_i - \mu)(x_j - \mu) \rangle. \quad (1.7)$$

Statistical independence, however, implies

$$\langle (x_i - \mu)(x_j - \mu) \rangle = \sigma^2 \delta_{ij}. \quad (1.8)$$

Only terms with  $i = j$  will contribute to  $\sigma_X^2$ , therefore

$$\sigma_X^2 = N\sigma_x^2. \quad (1.9)$$

For large  $N$ ,

$$\frac{\delta X}{X} \sim \frac{\sigma_X}{\mu_X} \sim N^{-1/2}. \quad (1.10)$$

As an application, let us evaluate the fluctuation in the number  $N_a$  of molecules in a volume  $V_a \subset V$ . Indicate with  $N$  the total number of molecules in  $V$ , and introduce a random variable  $x_i$ ,  $i = 1, \dots, N$ , which is  $= 1$  or  $= 0$  depending on whether  $i \in V_a$  or  $\notin V_a$ . Indicate with  $p$  the probability that a given molecule at a given time lies in  $V_a$ . We expect that for small  $V_a$   $p \ll 1$ . We immediately find

$$\mu_x = p \quad \text{and}, \quad \sigma_x^2 = \langle x_i^2 \rangle - \mu_x^2 = p - p^2. \quad (1.11)$$

Therefore, from Eqs. (1.6) and (1.9),

$$\mu_{N_a} = pN, \quad \sigma_{N_a}^2 = (p - p^2)N, \quad (1.12)$$

which implies

$$\frac{\delta N_a}{N_a} \sim \frac{\sqrt{(p - p^2)N}}{pN} \simeq (pN)^{-1/2} \sim N_a^{-1/2}. \quad (1.13)$$

We likewise obtain

$$\frac{\delta n_a}{n} \sim \frac{\delta J_a}{J} \sim \frac{\delta u_a}{u} \sim \frac{\delta N_a}{N_a} \sim (na^3)^{-1/2}, \quad (1.14)$$

which allows us to reformulate the condition for a continuum limit as

$$nl^3 \gg 1. \quad (1.15)$$

We conclude the chapter by introducing a concept that will accompany us throughout the course: that of fluid element (or fluid parcel). A “fluid element” is simply a portion of the fluid, which, on the time scales of interest, is not significantly deformed by the flow. We can convince ourselves that a fluid volume of size linear size  $l$  will behave as a fluid element at time scales  $\ll (\partial_{\mathbf{x}} \mathbf{u})^{-1}$ , provided  $l\partial_x u \ll u$  (we shall discuss the point more in detail in the next chapter).

We define the boundary of the fluid element by the condition that points on its surface move with the local fluid velocity  $\mathbf{u}(\mathbf{x}, t)$ . Molecules continuously cross the volume boundary, but the molecule mean inflow and outflow will balance in the reference frame moving with velocity  $\mathbf{u}(\mathbf{x}, t)$ , and the mass in the volume will remain constant on the average. Note that the motion of a fluid element is identical to that of a solid particle small enough to be transported by the fluid without exerting any feedback force. We call such an object a passive tracer.

We will adopt subscript  $L$  to indicate that a given volume (not necessarily a fluid element) is transported by the flow.

## 1.1 Suggested reading

- L.D. Landau and E.M. Lifshitz, “Statistical Physics” Vol. 5, Secs. 1, 2 and 114 (Pergamon Press, 1980)

## 2 Fluid kinematics

### 2.1 Lagrangian and Eulerian description of a flow

We can achieve a kinematic description of a flow in two ways:

- We can work in a “laboratory frame” and study the flow evolution at a fixed position in space; this is called an Eulerian approach.
- We can study the evolution of the flow measured by a fluid parcel transported by that flow field; this is called a Lagrangian approach.

An Eulerian description may perhaps look more natural. Indeed, most evolution equations, such as the Navier-Stokes equation, are written in an Eulerian frame, likewise, most experimental measurements, e.g., that of  $\mathbf{u}(\mathbf{x}, t)$  by an anemometer, are carried out at a fixed position of space. However, there are counterexamples. The Bernoulli law is an example of an evolution equation in a Lagrangian frame; experiments in wind tunnels are often based on seeding the flow with tracer particles, and in one way or another, bring into play ideas from a Lagrangian point of view.

The first step in the Lagrangian description of a flow is to define the coordinate of a fluid parcel. Indicate with

$$\mathbf{x}_L(t) \equiv \mathbf{x}_L(t|\mathbf{x}_0, t_0) \tag{2.1}$$

the position at time  $t$  of the fluid element which at time  $t_0$  was (or will be) at  $\mathbf{x}_0$ . We call  $\mathbf{x}_L(t)$  a Lagrangian coordinate and refer to the associated trajectory as a Lagrangian trajectory.<sup>1</sup>

The couple  $(\mathbf{x}_0, t_0)$  plays the role of a label identifying the parcel and is arbitrary. The time  $t_0$  is itself arbitrary. In general, we could identify the parcel with a label that does not bear any reference to points the parcel visits in its motion. The choice in Eq. (2.1), however, allows us to identify

$$\mathbf{x}_L(t|\mathbf{x}_0, t) = \mathbf{x}_0, \tag{2.2}$$

which will come in handy when switching from a Lagrangian to an Eulerian description.

From  $\mathbf{x}_L$ , we define the Lagrangian velocity of the parcel,

$$\mathbf{u}_L(t) \equiv \mathbf{u}_L(t|\mathbf{x}_0, t_0) = \dot{\mathbf{x}}_L(t|\mathbf{x}_0, t_0) \equiv \partial_t \mathbf{x}_L(t|\mathbf{x}_0, t_0). \tag{2.3}$$

We can express the Lagrangian velocity  $\mathbf{u}_L(t)$  in terms of the Eulerian velocity  $\mathbf{u}(\mathbf{x}, t)$ ,

$$\mathbf{u}_L(t|\mathbf{x}_0, t_0) = \mathbf{u}(\mathbf{x}_L(t|\mathbf{x}_0, t_0), t) \Rightarrow \mathbf{u}_L(t|\mathbf{x}_0, t) = \mathbf{u}(\mathbf{x}_0, t). \tag{2.4}$$

---

<sup>1</sup>The formalism can be easily adapted to describe deformations in a solid medium. Suppose the medium is undeformed at time  $t_0$ . Indicate with  $\mathbf{x}_0$  the coordinate of a point of the undeformed medium;  $\mathbf{x}_L(t, \mathbf{x}_0|t_0) - \mathbf{x}_0$  will then be the deformation.

By combining Eqs. (2.3) and (2.4), we obtain the equation of motion of a fluid parcel in an Eulerian flow field  $\mathbf{u}(\mathbf{x}, t)$

$$\dot{\mathbf{x}}_L(t) = \mathbf{u}(\mathbf{x}_L(t), t). \quad (2.5)$$

The concept of Lagrangian trajectory is closely related to that of streamline (or flowline) The streamlines of a vector field  $\mathbf{U}(\mathbf{x})$  are defined as the trajectories of the points obeying the equation

$$\dot{\mathbf{x}}_s(t) = \mathbf{U}(\mathbf{x}_s(t)). \quad (2.6)$$

Indeed, the vector  $\mathbf{U}(\mathbf{x})$  is by construction tangent to the streamline passing through  $\mathbf{x}$  (this tells that if  $\mathbf{U}(\mathbf{x}) \neq 0$ , there is only one field line crossing  $\mathbf{x}$ ). We thus see that the Lagrangian trajectories of a time-independent flow  $\mathbf{u} = \mathbf{u}(\mathbf{x})$ , are the streamlines of the flow. A related concept is that of streakline, which is the set of points obtained by superposing all Lagrangian trajectories  $\mathbf{x}_L(t|\mathbf{x}_0, t_0)$  originating in  $\mathbf{x}_0$  for different values of  $t_0$  (think of it as the result of the continuous injection at  $x_0$ , of tracers, then transported away by the flow).

From Eq. (2.5) we can derive the equation for the instantaneous streamlines of a time-dependent flow field at a given time  $t$ ,

$$\dot{\mathbf{x}}_s(s) = \mathbf{u}(\mathbf{x}_s(s), t). \quad (2.7)$$

We see that in this case, the instantaneous flow lines, the Lagrangian trajectories and the streak lines of the field do not coincide. They do coincide in the case of time-independent flows.

We can extend the definitions in Eqs. (2.1) and (2.3) to the case of a generic field  $\phi(\mathbf{x}, t)$ . Indicate with

$$\phi_L(t|\mathbf{x}_0, t_0) = \phi(\mathbf{x}_L(t|\mathbf{x}_0, t_0), t) \quad (2.8)$$

the value of the field measured along the path of a fluid parcel. This expression allows us to characterize the dependence of the Lagrangian field on the variable  $t$ . Let us analyze the dependence on the initial position  $\mathbf{x}_0$ . The change of variable  $\phi(\mathbf{x}_L(t|\mathbf{x}_0), t) = \phi_L(t|\mathbf{x}_0)$  is an example of what in mathematical jargon is called the pull-back  $\phi_L = \mathbf{x}_L^* \phi$  of  $\phi$  by  $\mathbf{x}_L$ : the value of the field  $\phi$  is *pulled back* from the point  $\mathbf{x}_L$  to its original position  $\mathbf{x}_0$  at time  $t_0$ . We can thus interpret  $\phi_L$  both as the value of  $\phi$  measured by the fluid parcel along the trajectory  $\mathbf{x}_L$ , and the value of  $\phi$  that the flow transports from  $\mathbf{x}_0$  to the current position. In both cases, the dependence of  $\phi_L$  on  $t$  has a component that is not associated with transport, which corresponds to the explicit time dependence of  $\phi(\mathbf{x}_L, t)$ . An example of Eulerian field  $\phi = \phi(\mathbf{x})$  independent of time is a fixed orography;  $\mathbf{u}(\mathbf{x}, t)$  could be in this case, e.g., a horizontal wind velocity field. Conversely, it is the Lagrangian field  $\phi_L$  which may be constant (of course, the corresponding Eulerian field  $\Phi$  will in general not be constant). We say that the field  $\phi$  is “frozen in the flow”. The associated

process is called Lagrangian transport. An example is the transport of a dye in an incompressible flow. In the absence of diffusion, the dye concentration at the current position  $\mathbf{x}_L$  is equal to the concentration at the initial point  $\mathbf{x}_0$ ; the concentration at a fixed position (Eulerian description), instead, will change with time.

At this point, we may want to be able to switch from an Eulerian to a Lagrangian description of the flow. The operation is carried out by means of the so-called material derivative

$$D_t = \partial_t + \mathbf{u}(\mathbf{x}, t) \cdot \nabla. \quad (2.9)$$

We verify in fact that

$$\begin{aligned} \partial_t \phi_L(t|\mathbf{x}_0, t_0)|_{t_0=t} &= [\partial_t + \mathbf{u}_L(t|\mathbf{x}_0, t_0) \cdot \nabla_{\mathbf{x}_L}] \phi(\mathbf{x}_L(t|\mathbf{x}_0, t_0), t)|_{t_0=t} \\ &= [\partial_t + \mathbf{u}(\mathbf{x}_0, t) \cdot \nabla_{\mathbf{x}_0}] \phi(\mathbf{x}_0, t). \end{aligned}$$

More concisely,

$$\partial_t \phi_L(t|\mathbf{x}, t_0)|_{t_0=t} = D_t \phi(\mathbf{x}, t) \quad (2.10)$$

(note that the time  $t_0$  is a label and can be chosen at will). The term  $\mathbf{u} \cdot \nabla$  in Eq. (2.9) is called advection, which is the contribution to the variation of  $\phi_L$  from the motion of the fluid parcel along the Lagrangian trajectory  $\mathbf{x}_L$ . In the case  $\phi$  is frozen in the flow,  $\dot{\phi}_L = 0 \Rightarrow D_t \phi = 0$ , which implies

$$\partial_t \phi(\mathbf{x}, t) = -\mathbf{u}(\mathbf{x}, t) \cdot \nabla \phi(\mathbf{x}, t). \quad (2.11)$$

The material derivative describes the evolution of a field in the reference frame of the moving fluid element. By construction, it is therefore unaffected by the Galilean shift  $(\mathbf{x}, t) \rightarrow (\mathbf{x}', t) = (\mathbf{x} - \mathbf{U}t, t)$ :

$$(\partial_t + (\mathbf{u} + \mathbf{U}) \cdot \nabla) \phi(\mathbf{x} - \mathbf{U}t, t) = (\partial_t + \mathbf{u} \cdot \nabla) \phi(\mathbf{x}', t). \quad (2.12)$$

## 2.2 Lagrangian transport of a vector field

In the following, we will have to deal a lot with the transport of vector quantities, such as the fluid velocity and the vorticity. Other situations in which one is faced with the issue of vector transport is that of electrically conducting fluids, due to the role potentially played by electric density currents and magnetic fields.

The transport of a vector field presents several subtleties. We discuss them one by one.

### 2.2.1 Parallel transport

The simple way to extend the idea of transport to the case of a vector field  $\mathbf{v}(\mathbf{x}, t)$  is to require that  $\mathbf{v}_L(t|\mathbf{x}_0, t_0) = \mathbf{v}(\mathbf{x}_L(t|\mathbf{x}_0, t_0))$  along fluid trajectories. While the

stem of vector  $\mathbf{v}_L$  is dragged along the trajectory  $\mathbf{x}_L$ , neither the magnitude nor the direction of the vector changes; the operation is usually called parallel transport. Parallel transport is trivial in Euclidean space, as we can utilize global Cartesian coordinates which translate the condition  $\dot{\mathbf{v}}_L = 0$  into identical conditions on the components,  $\dot{v}_{Li} = 0$ . However, there are situations of practical interest in which the fluid flow develops in a curved space. Examples include the fluid flow on a cell surface or the wind dynamics at scales such that the earth's curvature cannot be disregarded.

Consider the transport of a vector on the earth's surface. Take a vector  $\mathbf{v}$  directed north in Rome and displace it parallel to itself to Chicago, which lies roughly at the same latitude as Rome but at the longitude  $\phi \simeq \pi/2$  west.

Indicate with  $\mathbf{v}_p$  the new vector. From space, the two vectors look identical, but while in Rome  $\mathbf{v}$  points north, in Chicago, it points north-west: the component of  $\mathbf{v}$  on the equatorial plane, which in Rome is perpendicular to the earth parallel in Chicago is tangent to it. The direction of the meridian line, however, has changed. This simple observation informs us that to describe in coordinate the transport of a vector at distance such as that from Rome to Chicago, we need to work with global coordinates that are necessarily curvilinear.

We see from Eq. (2.10) that the term that causes trouble in expressing the condition  $\dot{\mathbf{v}}_L = 0$  in coordinates, is the advection  $\mathbf{u} \cdot \nabla \mathbf{v}$ . The trouble comes from the dependence of the basis vectors  $\mathbf{e}_i$  on the coordinate; we need to be careful in this case to distinguish covariant indices (those of the basis) and contravariant indices (those of the components); we thus adopt the summation convention and write

$$\mathbf{v} = v^i \mathbf{e}_i, \quad \nabla = \mathbf{e}^i \partial_i, \quad \mathbf{e}_i \cdot \mathbf{e}^j = \delta_{ij}, \quad (2.13)$$

where we have introduced the contravariant basis  $\mathbf{e}^i$  to guarantee that the differential of a scalar remains a scalar:

$$d\mathbf{x} \cdot \nabla f = dx^i \partial_i f \equiv df. \quad (2.14)$$

We can now evaluate the components of the advection term:

$$(\mathbf{u} \cdot \nabla \mathbf{v})^i = [u^k \partial_k \mathbf{e}_j v^j]^i = u^k \partial_k v^j + u^k v^j (\partial_k \mathbf{e}_j)^i = u^k [\delta_j^i \partial_k + \Gamma_{jk}^i] v^j, \quad (2.15)$$

where

$$\Gamma_{kj}^i = (\partial_k \mathbf{e}_j)^i \equiv \mathbf{e}^i \cdot (\partial_k \mathbf{e}_j) \quad (2.16)$$

is called the Christoffel symbol and the operator  $[\delta_j^i \partial_k + \Gamma_{jk}^i] v^j$  is called the covariant derivative.

A well-known property of covariant derivation is that transport of vector parallel to itself takes place on geodesic curves. In fluid mechanics notation this corresponds to the statement that the Lagrangian trajectories of a flow field obeying the law  $D_t \mathbf{u} = 0$  are geodesics.

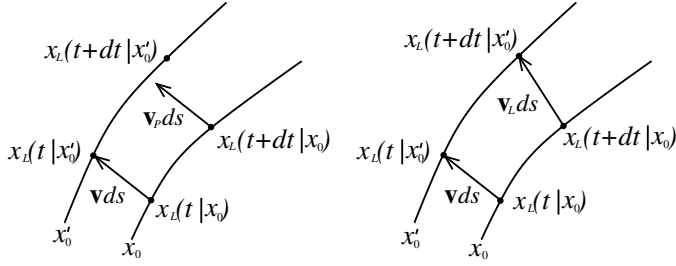


Figure 1: Comparison of parallel transport (left) and Lagrangian transport (right) of a vector field  $\mathbf{v}$  by the flow  $\mathbf{u}$ .

We shall confine our analysis in the rest of these notes to phenomena taking place at such a scale that effects from a possible curvature of the embedding space can be disregarded; we will then adopt Cartesian coordinates throughout, without distinguishing covariant from contravariant indices.

### 2.2.2 The Lie derivative

Now that we have been able to clarify the meaning of the advection of a vector as an operation of parallel transport, we may ask whether parallel and Lagrangian transport coincide. The fact is that we may interpret a vector field as a derived object, namely, the set of vectors tangent to a field of streamlines. The differential  $\mathbf{v}ds$  would represent in this case an infinitesimal segment of a streamline. The question arises whether Lagrangian transport should refer to the vector  $\mathbf{v}$  or to the streamlines of  $\mathbf{v}$ . The situation is illustrated in Fig. 1: in the case of parallel transport, one shifts the vector parallel to itself, as from definition; in the case of streamline transport, the stem and the tip of the vector  $\mathbf{v}ds$  are transported by  $\mathbf{u}$  like passive tracers (note that the endpoints of the vector  $\mathbf{v}$  lie at a given instant on a streamline of  $\mathbf{v}$ , which are however points on different streamlines of  $\mathbf{u}$ ). We shall speak in the second case of Lagrangian transport of the vector field  $\mathbf{v}$  by  $\mathbf{u}$ , and refer to  $\mathbf{v}$  as a frozen vector field.

An example of a vector field transported parallel to itself is the fluid velocity in a zero-pressure inviscid flow (Burgers dynamics). Examples of vector fields frozen in the flow are the vorticity in a zero-viscosity fluid and the magnetic field in a zero-viscosity zero-resistivity fluid.

Let us derive the evolution equation for a frozen vector field. The operation is illustrated in Fig. 2. Consider the following infinitesimal displacements,  $\mathbf{v}(\mathbf{x} - \mathbf{u}(\mathbf{x})dt, t)dt$  and  $\mathbf{v}(\mathbf{x}, t + dt)dt$ , produced by the field  $\mathbf{v}$ . The two coordinates  $\mathbf{x} - \mathbf{u}(\mathbf{x})dt$  and  $\mathbf{x}$  are the coordinates of the stem of the two displacements. The tip of the initial displacement vector is located at  $\mathbf{x} - \mathbf{u}(\mathbf{x})dt + \mathbf{v}(\mathbf{x} - \mathbf{u}(\mathbf{x})dt, t)dt$  and translates by an amount which can be obtained to the given order in  $dt$  by evaluating  $\mathbf{u}$  at the arrival point  $\mathbf{x} + \mathbf{v}(\mathbf{x}, t)dt$  (see Fig. 2). The final displacement  $\mathbf{v}(\mathbf{x}, t + dt)dt$

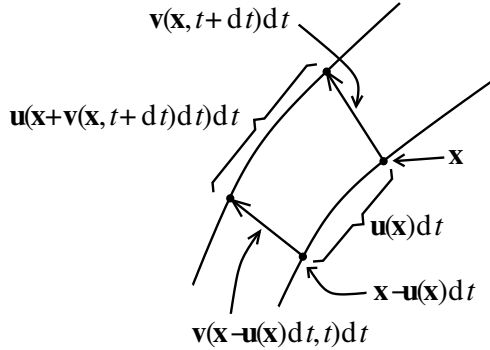


Figure 2: Graphical derivation of the evolution equation for a frozen vector field  $\mathbf{v}$ . The curved lines are the streamlines of  $\mathbf{u}$ .

is therefore the vector sum

$$\begin{aligned} & \mathbf{v}(\mathbf{x} - \mathbf{u}(\mathbf{x})dt, t)dt + \mathbf{u}(\mathbf{x} + \mathbf{v}(\mathbf{x}, t + dt)dt)dt - \mathbf{u}(\mathbf{x}, t) \\ & \simeq \left\{ [\mathbf{v}(\mathbf{x}, t) - \mathbf{u}(\mathbf{x}, t) \cdot \nabla \mathbf{v}(\mathbf{x}, t)]dt + \mathbf{v}(\mathbf{x}, t) \cdot \nabla \mathbf{u}(\mathbf{x})dt \right\} dt. \end{aligned}$$

We thus obtain for the time derivative of a vector field frozen in  $\mathbf{u}$ ,

$$\partial_t \mathbf{v}(\mathbf{x}, t) = -\mathbf{u}(\mathbf{x}, t) \cdot \nabla \mathbf{v}(\mathbf{x}, t) + \mathbf{v}(\mathbf{x}, t) \cdot \nabla \mathbf{u}(\mathbf{x}, t) := -\mathcal{L}_u \mathbf{v}(\mathbf{x}, t). \quad (2.17)$$

The operator  $\mathcal{L}_u \mathbf{v} = \mathbf{u} \cdot \nabla \mathbf{v} - \mathbf{v} \cdot \nabla \mathbf{u}$  is called the Lie derivative of  $\mathbf{v}$  in the direction of  $\mathbf{u}$ .

### 2.3 Vorticity, rate of strain and compression rate

The dynamics of fluids are governed by the stresses generated by the relative motions within the fluid. In the case of a simple fluid, the stresses are generated locally by the fluid velocity gradients, and can be analyzed in Cartesian coordinates even if the flow were to evolve on a curved surface.

Let us decompose the tensor  $\nabla \mathbf{u}$  into its trace, symmetric zero-trace, and anti-symmetric components,

$$\partial_i u_j = \frac{\delta_{ij}}{3} \nabla \cdot \mathbf{u} + \frac{1}{2} \left( \partial_i u_j + \partial_j u_i - \frac{2\delta_{ij}}{3} \nabla \cdot \mathbf{u} \right) + \frac{1}{2} \left( \partial_i u_j - \partial_j u_i \right). \quad (2.18)$$

We can express the antisymmetric component  $(1/2)[\nabla \mathbf{u} - (\nabla \mathbf{u})^t]$  in terms of the vorticity

$$\boldsymbol{\omega} = \nabla \times \mathbf{u}, \quad (2.19)$$

$$\nabla \mathbf{u} - (\nabla \mathbf{u})^t = \begin{pmatrix} 0 & \omega_3 & -\omega_2 \\ -\omega_3 & 0 & \omega_1 \\ \omega_2 & -\omega_1 & 0 \end{pmatrix}. \quad (2.20)$$

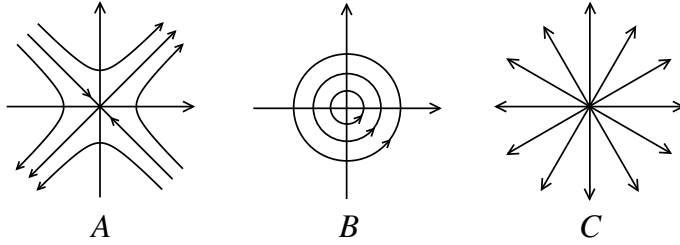


Figure 3: Sketch of 2D flows that are locally pure strain (A), pure vortical (B) or pure compressional (C).

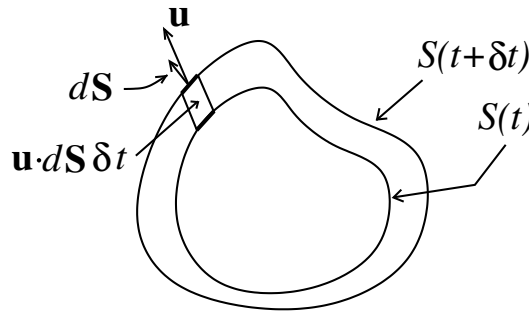


Figure 4: The motion of the boundary of a fluid volume induced by the flow  $\mathbf{u}$ .

The symmetric zero-trace component of  $\nabla \mathbf{u}$

$$\dot{s}_{ij} = \partial_i u_j + \partial_j u_i - \frac{2\delta_{ij}}{3} \nabla \cdot \mathbf{u} \quad (2.21)$$

is called the rate of strain, and the remaining trace component  $\nabla \cdot \mathbf{u} \delta_{ij}$  (taken with a minus sign) is called the compression rate.

We show in Fig. 3 the streamlines of two-dimensional (2D) velocity fields which are locally purely vortical, purely compressional, or purely strain flow. A flow with strain  $s$  and zero compression and vorticity is  $u_1 = sx_2$ ,  $u_2 = sx_1$ . We can obtain the streamlines of the flow from Eq. (2.6),  $\dot{x}_1 = sx_2$ ,  $\dot{x}_2 = sx_1 \Rightarrow 2dx_1^2/dt = sx_1x_2$ ,  $2dx_2^2/dt = sx_2x_1 \Rightarrow x_1^2 - x_2^2 = const.$ , which is the equation for the hyperbolas in case A of Fig. 3. The same procedure yields for a vortical flow  $x_1^2 + x_2^2 = const.$ , which corresponds to the circular orbits in case B of Fig. 3 (note that the flow field describes a fluid that rotates rigidly with angular frequency  $\omega$ ; such a flow is often called rotational, leaving the term vortical to situations in which  $\omega$  varies with the distance from the origin).

The compression rate gives the volume change of a portion of the fluid induced by the flow  $\mathbf{u}$ ; we illustrate the situation in Fig. 4. Indicate with  $d\mathbf{A}$  the oriented surface element of fluid volume  $V$ . In the time interval  $\delta t$  the volume  $V$  changes by

the amount

$$V(t + \delta t) - V(t) \simeq \delta t \int_{A(t)} d\mathbf{A} \cdot \mathbf{u}(\mathbf{x}, t) = \delta t \int_{V(t)} dV \nabla \cdot \mathbf{u}(\mathbf{x}, t). \quad (2.22)$$

Therefore, the compression rate of a fluid element is precisely

$$-\dot{V}/V = -\nabla \cdot \mathbf{u}. \quad (2.23)$$

A flow for which  $\nabla \cdot \mathbf{u} = 0$  is called incompressible.

## 2.4 Application to Hamiltonian dynamics

We can utilize the techniques developed in this chapter to characterize Hamiltonian flows. It is the flow of phase points in the  $2N$ -dimensional phase space labeled by coordinates  $(p_i, q_i)$ ,  $i = 1, \dots, N$ , where  $N$  is the number of degrees of freedom of the system. In the case of a system with just one degree of freedom, the phase points are identified by the 2D vector

$$\mathbf{x} = \begin{pmatrix} p \\ q \end{pmatrix} \quad (2.24)$$

Hamilton's equations define the fluid velocity

$$\mathbf{u}^H = \dot{\mathbf{x}} = \begin{pmatrix} -\partial_q H \\ \partial_p H \end{pmatrix}, \quad (2.25)$$

where  $H = H(\mathbf{x}) \equiv H(p, q)$  is the Hamiltonian of the system. Hamilton's equations can be written in the form

$$u_i^H = J_{ji} \partial_j H, \quad (2.26)$$

where

$$\mathbf{J} = \begin{pmatrix} 0 & 1 \\ -1 & 0 \end{pmatrix} \quad (2.27)$$

is called the symplectic matrix. In our fluid dynamics framework,  $\mathbf{u}^H = \mathbf{u}^H(\mathbf{x}, t)$  is an Eulerian field defined through Eq. (2.25) from the Lagrangian quantity  $\dot{\mathbf{x}}$ .

We verify that the Hamiltonian flow is incompressible,

$$\nabla \cdot \mathbf{u}^H = -\partial_p \partial_q H + \partial_q \partial_p H = 0, \quad (2.28)$$

which is the content of *Louville's theorem*.

If the Hamiltonian does not depend explicitly on time, the Hamiltonian flow is itself independent of time; let us take the specific example of the pendulum,

$$H = \frac{p^2}{2MR^2} - MgR \cos \theta, \quad \theta \equiv q. \quad (2.29)$$

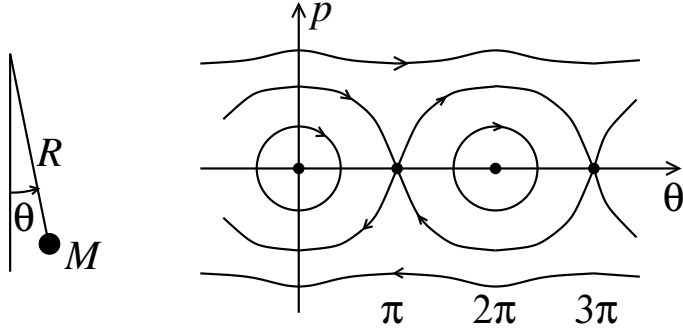


Figure 5: Phase portrait of the pendulum.

We show the streamlines of the flow in Fig. 5. We see that the stable equilibrium points at  $\theta = 2n\pi$  correspond to regions of vortical flow, while the unstable equilibrium points at  $\theta = (2n + 1)\pi$  correspond to strain flow, no sinks or wells in the form described in case *C* of Fig. 4 are possible due to the incompressibility of the flow.

One can write Hamilton's equations in terms of Poisson brackets,

$$\dot{x}_i = \{H, x_i\}, \quad \{f, g\} = J_{ij}\partial_i f \partial_j g \equiv \partial_p f \partial_q g - \partial_q f \partial_p g. \quad (2.30)$$

We can use the Poisson brackets to determine the variation of a field  $f$  measured by a phase point transported by the Hamiltonian flow  $\mathbf{u}$ ,

$$\dot{f} = \partial_t f + \mathbf{u}^H \cdot \nabla f = \partial_t f + J_{ij}\partial_i H \partial_j f = \partial_t f + \{H, f\}. \quad (2.31)$$

We can express energy conservation for a time-independent Hamiltonian  $H$  in the language of Poisson brackets,

$$\dot{E} \equiv \dot{H} = \{H, H\} = (J_{ij}\partial_i H)\partial_j H = \mathbf{u}^H \cdot \nabla H = 0, \quad (2.32)$$

which tells us that the streamlines of the Hamiltonian flow are the level curves of  $H$ . From a fluid mechanics point of view, we can say that  $H$  is frozen in the phase space flow determined by the Hamilton equations. Indeed, since the streamlines of the phase-space flow are the level curves of  $H$ , that function will be constant also when viewed as an Eulerian field,  $\partial_t H = 0$ .

Something more interesting occurs if we take  $H(p, q)$  as the initial condition of a time-dependent field  $H^K(p, q, t)$  undergoing Lagrangian transport by an auxiliary Hamiltonian  $K(p, q)$ . The field  $H^{H^K}$  is therefore frozen in the field  $u_i^K = J_{ji}\partial_j K$ . We shall discover that the time evolution of the Eulerian field  $u_i^{H^K} = J_{ji}\partial_{x_j} H^K$  is obtained as the Lie derivative of  $\mathbf{u}^{H^K}$  by  $\mathbf{u}^K$ , which is not surprising, considering that, as we have said, the streamlines of  $\mathbf{u}^{H^K}$  are the level curves of  $H^K$ .

The condition that the field  $H^K$  is frozen in the velocity field  $\mathbf{u}^K$  can be written in terms of Poisson brackets as

$$\dot{H}^K = \partial_t H^K + \{K, H^K\} = 0. \quad (2.33)$$

From here we readily obtain the time evolution of the Eulerian field  $\mathbf{u}^{H^K}(\mathbf{x}, t)$ ,<sup>2</sup>

$$\begin{aligned}
\partial_t u_i^{H^K} &= J_{ji} \partial_j \partial_t H^K = -J_{ji} \partial_j \{K, H^K\} \\
&= -J_{ji} \partial_j [J_{lm} (\partial_l K) \partial_m H^K] \\
&= -J_{ji} [(\partial_j \partial_l K) J_{lm} \partial_m H^K + (J_{lm} \partial_l K) \partial_j \partial_m H^K] \\
&= -J_{ji} [-(\partial_l \partial_j K) u_l^{H^K} + u_m^K \partial_j \partial_m H^K] \\
&= u_l^{H^K} \partial_l u_i^K - u_m^K \partial_m u_i^{H^K}
\end{aligned}$$

We can rewrite the result in terms of Lie derivatives as

$$\partial_t \mathbf{u}^{H^K} = -\mathbf{u}^K \cdot \nabla \mathbf{u}^{H^K} + \mathbf{u}^{H^K} \cdot \nabla \mathbf{u}^K \equiv -\mathcal{L}_{\mathbf{u}^K} \mathbf{u}^{H^K}, \quad (2.34)$$

which confirms the statement that the velocity field  $\mathbf{u}^{H^K}$  is frozen in  $\mathbf{u}^K$ .

## 2.5 Suggested reading

- S. Childress, “Topological fluid dynamics for fluid dynamicists”, <https://www.math.nyu.edu/~childres/tfd.pdf>

---

<sup>2</sup>We stress that the expression does not coincide with  $\dot{\mathbf{u}}^{H^K}$ , which is a Lagrangian quantity describing the motion of a phase space point in the velocity field generated by  $H^K$ .

### 3 Conservation of mass and momentum

The dynamics of a fluid is described by equations that are essentially local conservation laws for the mass, the momentum, and the energy.

Conservation of mass is expressed locally by imposing the condition that the mass  $M_a$  of a fluid element stays constant. We can write the condition in terms of the mass density along a fluid trajectory  $\rho_L$  and the volume  $V_L$  of the element,  $M \simeq V_L \rho_L$ ,

$$0 = \dot{M} \simeq V_L \dot{\rho}_L + \rho_L \dot{V}_L \quad (3.1)$$

An Eulerian version of this equation can be obtained by setting in  $\mathbf{x}_L(t|\mathbf{x}_0, t_0)$  and  $\mathbf{v}_L(t|\mathbf{x}_0, t_0)$  the labeling time  $t_0$  equal to  $t$ , and then using Eqs. (2.10) and (2.23) to set  $\dot{\rho}_L = D_t \rho$  and  $\dot{V}_L = V \nabla \cdot \mathbf{u}$ . From Eq. (3.1), we thus get the continuity equation

$$D_t \rho + \rho \nabla \cdot \mathbf{u} \equiv \partial_t \rho + \nabla \cdot (\rho \mathbf{u}) = 0. \quad (3.2)$$

We see that if the flow is incompressible. The density is “frozen” in the flow. Imagine an oil emulsion in water. The density  $\rho(\mathbf{x}, t)$  changes in response to the passage of oil droplets at  $\mathbf{x}$  (if the fluid is in motion), however, the density  $\rho_L(t)$  following the droplet remains constant.

In the absence of chemical reactions, the number density  $n(\mathbf{x}, t)$  obeys an equation identical to Eq. (3.2). Otherwise, we ought to include in Eq. (3.2) sources and sinks, and write separate equations for the different species, taking into account the diffusion of the different species across the fluid element boundaries. Difficulties in the identification of mass and matter (molecule) fluxes also arise in a relativistic context, since in this case we could equally interpret  $\rho$  and  $\mathbf{J}_m = \rho \mathbf{u}$ , as either the component of a 4-current or a momentum density (the time component of the stress-energy tensor). To avoid this sort of trouble, we shall assume throughout the notes that relativistic effects are negligible.

We can utilize the procedure adopted in the derivation of Eq. (3.2) to derive a local conservation law for the momentum. The starting point is the second law of Newton

$$M \dot{\mathbf{u}}_L(t) = \mathbf{F}(t), \quad (3.3)$$

where  $\mathbf{F}$  is the force on the fluid element. If the volume  $V$  is sufficiently large, it is possible to separate in  $\mathbf{F}$  a contact force component at the boundary of  $V$ . Let us consider an outward-oriented surface element  $d\mathbf{A}$  on the boundary of  $V$ . We could interpret the surface force  $d\mathbf{F}^S$  on  $d\mathbf{A}$  as a momentum flux through that surface element. In the case of the flow of a scalar quantity, such as the mass, the density current is a vector  $\mathbf{J}_m$ ; in the case of a vector, such as the force  $\mathbf{F}$ , the associated density current must be a second-order tensor  $\boldsymbol{\sigma}$ . Only in this way can  $\boldsymbol{\sigma} \cdot d\mathbf{A}$  be a vector. Indicate with  $\sigma_{ij}$  the momentum current density entering  $V$ , in such a way that

$$d\mathbf{F}^S = \boldsymbol{\sigma} \cdot d\mathbf{A}; \quad dF_i^S = \sigma_{ij} dA_j. \quad (3.4)$$

The tensor  $\boldsymbol{\sigma}$  is called the stress tensor of the fluid. The total force on  $V$  will be therefore

$$\mathbf{F} = \mathbf{F}^{ext} + \mathbf{F}^A = \mathbf{F}^{ext} + \int_{\partial V} d\mathbf{A} \cdot \boldsymbol{\sigma}, \quad (3.5)$$

where  $\mathbf{F}^{ext}$  is the contribution to  $\mathbf{F}$  from forces mediated by long-range fields such as gravity (note that such forces could be generated by portions of the fluid at macroscopic separations from  $V$ ). We can convert the surface integral in  $\mathbf{F}^S$  into a volume integral,  $\int_{\partial V} d\mathbf{A} \cdot \boldsymbol{\sigma} = \int_V dV \nabla \cdot \boldsymbol{\sigma}$ , and introduce force densities  $\mathbf{f} = \mathbf{F}/V$  and  $\mathbf{f}^{ext} = \mathbf{F}^{ext}/V$ . Equation (3.5) then becomes

$$\mathbf{f} = \mathbf{f}^{ext} + \nabla \cdot \boldsymbol{\sigma}. \quad (3.6)$$

We can now substitute Eq. (3.6) into Eq. (3.3) and exploit Eq. (2.10) to switch to an Eulerian description. The result is the conservation law for the momentum

$$\rho(\partial_t + \mathbf{u} \cdot \nabla)\mathbf{u} = \nabla \cdot \boldsymbol{\sigma} + \mathbf{f}^{ext}. \quad (3.7)$$

Proceeding as in the case of the tensor  $\nabla\mathbf{u}$ , when introducing vorticity, strain, and compression rate, we decompose the stress tensor  $\boldsymbol{\sigma}$  into its trace, symmetric zero-trace and antisymmetric components,

$$\sigma_{ij} = \frac{1}{3}\sigma_{ll}\delta_{ij} + \frac{1}{2}\left(\sigma_{ij} + \sigma_{ji} - \frac{2}{3}\sigma_{ll}\delta_{ij}\right) + \frac{1}{2}\left(\sigma_{ij} - \sigma_{ji}\right). \quad (3.8)$$

The terms in the decomposition are associated with separate contributions to the surface force on  $V$ . We see immediately that the trace component produces a force contribution  $(1/3)\sigma_{ll}d\mathbf{A}$  normal to the surface element, whose magnitude is independent of the orientation of  $d\mathbf{A}$ . In other words, we are dealing with a pressure force. The symmetric traceless component contributes normal and tangential forces. The antisymmetric ones only contribute tangential forces. We see that the symmetric traceless component tends to stretch  $V$ , while the antisymmetric induces rotation of the fluid element. We illustrate the situation in Fig. 6.

Let us focus on the rotation component. Indicate with  $a$  the characteristic scale of  $V$ . The contribution to  $\mathbf{F}^S$  from the antisymmetric stress component  $\sigma_{ij}^{as} = (1/2)(\sigma_{ij} - \sigma_{ji})$  has magnitude  $F^{as} \sim a^2 T^{as}$ . This induces a torque

$$\mathcal{T} \sim aF^{as} \sim a^3 T^{as} \quad (3.9)$$

on  $V$ . On the other hand, the inertia tensor of  $V$  is

$$I_{ij} = \int_V dV r_i r_j \rho \sim a^5 \rho, \quad (3.10)$$

where  $\mathbf{r}$  is evaluated with respect to some point in the interior of  $V$ . Comparison of Eqs. (3.9) and (3.10) tells us that  $T^{as}$  generates a response in the fluid on a time scale  $I/\mathcal{T} \sim a^2$  that vanishes in the continuum limit.

Any antisymmetric component of the stress tensor that is locally generated is going to be destroyed on this time scale. We thus reach the conclusion that the stress tensor does not have an antisymmetric component.

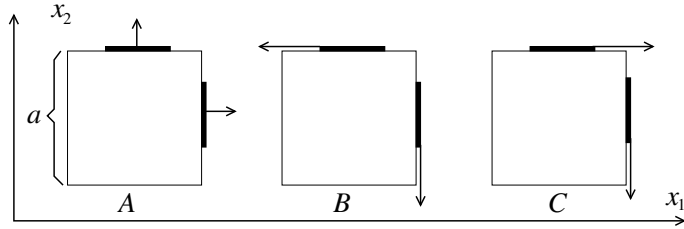


Figure 6: Examples of surface force contributions  $d\mathbf{F}^S$  from the trace ( $A$ ), the symmetric traceless ( $B$ ) and antisymmetric ( $C$ ) components of the stress tensor; in the example considered, we have taken  $\sigma_{11} = \sigma_{22} = \sigma_{33}$ , in such a way that the diagonal terms of the symmetric traceless component are identically zero.

### 3.1 Suggested reading

- P. Kundu, I.M. Cohen and D.R. Dowling, “Fluid mechanics, Secs. 4.1-7 (Ac. Press 2015)
- L.D. Landau, E.M. Lifshitz, E.M. Koevich and L.P. Pitaevskii, “Theory of elasticity” Vol. 7, Secs. 1 and 2 (Elsevier, 1986)

## 4 Constitutive laws

To describe the state of a fluid, we must know the spatial profile of The fluid density, velocity, and temperature (in the case of a mixture, or a conducting fluid, we also need the concentration and the current density of the different species). To fix the dynamics, we need closed expressions relating the stress tensor with these quantities and their gradients. A relation fixing such dependency is called a constitutive law.

We will see in the next sections that if the microscopic dynamics are sufficiently simple and the fluid is not too far from equilibrium, the macroscopic dynamics is local, and it is possible to carry out a gradient expansion,  $\sigma_{ij} = \sigma_{ij}^{(0)} + \sigma_{ij}^{(1)} + \dots$ , where

$$\sigma_{ij}^{(0)} = \sigma_{ij}^{(0)}(\rho, T), \quad \sigma_{ij}^{(1)} = \mu_{ijklm}^u(\rho, T)\partial_l u_m + \mu_{ijl}^\rho(\rho, T)\partial_l \rho + \mu_{ijl}^T(\rho, T)\partial_l T, \quad (4.1)$$

and higher-order terms take into account higher-order derivatives as well as larger powers of the different derivatives.

If it is possible to stop the gradient expansion to the first order, we say that the fluid is Newtonian. We say that the fluid is simple if it is also isotropic, in which case the stress tensor has the form

$$\sigma_{ij}^{(0)} = -P\delta_{ij}, \quad \text{and} \quad \sigma_{ij}^{(1)} = \mu^B \nabla \cdot \mathbf{u} \delta_{ij} + \mu \dot{s}_{ij}, \quad (4.2)$$

where  $P$  is the pressure, and  $\mu_B$  and  $\mu$  are called the bulk and dynamic viscosity. Since  $\sigma_{ij}$  is always symmetric, the stress tensor of a simple fluid is by construction independent of vorticity.

### 4.1 Condition of local thermodynamic equilibrium

The description of a fluid in terms of temperature, density, and velocity rests on the fact that the fluid is not too far from equilibrium, which means that the velocity distribution of the molecules is close to Maxwellian, and concepts from equilibrium thermodynamics—in particular temperature—at least locally, continue to apply. Local thermodynamic equilibrium is only possible if the spatial inhomogeneity of the fluid at scale  $\lambda$  is small, as molecular collisions could not smooth out inhomogeneities at scales below  $\lambda$ . The condition of slow space variation of macroscopic quantities, in turn, requires the macroscopic dynamics to be slow and thus give time to collisions to counteract the formation of sharp gradients.

The magnitude of the mean free path  $\lambda$  is determined by the geometry of the collision process. Let  $r_0$  be the characteristic size of a molecule, and define the molecular volume  $n^{-1} \equiv a_0^3$  as the typical volume in the gas (or liquid) containing just one molecule. The cross-section of a molecule is  $r_0^2$ , and the probability that a second molecule crossing the molecular volume of the first one hits that molecule is  $\sim (r_0/a_0)^2$ . Typically, a molecule crosses  $\sim (a_0/r_0)^2$  molecular volumes, each of

length  $a_0$ , before making a collision. The total distance traveled defines the mean free path

$$\lambda = a_0^3/r_0^2 = \frac{1}{nr_0^2}. \quad (4.3)$$

The condition of local thermodynamic equilibrium can be expressed in terms of the Knudsen number

$$\text{Kn} = \frac{\lambda}{l} \sim \frac{1}{nr_0^2 l} \ll 1. \quad (4.4)$$

Since  $\lambda \geq a_0$ , the condition for local thermodynamic equilibrium  $l \gg \lambda$  is stronger than the one for the continuum  $l \gg a_0$ , discussed in Sec. 1.

#### 4.1.1 Digression into plasma physics

Hot plasmas provide an example of a system for which the continuum limit is satisfied but local equilibrium is not.

Due to the long-range nature of electromagnetic interactions, the collision cross-section of the charged particles in a plasma is not well defined. A possibility is to introduce the concept of “hard” collision, as a scattering event involving a substantial change of direction in the motion of the particles. The total kinetic and potential energies of the two particles are going to be of the same order of magnitude when the particles get close. Indicate with  $e$  and  $m$  the charge and reduced mass of the particles (for a typical plasma, in which the lighter particles are the electrons,  $m$  is the electron mass). We thus define the minimum separation  $r(v)$  in a hard collision as

$$mv^2 \sim \frac{e^2}{r(v)} \quad (4.5)$$

and identify with  $r(v) = e^2/(mv^2)$  the effective interaction radius of the particles at relative velocity  $v$ . By taking  $r_0 \sim r(v_{th})$ , with  $v_{th}$  the thermal velocity of the electrons, we get the estimate of the mean free path

$$\lambda = \frac{1}{nr_0^2} \sim \frac{1}{n} \left( \frac{mv_{th}^2}{e^2} \right)^2 \sim n \left( \frac{k_B T}{e^2} \right)^2, \quad (4.6)$$

where  $k_B$  is the Boltzmann constant.

We point out that for our estimate to be correct, the plasma must be sufficiently dilute for binary collisions to be dominant; in other words, the plasma must be weakly correlated. This requires  $r_0 \ll a_0$ , which together with the continuum limit condition  $nl^3 \gg 1$  implies

$$\frac{k_B T}{e^2} \gg n^{1/3} \gg l^{-1}. \quad (4.7)$$

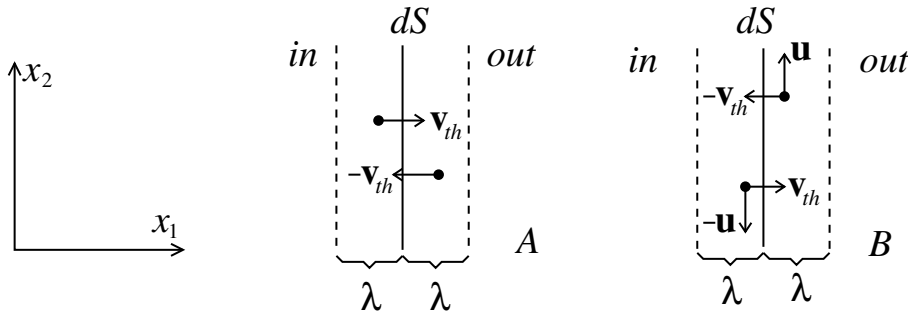


Figure 7: Sketch of the microscopic mechanisms responsible for pressure (*A*) and viscous (*B*) forces at the surface of a fluid element. All the velocities are measured in the reference frame of  $d\mathbf{A}$ .

A plasma may satisfy the continuum and weak correlation conditions in Eq. (4.7); however, if its temperature is too high, the effective Knudsen number  $\lambda/l$  will be so large that local thermal equilibrium is impossible. A hot plasma would not admit a fluid description and a kinetic theory approach based on the use of the Vlasov equation would be required.

## 4.2 Microscopic interpretation of pressure and viscosity

To determine the law of state  $P = P(\rho, T)$  and the functional form of the viscosity coefficient  $\mu = \mu(\rho, T)$ , we must have some information on the microscopic structure of the fluid. The operation is possible for  $\text{Kn} \ll 1$ , in which case we can describe the pressure and viscous forces acting on a fluid element  $V$  as the result of a process of deposition of momentum by the molecules crossing the boundary of that volume. The process takes place in a layer of thickness  $\lambda$  at the boundary of the fluid element, as described in Fig. 7. Case *A* of Fig. 7 illustrates how pressure is generated.

Molecules on the right of  $dA$  travel to the left with velocity  $-\mathbf{v}_{th}$ , and deposit momentum  $-m\mathbf{v}_{th}$  in the layer of thickness  $\lambda$  to the left of  $dA$  (consider, for simplicity, the case of a single molecular species). At the same time, molecules on the left travel to the right with velocity  $\mathbf{v}_{th}$  and deposit momentum  $m\mathbf{v}_{th}$  out of  $V$ , thus contributing other  $-m\mathbf{v}_{th}$  to the balance for  $V$ . The current from right to left and the one from left to right both have magnitude  $\sim nv_{th}dA/2$  (one-half of the molecules to the right travel to the left, and one-half of those to the left travel to the right). The total flow of momentum to the left, which is the portion of the normal component of  $\mathbf{F}^S$  exerted on  $dA$ , is therefore  $dF^\perp \sim nmv_{th}^2dA$ , from which we get the law of state

$$P \sim nmv_{th}^2 \sim nK_B T, \quad (4.8)$$

where  $k_B$  is the Boltzmann constant. We could turn the order of magnitude relation into an equality by a more careful analysis based on kinetic theory.

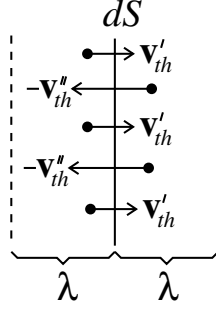


Figure 8: Mechanism for the generation of a heat flux. A positive temperature gradient is present such that  $v''_{th} > v'_{th}$  and at the same time  $n'' < n'$ , in such a way that  $P'' = P'$ . But this implies  $n'v_{th}^3 < n''v_{th}^3$ , which means that there is a heat flux to the left.

The mechanism for viscous force generation is illustrated in Fig. 7B. We are interested in this case in the tangential forces produced by the transfer of vertical momentum across  $dA$ .

Suppose that there is a horizontal gradient  $\partial_1 u_2 > 0$ . Molecules that have equilibrated at distance  $\lambda$  to the right of  $dA$  will have average vertical momentum  $m\lambda\partial_1 u_2$ . The molecular current from right to left will be as before  $\sim nv_{th}dA/2$ . At the same time, molecules that have equilibrated at distance  $\lambda$  to the left of  $dA$  will have average vertical momentum  $-m\lambda\partial_1 u_2$  and the current to the right will be  $\sim nv_{th}dA/2$ . Therefore, the total flow of momentum to the left, which is the portion of the tangential component of  $\mathbf{F}^S$  exerted on  $dA$  will be

$$dF^{\parallel} \sim nmv_{th}\lambda\partial_1 u_2 dA, \quad (4.9)$$

corresponding to the viscous stress

$$\sigma_{12} = \mu\partial_1 u_2, \quad \mu \sim nmv_{th}\lambda \sim \frac{mv_{th}}{r_0^2}. \quad (4.10)$$

The dynamic viscosity of a gas is independent of its density. The experimental verification of this fact by J.C. Maxwell provided the first evidence in support of the kinetic theory of gases. By combining with Eq. (4.10) with Eq. (5.4), we obtain for the kinematic viscosity

$$\nu \sim \lambda v_{th}. \quad (4.11)$$

A similar mechanism of generation is at play in the case of heat diffusion as illustrated in Fig. 8. Suppose  $\partial_1 T > 0$ , which means  $T' \simeq T - \lambda\partial_1 T$  and  $T'' \simeq T + \lambda\partial_1 T$ , and therefore also  $v'_{th} \simeq v_{th} - (v_{th}/(2T))\lambda\partial_1 T$  and  $v''_{th} \simeq v_{th} + (v_{th}/(2T))\lambda\partial_1 T$ . At the same time, the equilibrium of pressure forces requires  $n'T' = n''T'' = nT$ . The heat current density to the right is  $\sim n'v'_{th}k_B T'/2 = nv'_{th}k_B T/2$  and the one to the

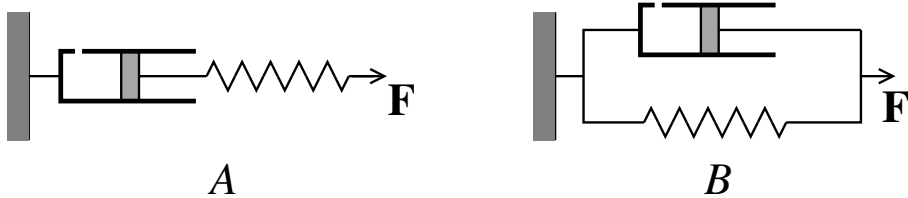


Figure 9: Mechanical analogs of a Maxwell fluid (A) and a Kelvin-Voigt solid (B).

left is  $\sim -n''v_{th}''k_B T''/2 = -nv_{th}''k_B T/2$ . The total heat current density along  $x_1$  is therefore

$$q_1 \sim nk_B T(v'_{th} - v''_{th})/2 \sim -\kappa n k_B \partial_1 T, \quad \kappa \sim \lambda v_{th}. \quad (4.12)$$

The diffusivity  $\kappa$  is typically of the same order as the kinematic viscosity  $\nu$ .

### 4.3 Non-Newtonian fluids

Non-Newtonian fluids comprise a vast zoo of behaviors. Some materials have a viscosity coefficient that depends on the magnitude of the strain rate. The viscosity of these materials may increase with  $s$  (shear-thickening materials, such as corn starch) or decrease with  $s$  (shear-thinning materials, such as sand in water). In some cases, memory effects may be present, and the viscosity may depend on the duration of the stress.

Other continuous media are characterized by a stress tensor depending on the strain rate and the strain. We speak in this case of viscoelastic materials. We can distinguish two main classes: materials in which the elastic component of the stress appears as transient, with viscous stresses dominating the steady-state dynamics, and materials in which viscous stresses are significant in the transient, and elastic forces are dominant at the steady-state. Materials in the first class are called Maxwell fluids (or solid-like fluids); materials in the second class are called Kelvin-Voigt solids (or fluid-like solids). Examples in the first class include whipped cream, mucus, and the silly putty. The second class comprises living tissues and some plastics. A mechanical analog of the dynamics of Maxwell fluids and Kelvin-Voigt solids is illustrated in Fig. 9.

It is interesting to note that the elastic stress of a solid and the viscous stress of a fluid have the same functional form, with the compression  $\nabla \cdot \mathbf{y}$  replacing the compression rate  $\nabla \cdot \mathbf{u}$  and the strain  $s_{ij} = \partial_i y_j + \partial_j y_i - (2/3)\nabla \cdot \mathbf{y} \delta_{ij}$  replacing the strain rate  $\dot{s}_{ij} = \partial_i u_j + \partial_j u_i - (2/3)\nabla \cdot \mathbf{u} \delta_{ij}$ , where  $\mathbf{y}(t|\mathbf{x}_0) = \mathbf{x}_L(t|\mathbf{x}_0) - \mathbf{x}_0$  is the dislocation of the solid element with equilibrium coordinate  $\mathbf{x}_0$ .

The mechanical analogs in Fig. 9 allow us to derive constitutive laws for Maxwell and Kelvin-Voigt materials. The spring and the friction-generating piston-cylinder assembly in the figure, could be seen as the microscopic components responsible for the stress at the surface of a fluid element, all assumed to have zero inertia.

In the case of a Maxwell material, the friction and the spring act in series; at a steady state, the spring reaches the equilibrium elongation corresponding to the friction force on the moving piston. In the case of a Kelvin-Voigt material, the two forces act in parallel; at the steady state, the spring reaches the equilibrium elongation corresponding to the external forces  $\mathbf{F}$  on the assembly, while the friction force is zero.

Identify with subscript  $S$  and  $P$  the spring and piston components of stress, strain, and rate of strain. In the Maxwell case, the stress is constant along the chain (because of zero inertia). Hence

$$\sigma = \alpha s_A = \mu \dot{s}_P, \quad s_A + s_P = s \quad \Rightarrow \quad \dot{s} = \frac{\dot{\sigma}}{\alpha} + \frac{\sigma}{\mu}, \quad (4.13)$$

where  $\alpha$  plays the role of elasticity modulus (Lamé coefficient) of the material. In the Kelvin-Voigt case, the deformations of the spring and cylinder-piston assembly are equal. Total stress is the sum of the two components

$$s_A = s_P = s \quad \Rightarrow \quad \text{and} \quad \sigma = \sigma_A + \sigma_P = \alpha s + \mu \dot{s}. \quad (4.14)$$

#### 4.4 Suggested reading

- P. Kundu, I.M. Cohen and D.R. Dowling, “Fluid mechanics, Secs. 4.8-9 (Ac. Press 2015)

## 5 The Navier-Stokes equation

Back to the realm of Newtonian fluids, if the deviations from equilibrium of  $\rho$  and  $T$  are weak enough, it is possible to disregard the dependence of  $\mu_B$  and  $\mu$  on  $\rho$  and  $T$  and approximate in Eq. (3.7)

$$\nabla \cdot \boldsymbol{\sigma} \simeq \mu_B \nabla \nabla \cdot \mathbf{u} + \mu \nabla \cdot \dot{\mathbf{s}}.$$

The bulk viscosity of most fluids is small and usually disregarded. In this case, the viscous stress simplifies to

$$\sigma_{ij}^{(1)} = \mu \dot{s}_{ij}, \quad (5.1)$$

and the momentum conservation equation (3.7) becomes

$$\rho(\partial_t + \mathbf{u} \cdot \nabla) \mathbf{u} + \nabla P = \mu \left( \nabla^2 \mathbf{u} + \frac{1}{3} \nabla \nabla \cdot \mathbf{u} \right) + \mathbf{f}^{ext}, \quad (5.2)$$

called the Navier-Stokes equation.

To solve the system formed by the continuity equation (3.2) and the Navier-Stokes equation (5.2), we need a law of state  $P = P(\rho, T)$  and therefore also an evolution equation for the temperature. We shall deal with the issue in the coming section. A special case is that of incompressible of. If the density is constant in the domain, Eqs. (3.2) and (5.2) take the form

$$\nabla \cdot \mathbf{u} = 0, \quad (\partial_t + \mathbf{u} \cdot \nabla) \mathbf{u} + \nabla P / \rho = \nu \nabla^2 \mathbf{u} + \mathbf{f}^{ext} / \rho, \quad (5.3)$$

and no temperature equation is needed. The parameter in Eq. (5.3)

$$\nu = \mu / \rho \quad (5.4)$$

is called kinematic viscosity; for water  $\nu \simeq 0.01 \text{ cm}^2/\text{s}$ ; for air at sea level  $\nu \simeq 0.15 \text{ cm}^2/\text{s}$ . An equation for the pressure can be obtained by taking the divergence of the second equation,

$$\nabla^2 P + \rho \nabla \cdot (\mathbf{u} \cdot \nabla \mathbf{u}) = \nabla \cdot \mathbf{f}^{ext}. \quad (5.5)$$

To solve Eqs. (5.3) and (5.5), we need boundary conditions on both  $\mathbf{u}$  and  $P$ . Equations (5.3) and (5.5) contain Laplacians of the fields  $\mathbf{u}$  and  $P$ . The boundary conditions thus involve some combinations of the fields and their normal derivatives.

An analytical solution of the Navier-Stokes equation is not possible, in general, due to the equation's nonlinearity. We can estimate the nonlinearity strength from the relative magnitude of the advection and viscous terms,

$$\mathbf{u} \cdot \nabla \mathbf{u} \sim \frac{(\delta u)^2}{L}, \quad \nu \nabla^2 \mathbf{u} \sim \frac{\nu \delta u}{L^2}, \quad (5.6)$$

from which we can form a dimensionless quantity called the Reynolds number

$$\text{Re} = \frac{L\delta u}{\nu}. \quad (5.7)$$

We can obtain a non-dimensional version of the incompressible Navier-Stokes equation (5.3) by expressing length velocities and mass in units  $L$ ,  $\delta u$  and  $M_L = L\rho$ . The result is

$$(\partial_{\hat{t}} + \hat{\mathbf{u}} \cdot \hat{\nabla})\hat{\mathbf{u}} + \hat{\nabla}\hat{P} = \frac{\hat{\nabla}^2\hat{\mathbf{u}}}{\text{Re}} + \hat{\mathbf{f}}^{ext}. \quad (5.8)$$

For large  $\text{Re}$ , the flow will typically be turbulent, and velocity fluctuations at a multiplicity of scales will be generated. There will be, in this case, a multiplicity of Reynolds numbers

$$\text{Re}_l = \frac{l\delta_l u}{\nu}, \quad (5.9)$$

giving the relative strength of inertial and viscous forces at the different flow scales.

In the case of a turbulent flow, the scale  $L$  and the characteristic velocity  $\delta u \equiv \delta_L u$  correspond to the scale of the largest eddies, determined by the boundary conditions of the flow (say, the width of a duct). Typically (as we shall see in the last section of these notes),  $\text{Re}_l$  is an increasing function of  $l$ , thus  $\text{Re} \equiv \text{Re}_L = \max_l \text{Re}_l$ .

## 5.1 Viscous flows

For  $\text{Re} \ll 1$ , Eq. (5.3) takes the limit form

$$\rho\partial_t\mathbf{u} + \nabla P = \mu\nabla^2\mathbf{u} + \mathbf{f}^{ext}, \quad \nabla \cdot \mathbf{u} = 0. \quad (5.10)$$

called the Stokes equation. If we disregard transients, the equation reduces to a balance of viscous, pressure and external forces

$$\nabla P = \mu\nabla^2\mathbf{u} + \mathbf{f}^{ext}, \quad \nabla \cdot \mathbf{u} = 0. \quad (5.11)$$

a regime called creeping flow. Clearly, a creeping flow regime is only possible if the boundary conditions and external forces vary on a time scale much slower than the viscous timescale  $\tau = L^2/\nu$ , where  $L$  is the characteristic scale of the flow.

Linearity of Eq. (5.11) makes analytical progress possible. However, except for simple geometries, solving Eqs. (5.10) and (5.11) can be laborious. In many cases, dimensional reasoning is the only viable strategy. We can, e.g., make estimates on the drag force on a body of size  $L$  moving with velocity  $U$  in the fluid,

$$F \sim L^3\mu\nabla^2\mathbf{u} \sim \mu LU. \quad (5.12)$$

An exact solution of Eq. (5.11) is possible in the case of the Couette flow, which is the flow between two flat surfaces sliding at constant relative speed  $U$ . The geometry

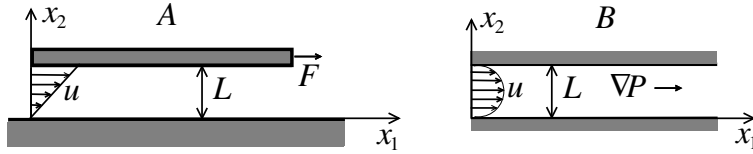


Figure 10: Sketch of Couette flow (A) and channel flow (B).

of the system is shown in Fig. 10a; we can evaluate the force that is required to keep the system in motion. Let us assume the gap width is much smaller than its length. We can thus disregard boundary effects and write  $\mathbf{u} = (u_1(x_2), 0, 0)$ . Since the velocity  $U$  of the body is constant, the force  $F$  exactly balances the viscous and pressure forces in the fluid. On the other hand, since the fluid does not accelerate, we must have  $\partial_1 P + \mu \partial_2^2 u = 0$ , so that for zero pressure forces,

$$\partial_2 u_1 = \text{constant}. \quad (5.13)$$

We can then impose no-slip conditions (Eq. (8.8)) on the solid surfaces bounding the gap, and we get

$$u_1(x_2) = U x_2 / L. \quad (5.14)$$

From here, we obtain the expression for the drag force

$$F_1 = \mu A U / L, \quad (5.15)$$

where  $A$  is the area of the body.

Another example of a flow for which a simple description is possible is the channel flow in Fig. 10b. We have a pressure difference  $\Delta P$  at the two ends of the interstice between two flat solid objects. Again, the width of the gap is assumed to be small. We thus set  $\mathbf{u} = (u_1(x_2), 0, 0)$  and impose stationarity,

$$\mu \partial_2^2 u_1 = \partial_1 P = \Delta P / X. \quad (5.16)$$

By imposing no-slip conditions on the surfaces at  $x_2 = 0$  and  $x_2 = L$ , we find the parabolic flow profile

$$u_1(x_2) = \frac{\Delta P}{2\mu X} (L - x_2)x_2. \quad (5.17)$$

The same calculation can be carried out in the case of a flow in a cylindrical pipe (Poiseuille flow), in which case it is possible to show that

$$u_1(r) = \frac{\Delta P}{4\mu X} (R^2 - r^2), \quad (5.18)$$

where  $R$  is the pipe's radius and  $r$  is the radial coordinate.

## 5.2 Suggested reading

- P. Kundu, I.M. Cohen and D.R. Dowling, “Fluid mechanics, Secs. 4.8-9 (Ac. Press 2015)

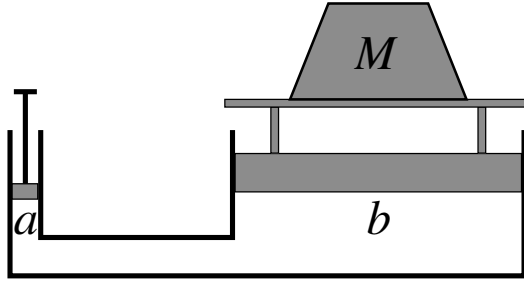


Figure 11: Mechanism of the hydraulic lift.

## 6 Hydrostatics

A fluid in equilibrium conditions obeys hydrostatic balance

$$\nabla P = \mathbf{f}^{ext}, \quad (6.1)$$

which descends straightforwardly from the Navier-Stokes equation (5.2). Equation (6.1) is the content of Pascal's principle, which states that at equilibrium, there must be a balance between pressure forces and external forces in the fluid. The solution of Eq. (6.1) is called the hydrostatic pressure.

We focus again on the case in which  $\mathbf{f}^{ext} = -\rho g \mathbf{e}_3$  is the gravitational force. In the case of a constant density fluid, such as, e.g., water, Eq. (6.1) can be integrated to give

$$P(x_3) = P(0) - x_3 \rho g, \quad (6.2)$$

which is called Stevino's law.

Stevino's law implies the law of communicating vessels, which states that the water level in the vessels must be identical at equilibrium. The proof is straightforward: if  $P_0$  is the pressure in a point of the fluid at height  $x_{3,0}$ , and  $x_{3,a}$  and  $x_{3,b}$  are the water levels in vessels  $a$  and  $b$ , the pressure at the water surface in the two vessels will be  $P_a = P_0 - (x_{3,a} - x_{3,0})\rho g$  and  $P_b = P_0 - (x_{3,b} - x_{3,0})\rho g$ . However, since at equilibrium  $P_a = P_b = P_{atm}$ , we must also have  $x_{3,a} = x_{3,b}$ . For the same reason, at equilibrium, the water surface in a tank must be horizontal.

Pascal's law explains how lifting and pressing devices work; we illustrate the mechanism in Fig. 11. The pressure on  $a$  and  $b$ , subtracted of the hydrostatic contribution  $\rho g(x_{3,a} - x_{3,b})$ , must be equal. The force on  $a$  required to lift the weight  $M$  on  $b$  is therefore

$$F_a = \frac{A_b}{A_a} M g, \quad (6.3)$$

where  $A_a$  and  $A_b$  are the areas of the pistons in  $a$  and  $b$ .

The same principle behind the hydraulic lift finds a spectacular realization in an experiment proposed by Pascal himself. Suppose that a barrel is communicating at the top with a thin and long vertical pipe and that the whole assembly is water-tight; pour water until the barrel and pipe are both full; the pressure at height  $x_3$  in the barrel is  $P = P_{atm} + (h - x_3)\rho g$ , where  $h$  is the length of the pipe. We then see that if  $h$  is sufficiently large, the pressure  $P$  will eventually cause the barrel to crack open. The remarkable fact is that the result is independent of the pipe radius (and therefore of the amount of water in the pipe).

Another physical law that can be derived from Eq. (6.1) is Archimedes' principle: an immersed body is subjected to a lift force equal to the weight of the displaced water. Indicate with  $A_w$  and  $A_a$ ,  $A = A_w \cup A_a$ , the portions of the body surface below and above the water surface, and with  $d\mathbf{A}$  the surface-element oriented out of the body. Let us put the origin of the axes at the water surface, pointing upwards; the lift force on the body is

$$\begin{aligned} F_3 &= - \int_A dA_3 P(x_3) = -P_{atm} \int_{A_a} dA_3 - \int_{A_w} dA_3 (P_{atm} - g\rho x_3) \\ &= g\rho \int_{A_w} dA_3 x_3 = g\rho V_w, \end{aligned} \tag{6.4}$$

where  $V_w$  is the underwater portion of the body, and where to reach the result we have exploited  $\int_A d\mathbf{A} = 0$ .

## 6.1 Suggested reading

- L.D. Landau and E.M. Lifshitz, "Fluid mechanics" Vol. 6, Secs. 3 and 4 (Pergamon Press 1987)

## 7 Conservation of energy

The continuity equation (3.2), the Navier-Stokes equation (5.2), and constitutive laws Eqs. (4.8) and (4.10) do not form a closed system. We need an additional equation for the temperature. We obtain such an equation by imposing energy conservation and separating the contributions from the kinetic and internal energy of the fluid.

### 7.1 Kinetic energy balance

An equation for the kinetic energy can be obtained in general form by taking the scalar product of Eq. (3.7) with  $\mathbf{u}$ ,

$$(1/2)\rho D_t u^2 = \mathbf{u} \cdot (\nabla \cdot \boldsymbol{\sigma} + \mathbf{f}^{ext}). \quad (7.1)$$

We exploit the continuity equation (3.2) to write Eq. (7.1) as

$$D_t(\rho u^2/2) = -\rho u^2 \nabla \cdot \mathbf{u}/2 + \mathbf{u} \cdot (\nabla \cdot \boldsymbol{\sigma} + \mathbf{f}^{ext}). \quad (7.2)$$

We note the advection term  $-\rho u^2 \nabla \cdot \mathbf{u}/2$  to RHS of the equation, which does contribute to the balance of kinetic energy  $K_L = \int_{V_L} dV \rho u^2/2$  in volume  $V_L$  following the fluid. Such a term is not present in Eq. (3.7) because of the condition of zero momentum advection into a fluid element,  $\int_{S_L} d\mathbf{A}_L \cdot \mathbf{u} = \int_{V_L} dV \nabla \cdot \mathbf{u} = 0$ . We exploit Eqs. (4.2) and (5.1), and write

$$\begin{aligned} \mathbf{u} \cdot (\nabla \cdot \boldsymbol{\sigma}) &= -\mathbf{u} \cdot \nabla P + \mu \mathbf{u} \cdot (\nabla \cdot \dot{\mathbf{s}}) \\ &= -\nabla \cdot (\mathbf{u}P) + P \nabla \cdot \mathbf{u} + \mu \nabla \cdot (\mathbf{u} \cdot \dot{\mathbf{s}}) - \mu \dot{\mathbf{s}} : (\nabla \mathbf{u}) \\ &= \nabla \cdot (\mathbf{u} \cdot \boldsymbol{\sigma}) + P \nabla \cdot \mathbf{u} - \mu \|\dot{\mathbf{s}}\|^2/2, \end{aligned} \quad (7.3)$$

where  $\|\dot{\mathbf{s}}\|^2 \equiv s_{ij}s_{ij}$ . We substitute the expression into Eq. (7.2) and get

$$D_t(\rho u^2/2) = -\rho u^2 \nabla \cdot \mathbf{u}/2 + \nabla \cdot (\mathbf{u} \cdot \boldsymbol{\sigma}) + P \nabla \cdot \mathbf{u} - \mu \|\dot{\mathbf{s}}\|^2/2 + \mathbf{u} \cdot \mathbf{f}^{ext}, \quad (7.4)$$

which we can rewrite in the form

$$\partial_t(\rho u^2/2) = \nabla \cdot (\mathbf{u} \cdot \boldsymbol{\sigma} - \rho u^2 \mathbf{u}/2) + P \nabla \cdot \mathbf{u} - \mu \|\dot{\mathbf{s}}\|^2/2 + \mathbf{u} \cdot \mathbf{f}^{ext}. \quad (7.5)$$

Integrating Eq. (7.5) over a fixed volume  $V$  yields the balance equation for the kinetic energy in the volume,  $K = (1/2) \int_V dV \rho u^2$ :

$$\dot{K} = \int_{\partial V} d\mathbf{A} \cdot [\mathbf{u} \cdot \boldsymbol{\sigma} - \rho u^2 \mathbf{u}/2] + \int_V dV [P \nabla \cdot \mathbf{u} - \mu \|\dot{\mathbf{s}}\|^2/2 + \mathbf{u} \cdot \mathbf{f}^{ext}]. \quad (7.6)$$

The surface integral to the RHS of the equation accounts for the kinetic energy flow into  $V$  produced by advection and the work by the stress forces on  $S$ . The first two terms in the volume integral describe the conversion of kinetic energy into internal energy through compression and viscous dissipation. The contribution of viscous dissipation is always negative. Thus, if an incompressible fluid lies in a tank with fixed walls, and  $\mathbf{f}^{ext} = 0$ ,  $\dot{K}$  will be negative. Any initial motion in the fluid will come to a halt.

## 7.2 Heat transport

Let us indicate the fluid thermal energy per unit mass with  $\mathcal{E}$ . The total energy in a fluid element  $V_L$  will be, therefore,

$$E_L \simeq V_L \rho (u_L^2/2 + \mathcal{E}_L) = K_L + E_L^{th}, \quad (7.7)$$

where  $K_L = M_L u_L^2/2$  is the kinetic energy of the fluid element and  $E_L^{th} = M_L \mathcal{E}_L$ . We can obtain an equation for  $K_L$  from Eqs. (7.1) and (7.3),

$$\dot{K}_L = \int_{\partial V_L} d\mathbf{A} \cdot \mathbf{u} \cdot \boldsymbol{\sigma} + \int_{V_L} dV [P \nabla \cdot \mathbf{u} - \mu \|\dot{\mathbf{s}}\|^2/2 + \mathbf{u} \cdot \mathbf{f}^{ext}]. \quad (7.8)$$

The terms to RHS of Eq. (7.8) represent the work on the fluid element by the viscous stresses and the pressure forces of the rest of the fluid, the mechanical energy gain and loss from compression and viscous dissipation in  $V_L$ , and the work by the external forces. The change of mechanical energy from compression and viscous dissipation results in a change of opposite sign in the internal energy  $\mathcal{E}_L$ . To obtain an equation for the latter, we need to take into account the energy flux  $\mathbf{q}$  through  $\partial V_L$  and the possible contribution  $\rho h^{ext}$  to  $\mathcal{E}_L$  from the radiation influx and the conversion from chemical to thermal energy. We reach the result

$$\rho D_t \mathcal{E} + P \nabla \cdot \mathbf{u} = -\nabla \cdot \mathbf{q} + \mu \|\dot{\mathbf{s}}\|^2/2 + \rho h^{ext}. \quad (7.9)$$

We can apply Eq. (7.9) to study the evolution of the internal energy content  $E_L$  of fluid element  $V_L$  transported by the flow. Equation (2.23) and mass conservation allow us to write  $\int_{V_L} dV (\rho D_t \mathcal{E} + P \nabla \cdot \mathbf{u}) = \dot{E}_L^{th} + P \dot{V}_L$ , from which we get

$$\dot{E}_L^{th} + P \dot{V}_L = \dot{Q}_L, \quad (7.10)$$

where

$$\dot{Q}_L = - \int_{\partial V_L} d\mathbf{A} \cdot \mathbf{q} + \mu \int_{V_L} dV [\|\dot{\mathbf{s}}\|^2/2 + \rho h^{ext}] \quad (7.11)$$

is the rate at which heat enters the volume element. We recognize in Eq. (7.10) the first law of thermodynamics applied to the fluid element  $V_L$ . Of particular interest is the case that pressure is constant along a fluid trajectory. Equation (7.10) then becomes

$$\dot{E}_L^{th} + P V_L \nabla \cdot V_L (\rho D_t \mathcal{E} + P \nabla \cdot \mathbf{u}) = \frac{d}{dt} [E_L^{th} + P V_L] = \dot{W}_L, \quad (7.12)$$

where  $\dot{W}_L$  is the rate of heat transfer to the fluid element at a constant pressure,

$$\dot{W}_L = - \int_{\partial V_L} d\mathbf{A} \cdot \mathbf{q} + \int_{V_L} dV \left[ h^{ext} + \frac{\mu}{2} \|\dot{\mathbf{s}}\|^2 \right]. \quad (7.13)$$

We can convert the heat transport equation (7.9) to one for the temperature. The operation is transparent in the case of a uniform quiescent fluid. Equation (7.8) then takes the form

$$\rho d\mathcal{E} = \rho h^{ext} dt = n c_V k_B dT, \quad (7.14)$$

where  $c_V$  is the specific heat per molecule at constant volume (in the case of a gas of monoatomic molecules,  $c_V = 3/2$ ). We can then rewrite Eq. (7.9) in the form

$$n c_V k_B D_t T + P \nabla \cdot \mathbf{u} = -\nabla \cdot \mathbf{q} + \mu \|\dot{\mathbf{s}}\|^2 / 2 + \rho h^{ext}. \quad (7.15)$$

We can consider again a constant pressure situation and rewrite the RHS of the equation in the form

$$\begin{aligned} n c_V k_B D_t T + P \nabla \cdot \mathbf{u} &= n c_V k_B \dot{T}_L + (P/V_L) \dot{V}_L \\ &= \left[ n c_V k_B + \frac{P}{V_L} \left( \frac{\partial V_L}{\partial T} \right)_P \right] \dot{T}_L := n c_P k_B \dot{T}_L. \end{aligned} \quad (7.16)$$

which defines the specific heat at constant pressure  $c_P$ . In the case of an ideal gas,  $V = N k_B T / P \Rightarrow (P/V_L)(dV/dT)_P = n k_B \Rightarrow c_P = c_V + 1$ .

For Eqs. (3.2), (5.2), and (7.15) to form a closed system of equations, we still need constitutive equations for the pressure and the heat flux. In the case of a gas, the pressure obeys the law of state Eq. (4.8), and one usually reabsorbs the constant  $c_V$  in the definition of the diffusivity  $\kappa$  (see Eq. (4.12)):

$$\mathbf{q} = -n \kappa k_B \nabla T. \quad (7.17)$$

As previously done with the viscosity, effects from the spatial variation of  $n \kappa$  are disregarded, and Eq. (7.9) takes the final form

$$c_V D_t T + T \nabla \cdot \mathbf{u} = \kappa \nabla^2 T + k_B^{-1} [\nu \|\dot{\mathbf{s}}\|^2 / 2 + m h^{ext}]. \quad (7.18)$$

In the case of a fluid at constant pressure,

$$c_P D_t T = \kappa \nabla^2 T + k_B^{-1} [\nu \|\dot{\mathbf{s}}\|^2 / 2 + m h^{ext}]. \quad (7.19)$$

Note that in the absence of thermal diffusion and thermal sources, Eq. (7.19) becomes  $D_t T = 0$ , which means that  $T$  is frozen in the field  $\mathbf{u}$ . We shall see in Sec. 11.2 that setting  $\nabla \cdot \mathbf{u} = 0$  is not sufficient to impose incompressibility in Eq. (7.18). It is an example of singular perturbation, as the pressure must large enough to prevent any volume change of the fluid element. The consequence is that the product  $P \nabla \cdot \mathbf{u}$  is never small and incompressible energy transport is described by Eq. (7.19).

We have seen in Sec. 5.1 that for small  $\text{Re}$  the advection term the dynamics of the fluid reduces to a balance of viscous, pressure and external forces. The same line of reasoning leading for  $\text{Re} \rightarrow 0$  to the Stokes equation (5.10) yields in the case of Eq. (7.19) the heat equation

$$c_P \partial_t T = \kappa \nabla^2 T + \text{heat sources}, \quad \frac{u_L L}{\kappa} = \text{Re Pr} \ll 1, \quad (7.20)$$

where  $L$  and  $u_L$  are the characteristic length and velocity of the flow and  $\text{Pr} = \nu / \kappa$  is called the Prandtl number. For most gases  $\text{Pr} \sim 1$ .

### 7.2.1 The enthalpy of a fluid

The heat transfer at constant pressure is called enthalpy. We recall here some of its properties, which will be helpful when dealing with compressible flows. We define enthalpy from the relation

$$dW|_P = Mdw = (dE^{th} + PdV)_P = d(E^{th} + PV)_P = TdS|_P,$$

where subscript  $P$  indicates variation at constant pressure,  $E^{th} = \mathcal{E}M$  is the thermal energy,  $S$  is the entropy, and  $V = V(P, S)$  is the volume of the fluid element. Thus, enthalpy is a function of entropy and pressure,  $W = W(S, P) \Rightarrow dW = T(S, P)dS + V(S, P)dP$  (in this framework, energy  $E^{th} = E^{th}(S, V)$  is understood as a function of volume and entropy, and  $dE^{th} = TdS - PdV$ ). Define the enthalpy per unit mass  $w = W/M = \mathcal{E} + P/\rho$ . In isentropic conditions, we have the useful relation

$$dw = dW|_S/M = VdP/M = \rho^{-1}dP. \quad (7.21)$$

### 7.2.2 The entropy of a fluid

We can rewrite the thermal energy balance equation (7.10) in terms of the entropy gain in an infinitesimal displacement,

$$TdS_L - PdV_L = dE_L^{th}, \quad (7.22)$$

where we neglect the contribution to  $dS_L$  from entropy production inside the fluid element. We can write equivalently

$$TdS_L - Pd(1/\rho_L) = d\mathcal{E}_L = \frac{c_V k_B}{m} dT_L. \quad (7.23)$$

where  $s = S/M$ . From here we get the entropy change along a fluid trajectory

$$s_f - s_i = \frac{k_B}{m} \left[ c_V \ln(T_f/T_i) - \ln(\rho_f/\rho_i) \right]. \quad (7.24)$$

We can derive an expression for the entropy change as a function of the temperature and the pressure starting from Eq. (7.21),

$$TdS_L + \rho^{-1}dP_L = dw_L = \frac{c_P k_B}{m} dT_L. \quad (7.25)$$

The result is

$$s_f - s_i = \frac{k_B}{m} \left[ c_P \ln(T_f/T_i) - \ln(P_f/P_i) \right]. \quad (7.26)$$

### 7.3 An equation for the total energy

We can combine Eqs. (7.2) and (7.9) to derive an Eulerian equation for the total energy density. We first exploit the continuity equation (3.2) to rewrite in Eq. (7.9)

$$\begin{aligned}\rho D_t \mathcal{E} + P \nabla \cdot \mathbf{u} &= D_t(\rho \mathcal{E}) + (P + \rho \mathcal{E}) \nabla \cdot \mathbf{u} \\ &= \partial_t(\rho \mathcal{E}) + \mathbf{u} \cdot \nabla(\rho \mathcal{E}) + (P + \rho \mathcal{E}) \nabla \cdot \mathbf{u} \\ &= \partial_t(\rho \mathcal{E}) + \nabla \cdot [\mathbf{u}(P + \rho \mathcal{E})] - \mathbf{u} \cdot \nabla P.\end{aligned}\quad (7.27)$$

We next exploit Eq. (7.3) to rewrite in Eq. (7.2)

$$\begin{aligned}D_t(\rho u^2/2) + \rho u^2 \nabla \cdot \mathbf{u}/2 - \mathbf{u} \cdot (\nabla \cdot \boldsymbol{\sigma}) \\ = \partial_t(\rho u^2/2) + \nabla \cdot (\rho u^2 \mathbf{u}/2) + \mathbf{u} \cdot \nabla P + \dots,\end{aligned}\quad (7.28)$$

where the dots stand for the viscous and external force terms. We sum Eqs. (7.27) and (7.28) and obtain

$$\partial_t[\rho(u^2/2 + \mathcal{E})] + \nabla \cdot [\mathbf{q} + \rho \mathbf{u}(u^2/2 + w)] = \mathbf{f}^{ext} \cdot \mathbf{u} + \rho h^{ext},\quad (7.29)$$

where  $w$  is the enthalpy per unit mass of the fluid.

### 7.4 Isoentropic flow

The entropy gain of a fluid element, assuming reversible conditions, reads, from Eqs. (7.10), (7.11) and (7.22),

$$\dot{S}_L = \int_{V_L} dV \frac{-\nabla \cdot \mathbf{q} + \mu \|\dot{\mathbf{s}}\|^2 + \rho h^{ext}}{T}.\quad (7.30)$$

By substituting Eq. (7.17) into Eq. (7.30), we can verify that the entropy of an isolated system does not decrease with time, which is the content of the second principle of thermodynamics. In the case of an isolated system, we have in fact

$$\begin{aligned}\dot{S} &= \int_V dV T^{-1} [nk_B \kappa \nabla^2 T + \mu \|\dot{\mathbf{s}}\|^2] \\ &\leq nk_B \kappa \int_V dV \left[ \nabla \cdot \frac{\nabla T}{T} - \nabla T \cdot \nabla \frac{1}{T} \right] \\ &= - \int_{\partial V} \frac{d\mathbf{A} \cdot \mathbf{q}}{T} + nk_B \kappa \int_V dV \frac{|\nabla T|^2}{T^2},\end{aligned}\quad (7.31)$$

and since  $\mathbf{q} = 0$  on  $\partial V$ ,  $\dot{S}_L \geq 0$ .

If the entropy  $S_L$  of fluid elements is constant along a fluid trajectory, also the entropy density  $s_L = S_L/M$  is constant, which means that the entropy density  $s(\mathbf{x}, t)$  is a frozen field,

$$D_t s = 0.\quad (7.32)$$

If  $s$  is conserved along the flow, an initially uniform distribution of  $s$  will remain uniform also afterward, and we say that the flow is isentropic.

In isentropic conditions, the values of  $\rho$  and  $T$  along a fluid trajectory are related by an adiabatic transformation. From Eqs. (2.23) and (7.15) we have

$$n\rho c_V k_B D_t T = P D_t \rho \quad \Rightarrow \quad \rho^2 \frac{dT}{d\rho} = \frac{m}{c_V k_B} P(\rho, T), \quad (7.33)$$

which is replaced, in the case of a gas for which  $P = nk_B T$ , by the familiar relation

$$\rho \frac{dT}{d\rho} = \frac{T}{c_V} \Leftrightarrow T \rho^{-1/c_V} = C, \quad (7.34)$$

where  $C$  is constant throughout the fluid.

Equation (7.33) implies

$$P = P(\rho, T(\rho)). \quad (7.35)$$

A flow such that the pressure only depends on the density is said to be barotropic, and since the implication in Eq. (7.34) goes both ways, the flow will be isentropic as well. Surfaces at constant pressure coincide in a barotropic flow with those at constant density, and therefore, through the law of state, also with those of constant temperature.

## 7.5 Bernoulli's equation

The total energy balance equation (7.29) can be specialized to the case of a stationary ideal flow, for which  $\kappa = \mu = 0$ , and there are no external heat sources. If we furthermore assume that the external force can be derived from a potential,  $\mathbf{f}^{ext} = -\rho \nabla \Psi$ , and exploit the fact that at stationarity the continuity equation (3.2) dictates  $\nabla \cdot (\rho \mathbf{u}) = 0$ , we can write

$$\mathbf{u} \cdot \nabla [u^2/2 + w + \Psi] = 0, \quad (7.36)$$

where we recall  $w = \mathcal{E} + P/\rho$  is the enthalpy per unit mass of the fluid. By integrating Eq. (7.36) along a field line, we obtain Bernoulli's equation

$$\frac{u^2}{2} + w + \Psi = \text{constant}. \quad (7.37)$$

Of particular interest is the case the flow is incompressible, and  $\Psi = gx_3$  is the gravitational potential. Of course, an incompressible flow can be time-independent only if  $\rho$  is constant in space. Equation (7.37) reads in this case

$$\frac{1}{2} \rho u^2 + P + \rho g x_3 = \text{constant}, \quad (7.38)$$

which is the original form Bernoulli derived his equation in 1738.

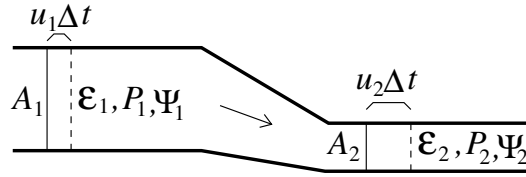


Figure 12: Control domain for Bernoulli's principle.

The physical content of Bernoulli's equation is that the pressure of a fluid flowing at a constant height increases where it slows down and decreases where it accelerates; in the case the height of the fluid changes during the motion, the pressure and the kinetic energy must compensate for the change in potential energy.

The equation has a nice geometrical interpretation illustrated in Fig. 12. A mass amount  $\Delta M = \rho_1 A_1 u_1 \Delta t = \rho_2 A_2 u_2 \Delta t$  travels the control surfaces  $A_1$  and  $A_2$  in a time  $\Delta t$ . A change of potential energy  $(\Psi_2 - \Psi_1)\Delta M$  takes place in the time interval in the fluid element bounded initially by  $A_1$  and  $A_2$ . Concurrently, an amount of work is exerted on the fluid element by the fluid to the left of  $A_1$  and an amount  $-A_2 P_2 u_2 \Delta t$  is exerted on the same fluid element by the fluid to the right of  $A_2$ . As a result of the displacement, there is a change  $\Delta M(\mathcal{E}_2 + u_2^2/2) - \Delta M(\mathcal{E}_1 + u_1^2/2)$  in the sum of the kinetic and internal energy of the fluid element. Imposing energy conservation yields, in the absence of tangential stresses at the boundaries,

$$\Delta M(\Psi_1 + \mathcal{E}_1 + u_1^2/2) - \Delta M(\Psi_2 + \mathcal{E}_2 + u_2^2/2) + (P_1 A_1 u_1 - P_2 A_2 u_2)\Delta t = 0,$$

which implies Bernoulli's equation (7.37).

Combining Stevino's law and Bernoulli's equation allows us to derive Torricelli's law, which gives the speed of water out of an orifice in a tank as a function of the height  $h$  of the water column above the orifice. The pressure at the water surface and outside the orifice equals the atmospheric pressure  $P_{atm}$  (in this and the following examples, we disregard the change of  $P_{atm}$  at the scales under consideration). Inside the tank, the pressure at the orifice level, from Eq. (6.2), equals  $P_{atm} + \rho gh$ , and the fluid velocity is zero. Bernoulli's equation (7.38) then implies  $P_{atm} + \rho gh = P_{atm} + (1/2)\rho u^2$ , where  $u$  is the flow velocity just out of the orifice. We thus get

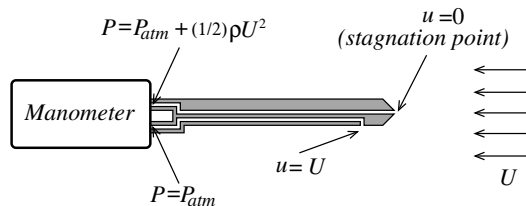


Figure 13: Schematics of the Pitot pipe

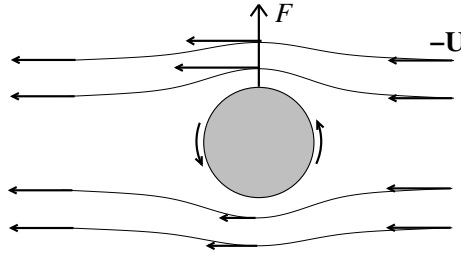


Figure 14: The Magnus effect.

Torricelli's law

$$u = \sqrt{2gh}. \quad (7.39)$$

The Pitot pipe is an example of a device that works thanks to Bernoulli's law. We illustrate the mechanics of the device in Fig. 13. The Pitot pipe allows one to determine the flow velocity of the fluid from the pressure difference generated in two channels: one facing the flow, in the so-called stagnation point, where the fluid velocity is zero, the other tangent to the flow, where the fluid velocity is approximately equal to its value far from the device.

Another application of Bernoulli's equations is the explanation of the Magnus effect. The effect allows a football player to make a ball follow a curved trajectory by giving the ball a spin. We illustrate the idea in Fig. 14, which depicts a ball flying to the right with velocity  $\mathbf{U}$ , spinning counterclockwise, and consequently subjected to an upward lift force  $\mathbf{F}$ .

In the reference frame of the ball, the air approaches the ball with speed  $-\mathbf{U}$ ; when it gets close, however, it slows down and tends to be dragged along by the spinning ball. The air on top of the ball will flow faster than the air below; by Bernoulli's equation, the velocity decrease of the air along its streamlines must be compensated by an increase the pressure, which is the strongest under the ball; the result is a lift force  $\mathbf{F}$  pushing the ball upwards.

The explanation of the Magnus effect provided by Bernoulli's equation has several limitations. In the first place, the air, to feel the drag of the rotating ball, must have finite viscosity. This, however, violates the hypothesis at the basis of Bernoulli's equation, that the flow is inviscid. A second difficulty is that the flow near the ball becomes turbulent and thus is not stationary, which is problematic since the turbulence-induced drag on the ball may have a lateral component and contribute to the lift.

Limitations in the applications of Bernoulli's equation, similar to the one just discussed, arise in several contexts. As a rule of thumb, Bernoulli's equation approach allows a qualitative understanding of a process but often falls short when the goal is quantitative estimates.

We conclude the section by noting that Eq. (7.29), which stands at the basis of Bernoulli's law, is also valid for viscous fluids, suggesting that we could extend

Bernoulli's law to non-ideal conditions, provided the strain is zero at the ends of the control domain. We shall consider such a situation in Sec. (10.3) when dealing with shock waves. Note that if the flow is compressible, knowing the pressure and the vertical coordinate at the ends of the domain does not fix the fluid velocity, as we need to know the density. Once the pressure and the density are fixed, we could determine the fluid velocity and, through Eq. (7.26) and the equation of state, the entropy. We immediately realize that entropy is not conserved, as viscous dissipation and other processes may lead to entropy production in the central part of the control domain.

## 7.6 Suggested reading

- L.D. Landau and E.M. Lifshitz, "Fluid mechanics" Vol. 6, Secs. 2, 5, 6 and 16 (Pergamon Press 1987)
- P. Kundu, I.M. Cohen and D.R. Dowling, "Fluid mechanics, Secs. 4.12-16 (Ac. Press 2015)

## 8 Ideal hydrodynamics

We say that a fluid is ideal if its viscosity equals zero. Unfortunately, the zero viscosity limit of the Navier-Stokes equation (5.2) is singular, which means that the zero viscosity limit of a solution of the Navier-Stokes equation does not coincide, in general, with the solution of the zero-viscosity version of that equation, called the Euler's equation

$$\rho D_t \mathbf{u} + \nabla P = \mathbf{f}^{ext}. \quad (8.1)$$

Identifying a large Reynolds number flow with an ideal flow is thus problematic, and vorticity plays crucial role. The key issue is the dynamics of the fluid near solid obstacles, which calls back the question of how to impose boundary conditions on the flow.

Consider a fluid of arbitrarily small but non-zero viscosity flowing in the vicinity of a fixed solid obstacle, and consider a portion of the surface of the solid, sufficiently small to be approximated by its tangent plane, which we take to be the  $x_1x_2$  plane. Near the body, the flow is almost parallel to the body's surface and is a linear function of  $x_3$ . Taking the flow locally along  $x_1$ ,  $\mathbf{u} = (\alpha x_3, 0, 0)$ , which corresponds to values of the viscous stress and the viscosity  $\sigma_{13} = \alpha\mu$  and  $\boldsymbol{\omega} = (0, \alpha, 0)$ .

What happens in high Reynolds number flows is that the velocity gradient tends to concentrate in a boundary layer whose thickness decreases with the viscosity. In the case of slowly varying flows, the boundary layer thickness  $l$  can be estimated from the Navier-Stokes equation (5.2) as the distance from the body where inertia and viscous dissipation become of the same order,  $l \sim \nu/U$ , where  $U$  is the velocity scale of the flow relative to the body. On the other hand, the viscous dissipation per unit area and unit mass is, from Eq. (7.9),  $l\nu\|\dot{\mathbf{s}}\|^2 \sim \nu U^2/l \sim U^3$ , which tells us that even though the thickness of the boundary layer tends to zero with the viscosity, the viscous dissipation (and hence the drag) remains finite. We note that the viscous boundary layer is not stationary. We can convince ourselves of this by considering that viscosity diffuses momentum away from the body surface while advection carries the fluid longitudinally. For a body of size  $L$ , diffusion acts for a time  $\sim L/U$ , which yields the diffusion length  $l_\nu \sim (\nu L/U)^{1/2} = \text{Re}^{-1/2}L$ . Indeed, the situation is more complicated. One can show that the viscous boundary layer is unstable, and the flow is not parallel to the body surface, becoming turbulent in the process. The boundary layer then turns into a tangle of thin vortex filaments that are transported away from the body at a rate much higher than that provided by viscosity, and end up filling a significant portion of the fluid volume.

The upshot of the present discussion is that zero viscosity does not imply zero viscous dissipation. Qualitative estimates of the kind obtained in the case of the Magnus effect discussed in Sec. 7.5 are nevertheless possible if turbulence remains confined to a limited portion of the fluid, and the flow could be treated as ideal away from solid obstacles and the turbulence in their proximity.

## 8.1 Potential flows

The velocity field of a vorticity-free flow can be written as the gradient of a scalar potential

$$\mathbf{u} = \nabla\Phi. \quad (8.2)$$

We speak in this case of a potential flow. If the fluid is barotropic, and the external force can itself be derived from a potential,  $\mathbf{f}^{ext}/\rho = -\nabla\Psi$ , the Navier-Stokes equation can be converted into an equation for the potential

$$\partial_t\Phi + \frac{1}{2}|\nabla\Phi|^2 + w + \Psi - \frac{4}{3}\nu\nabla^2\Phi = \text{constant}, \quad (8.3)$$

where we have exploited the relation

$$\begin{aligned} \mathbf{u} \cdot \nabla u_j &= (\partial_i\Phi)\partial_j\partial_i\Phi = \partial_j[(\partial_i\Phi)\partial_i\Phi] - (\partial_j\partial_i\Phi)\partial_i\Phi \\ &= \partial_j[(\partial_i\Phi)\partial_i\Phi] - \frac{1}{2}\partial_j[(\partial_i\Phi)\partial_i\Phi] = \frac{1}{2}\partial_j|\nabla\Phi|^2, \end{aligned} \quad (8.4)$$

together with the fact that in barotropic conditions  $\rho^{-1}dP = dw$ , where  $w$  is the enthalpy per unit mass. We note that the constant in Eq. (8.3) may still depend on time; such time dependence would produce a contribution to  $\Phi$ , which is time-dependent but constant in space, and thus does not modify  $\mathbf{u}$ .

Equation (8.4) tells us that, in barotropic conditions, a vorticity-free initial condition produces zero curl terms in the Navier-Stokes equation. A flow with zero vorticity initially will thus remain vorticity-free at later times.

Equation (8.3) takes a simple form in the incompressible case

$$\partial_t\Phi + \frac{1}{2}|\nabla\Phi|^2 + \frac{P}{\rho} + \Psi = \text{constant}, \quad \nabla^2\Phi = 0, \quad (8.5)$$

in which the viscous terms disappear, and the dynamics becomes identical to that of an ideal fluid (in this case, the flow contains only strain). We note that in the case of a time-independent ideal flow, Eq. (8.3) takes a form reminiscent of Bernoulli's equation

$$\frac{1}{2}|\nabla\Phi|^2 + w + \Psi = \text{constant}. \quad (8.6)$$

The only difference is that in the case of Bernoulli's equation the sum  $u^2/2 + w + \Psi$ , is constant along flow lines, while in the case of Eq. (8.6) the sum is constant in the whole flow domain.

To solve Eq. (8.3), we must impose boundary conditions on the potential  $\Phi$ ; we require that the fluid cannot penetrate solid objects (impermeability boundary conditions), which leads to Neumann boundary conditions at the body surface  $s$

$$\mathbf{u}_\perp^{solid} = \mathbf{u}_\perp^s = \nabla_\perp\Phi^s, \quad (8.7)$$

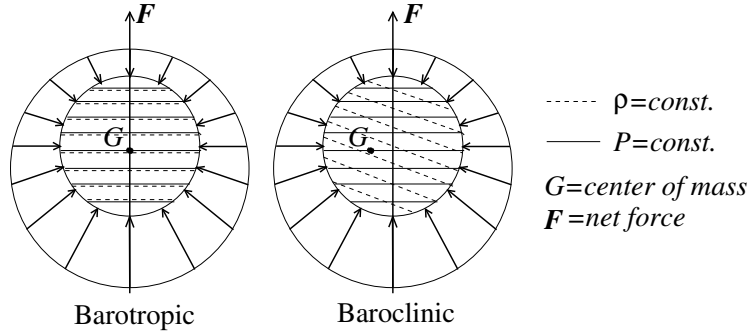


Figure 15: Mechanism of vorticity generation in baroclinic conditions (from *Fluid Mechanics* by P. Kundu).

where  $\mathbf{e}_\perp$  is the local normal to the solid surface. We note that no boundary conditions are imposed on the tangential component of the velocity; however, we know that viscosity generates tangential stress at the solid surface, which forces the tangential components of  $\mathbf{u}$  and  $\mathbf{u}^{solid}$  at the solid surface to be equal:

$$\mathbf{u}_\parallel^{solid} = \mathbf{u}_\parallel^s. \quad (8.8)$$

In general  $\mathbf{u}_\parallel^{solid} \neq \nabla_\parallel \Phi$ , and the difference  $\mathbf{u}_\parallel^{solid} - \nabla_\parallel \Phi$  acts as a source of vorticity.

Another mechanism for vorticity production is the presence of baroclinic conditions, as illustrated in Fig. 15. The baroclinic case in the figure corresponds to a situation in which the temperature is higher on the right (the fluid element may represent the left lobe in the vertical section of a rising mushroom cloud). The center of mass of the fluid element shifts to the left, which causes the gravitational force to generate a counterclockwise torque on the fluid element.

## 8.2 Fluid inertia

We want to study the dynamics of a solid body in an infinite incompressible fluid. Indicate with  $\mathbf{U}$  the velocity of the body, assumed constant, and with  $\mathbf{u}(\mathbf{x}, t)$  the velocity perturbation generated in the fluid. Consider, for simplicity, the case of a sphere of radius  $R$  moving along the axis  $x_1$ . Assume potential flow, and indicate with  $\hat{\mathbf{u}} = \nabla \hat{\Phi}$  the fluid velocity perturbation in the reference frame of the moving sphere,

$$\hat{\mathbf{u}}(\mathbf{x}, t) = \mathbf{u}(\mathbf{x} + \mathbf{U}t, t). \quad (8.9)$$

Take the origin of the axis of the moving reference frame at the center of the sphere. The field  $\hat{\mathbf{u}}$  is obtained as the solution of the boundary value problem

$$\nabla^2 \hat{\Phi} = 0, \quad \mathbf{x} \cdot (\mathbf{U} + \hat{\mathbf{u}})_A = 0, \quad (8.10)$$

where  $A$  is the sphere's surface.

The potential  $\hat{\Phi}$  has the same structure of the potential of an electric multipole,

$$\Phi(\mathbf{x}) = -\frac{M^{(0)}}{x} - \frac{\mathbf{M}^{(1)} \cdot \mathbf{x}}{x^3} - \frac{\mathbf{M}^{(2)} : \mathbf{x}\mathbf{x}}{x^5} + \dots \quad (8.11)$$

We know from incompressibility that the point charge contribution to  $\hat{\mathbf{u}}$ ,  $\hat{\mathbf{u}}^{(0)} = M^{(0)}\mathbf{x}/x^3$ , vanishes. We verify that to enforce the boundary conditions in Eq. (8.10), it is sufficient to keep the dipole contribution,

$$\hat{\mathbf{u}} = \hat{\mathbf{u}}^{(1)} = \frac{3(\mathbf{M}^{(1)} \cdot \mathbf{x})\mathbf{x} - \mathbf{M}^{(1)}x^2}{x^5}. \quad (8.12)$$

Indeed, we know from symmetry that  $\mathbf{M}^{(1)}$  is directed along  $x_1$ . Equation (8.10) thus becomes

$$\mathbf{x} \cdot (\mathbf{U} + \hat{\mathbf{u}})_A = \frac{2x_1}{R^2x}(M^{(1)} + UR^3) = 0, \quad (8.13)$$

and substituting the resulting expression for  $M^{(1)}$  into Eq. (8.12) yields

$$\hat{\mathbf{u}} = \frac{[\mathbf{U}x^2 - 3(\mathbf{U} \cdot \mathbf{x})\mathbf{x}]R^3}{2x^5}. \quad (8.14)$$

We can calculate from Eq. (8.14) the kinetic energy content of the fluid velocity perturbation generated by the sphere,

$$K = \frac{\pi\rho R^6 U^2}{4} \int_R^{+\infty} \frac{dx}{x^4} \int_{-1}^1 dz (3z^2 + 1) = \frac{\pi\rho R^3 U^2}{3}. \quad (8.15)$$

Equation (8.15) tells us that the work required to accelerate the body has a component associated with the induced fluid motion. The effect is the same as a renormalization of the body mass, called the added mass. In the case of a radius  $R$  sphere,

$$\delta M = \frac{2\pi\rho R^3}{3}. \quad (8.16)$$

From Eq. (8.15), we can define the linear momentum of the flow perturbation

$$\delta\mathbf{P} = \frac{\partial K}{\partial \mathbf{U}} = \delta M \mathbf{U}. \quad (8.17)$$

Note that  $\delta\mathbf{P}$  cannot be expressed as an integral over the linear momenta of the fluid elements, as  $K$  receives contributions from momenta along  $\delta\mathbf{P}$  and perpendicular to it. Indeed, the integral  $\rho \int d^3x \hat{\mathbf{u}}$  does not even converge. A simple mechanical analog showing a similar mismatch between the total momentum and the sum of the momenta of the parts is shown in Fig. 16. The Lagrangian of the system is

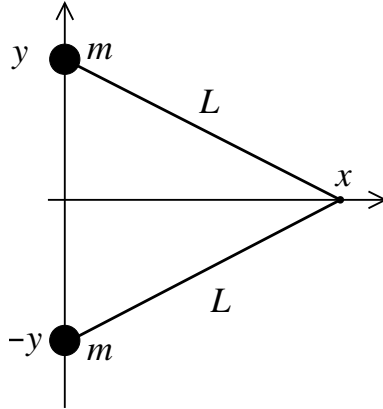


Figure 16: Mechanical analog of the incompressible fluid. The two beads, which represent the fluid, are free to slide vertically on the  $y$  axis and are connected to the hinge in  $x$  (the solid body) by two rigid sticks of length  $L$  (the pressure and impermeability constraints).

$$L(x, \dot{x}) = m\dot{y}^2 = \frac{mx^2\dot{x}^2}{L^2 - x^2}. \quad (8.18)$$

The momentum conjugate to  $x$  is

$$p = \frac{\partial L}{\partial \dot{x}} = \frac{2mx^2\dot{x}}{L^2 - x^2}, \quad (8.19)$$

while the sum of the momenta of the two beads,  $m\dot{y}$  and  $-m\dot{y}$ , is by construction equal to zero.

If the velocity  $\mathbf{U}$  of the solid body is constant, the total linear momentum  $\mathbf{P} = (M + \delta M)\mathbf{U}$  of the system and the fluid is conserved. We thus reach the remarkable conclusion (d’Alambert’s paradox) that no force is required to keep a body in motion in an inviscid infinite fluid. Note that the condition that the fluid is infinite cannot be relaxed, as momentum could flow out of a finite domain without the need for dissipation. A trivial mechanism is the interaction with a moving solid boundary.

To accelerate or slow down a body in an infinite inviscid fluid, we still need to impose a force  $\mathbf{F} = (M + \delta M)\dot{\mathbf{U}}$ . We can use this information to determine the law of motion for a solid body immersed in an accelerating fluid. Suppose that the only force on the body is Archimedes’ push from the acceleration of the fluid,

$$V\rho D_t \mathbf{U}_f \equiv V\rho(\partial_t + \mathbf{U} \cdot \nabla) \mathbf{U}_f, \quad (8.20)$$

where  $V$  is the volume of the body,  $\mathbf{U}_f$  the fluid velocity and  $D_t \mathbf{U}_f$  the change of fluid velocity experienced by the moving body. The Archimedes forces generate a variation in the body momentum,  $M\mathbf{U}$ , and in the momentum of the fluid  $\delta M(\mathbf{U} - \mathbf{U}_f)$ . The result is

$$(M + \delta M)\dot{\mathbf{U}} = (V\rho + \delta M)D_t \mathbf{U}_f. \quad (8.21)$$

### 8.3 Gravity waves

Gravity waves provide an example of potential flow. We focus on the case of small amplitude gravity waves in deep water.

Let us choose our reference system with  $x_1$  along the propagation's direction of the wave, with  $x_3$  pointing upwards and the origin of the axes at the unperturbed water surface, and we look for solutions in the form

$$\Phi(\mathbf{x}, t) = \Phi_0(x_3) \exp[i(kx_1 - \omega t)]. \quad (8.22)$$

Incompressibility guarantees that the velocity potential obeys Laplace's equation  $\nabla^2\Phi = 0$ . In the case of the wave solution in Eq. (8.22),

$$(\partial_3^2 - k^2)\Phi_0 = 0 \Rightarrow \Phi_- e^{-kx_3} + \Phi_+ e^{kx_3}. \quad (8.23)$$

The term  $\Phi_- e^{-kx_3}$  grows exponentially with the depth and is absent in the case of infinitely deep water.

To obtain a dispersion relation, we require that the fluid pressure at the perturbed water surface equals the atmospheric pressure. We can thus write

$$\partial_t P_L(t|\mathbf{x}, t_0) = 0, \quad (8.24)$$

where  $P_L(t|\mathbf{x}, t_0)$  is the pressure at the current fluid element position, and  $\mathbf{x} = (x_1, x_2, 0)$  is the position of the fluid element at the time  $t_0$  when it crosses the reference unperturbed water surface level (different fluid elements have different time labels  $t_0$ ). We determine  $P_L(t|\mathbf{x}, 0)$  from  $P(\mathbf{x}, t)$  by solving Eq. (8.5). The equation can be linearized provided  $k\Phi^2 \ll \omega\Phi$ , which, expressed in terms of the wave height  $A = k\Phi_0(0)/\omega$ , reads

$$kA \ll 1. \quad (8.25)$$

The linearized version of Eq. (8.5) reads

$$P/\rho = -\partial_t\Phi + gx_3 + \text{constant}. \quad (8.26)$$

We likewise linearize  $P_L$ ,

$$\begin{aligned} P_L(t|\mathbf{x}, 0) \equiv P(\mathbf{x}_L(t|\mathbf{x}, 0), t) &= \rho[gx_{3,L}(t|\mathbf{x}, 0) - \partial_t\Phi(\mathbf{x}_L(t|\mathbf{x}, 0), t)] \\ &\simeq \rho[gx_{3,L}(t|\mathbf{x}, 0) - \partial_t\Phi(\mathbf{x}, t)]. \end{aligned} \quad (8.27)$$

We substitute Eq. (8.27) into Eq. (8.24), exploit the relation

$$\dot{x}_{3,L}(t|\mathbf{x}, 0) = u_{3,L}(t|\mathbf{x}, 0) \simeq u_3(\mathbf{x}, t), \quad (8.28)$$

again drop terms quadratic in  $\Phi$ , and we get

$$0 = [g\partial_3 - \partial_t^2]\Phi = 0. \quad (8.29)$$

We finally substitute Eqs. (8.22) and (8.23) into Eq. (8.29) and we obtain the dispersion relation

$$\omega^2 = kg. \quad (8.30)$$

From Eq. (8.30), we find the phase velocity of the wave

$$c_w = g/\omega^2. \quad (8.31)$$

Gravity waves in nature do not always have a small amplitude. We are going to see that nonlinearities generate a transport component in the motion of the fluid, called the Stokes drift. Let us study the trajectory of a fluid element at the water surface. Such fluid element will move with velocity  $\dot{\mathbf{x}}_L(t|\mathbf{x}) = \mathbf{u}_L(t|\mathbf{x})$ . To the lowest order in the parameter  $kA$ , we can approximate

$$\mathbf{x}_L \simeq \mathbf{x} - A \begin{pmatrix} \cos(\alpha_0 + kx_1 - \omega t) \\ \sin(\alpha_0 + kx_1 - \omega t) \end{pmatrix}, \quad (8.32)$$

where  $A = k|\Phi_0(0)|/\omega$  and  $\alpha_0$  is the initial phase of  $\Phi_0$ . The fluid element moves along a circular trajectory.

Let us evaluate the next order in the expansion

$$\begin{aligned} u_{L,1}^{(2)} &= (\mathbf{x}_L(t|\mathbf{x}) - \mathbf{x}) \cdot \nabla u_1(\mathbf{x}, t) \\ &= \frac{A}{\omega} (\mathbf{x}_L(t|\mathbf{x}) - \mathbf{x}) \cdot \nabla [e^{kx_3} \sin(\alpha_0 + kx_1 - \omega t)]. \end{aligned}$$

We find from Eq. (8.32), the drift velocity at the water surface,

$$u_{L,1}^{(2)} = \frac{kA^2}{\omega} [\sin^2(\alpha_0 + kx_1 - \omega t) + \cos^2(\alpha_0 + kx_1 - \omega t)] = (kA)^2 c_w. \quad (8.33)$$

We see that the fluid motion at the water surface has an  $O((kA)^2)$  drift component, which can generate transport in the direction of the wave.

### 8.3.1 Viscous corrections

Working in a potential flow framework guarantees that continuity of the normal stress at the water surface, Eq. (8.24), suffices as a boundary condition for the problem. Finite viscosity requires us to impose continuity of the tangential stress as well. We verify that the result is of a boundary layer of thickness so minuscule that its effect on the wave dynamics is, in most circumstances, negligible.

Since  $\mu_{air} \sim 0.015\mu_{water}$ , we can the tangential stress at the water surface equal to zero. Continuity of the tangential stress

$$\partial_3 u_1 = \partial_3 (u_1^{vort} + \partial_1 \Phi) = 0 \Rightarrow \quad (8.34)$$

then yields the boundary condition for the vorticity  $\hat{\omega}$  at the water surface

$$\hat{\omega} \simeq -\partial_3 \partial_1 \Phi. \quad (8.35)$$

We can obtain an equation for the vorticity by taking the curl of the Navier-Stokes equation. In the case of linear waves, we can disregard the advection term, and we obtain the diffusion equation

$$\partial_t \hat{\omega} = \nu \nabla^2 \hat{\omega}. \quad (8.36)$$

The viscous boundary layer at the water surface has therefore thickness

$$l \sim \sqrt{\nu/\omega}, \quad (8.37)$$

which, for frequencies of the order of 1 Hz or smaller, is well below the millimeter scale.

We can estimate the damping rate  $\Gamma$  of the wave as the ratio of the dissipation per unit surface

$$\dot{E} \sim -\mu \int dx_3 \hat{\omega}^2 \sim \mu l |\Phi k^2|^2 \quad (8.38)$$

and the energy per unit surface of the wave

$$E \sim \rho \int dx_3 |\nabla \Phi|^2 \sim \rho |\Phi|^2 k, \quad (8.39)$$

where we have exploited Eq. (8.23). We find

$$\frac{\Gamma}{\omega} = \frac{\dot{E}}{\omega E} \sim \frac{\nu l k^3}{\omega} \sim \frac{\nu^{3/2} \omega^{9/2}}{g^3}, \quad (8.40)$$

where use has been made of Eq. (8.31). In order for the ratio  $\Gamma/\omega$  to become  $O(1)$ , it would be necessary to consider wavelengths at the millimeter scale, where surface tension becomes significant and capillary waves take the place of gravity waves.

## 8.4 Suggested reading

- L.D. Landau and E.M. Lifshitz, “Fluid mechanics” Vol. 6, Secs. 9, 11 and 12. (Pergamon Press 1987)
- P. Kundu, “Fluid Mechanics”, Secs. 5.1-3 (Ac. Press 2015)

## 9 Vorticity dynamics

We can obtain an evolution equation for the vorticity  $\boldsymbol{\omega} = \nabla \times \mathbf{u}$  by taking the curl of the Navier-Stokes equation (5.2) and exploiting the identity from vector analysis  $\nabla u^2/2 = \mathbf{u} \times (\nabla \times \mathbf{u}) + \mathbf{u} \cdot \nabla \mathbf{u}$ . The result is

$$D_t \boldsymbol{\omega} - \boldsymbol{\omega} \cdot \nabla \mathbf{u} \equiv (\partial_t + \mathcal{L}_{\mathbf{u}}) \boldsymbol{\omega} = -\nabla \times \frac{\nabla P}{\rho} + \nu \nabla^2 \boldsymbol{\omega} + \nabla \times (\mathbf{f}^{ext}/\rho), \quad (9.1)$$

where  $\mathcal{L}_{\mathbf{u}} \boldsymbol{\omega}$  is the Lie derivative defined in Eq. (2.17). We see that if the three conditions that viscosity is negligible, the fluid is barotropic, and the external force per unit mass is curl-free are all satisfied, vorticity will behave as a frozen vector field.

This remarkable property has a geometrical origin, which is best understood by looking at the behavior of the flow lines of the vorticity field (the vortex lines). We note that since  $\boldsymbol{\omega}$  is by construction divergence-free, the vortex lines must either close on themselves or terminate at the boundaries of the fluid.

We can define the vortex tube generated by a certain closed contour  $\Gamma$  as the set of the vortex lines girded by  $\Gamma$  (see Fig. 17). The vorticity flux through any surface  $A$  bounded by  $\Gamma$  has the same value

$$\varphi_\Gamma = \int_A d\mathbf{A} \cdot \boldsymbol{\omega} = \int_\Gamma d\mathbf{l} \cdot \mathbf{u}, \quad (9.2)$$

which defines the strength of the vortex tube.

We can verify that  $\varphi_\Gamma$  does not depend on the choice of the contour  $\Gamma$ . Consider the portion  $V$  of the vortex tube in Fig. 17. From vorticity being a zero-divergence field, we have indeed

$$0 = \int_V dV \nabla \cdot \boldsymbol{\omega} = \int_{\partial V} d\mathbf{A} \cdot \boldsymbol{\omega} = \int_{A'} d\mathbf{A}' \cdot \boldsymbol{\omega} - \int_A d\mathbf{A} \cdot \boldsymbol{\omega} = \varphi_{\Gamma'} - \varphi_\Gamma, \quad (9.3)$$

where we have exploited the fact that  $\boldsymbol{\omega}$  is by construction parallel to the surface of the vortex tube.

### 9.1 Kelvin's theorem

If the flow is time-dependent, the geometry of vortex lines and vortex tubes will not remain constant. However, if the flow is inviscid and barotropic, and the external force is derived from a potential,  $\mathbf{f}^{ext}/\rho = -\nabla\Psi$ , the strength  $\varphi_\Gamma$  of vortex tubes is conserved. The statement is equivalent to that of Kelvin's theorem, that if the above conditions are satisfied, the velocity circulation along a contour  $\Gamma_L(t)$  moving with the fluid is a constant of the motion,

$$\varphi_{\Gamma_L} = \int_{\Gamma_L} d\mathbf{l} \cdot \mathbf{u} = \text{constant}. \quad (9.4)$$

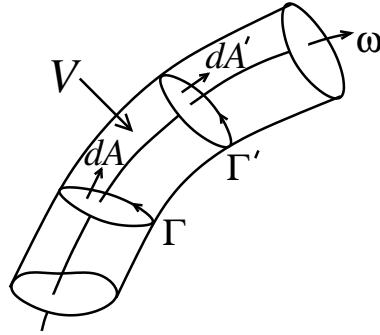


Figure 17: Representation of a vortex tube.

Let us prove the result. The circulation of  $\mathbf{u}$  along a path  $\Gamma$ , which coincides with the strength of the vortex tube encircled by  $\Gamma$ , can be written in the form

$$\varphi_{\Gamma_L}(t) = \sum_{\Gamma} \delta \mathbf{l}_L(t) \cdot \mathbf{u}_L(t), \quad (9.5)$$

where the  $\delta \mathbf{l}_L$  are infinitesimal elements of  $\Gamma_L$ . Differentiating in time Eq. (9.5) gives us

$$\begin{aligned} \dot{\varphi}_{\Gamma_L} &= \sum_{\Gamma} \mathbf{u}_L \cdot \frac{d\delta \mathbf{l}_L}{dt} + \sum_{\Gamma} \delta \mathbf{l}_L \dot{\mathbf{u}}_L \\ &= \sum_{\Gamma} \mathbf{u}_L \cdot \delta \mathbf{u}_L + \int_{\Gamma} \dot{\mathbf{u}}_L \cdot d\mathbf{l}. \end{aligned} \quad (9.6)$$

We can exploit Eq. (7.21) to cast Euler's equation (8.1) in the form

$$\dot{\mathbf{u}}_L = D_t \mathbf{u} = -\nabla(w - \Psi). \quad (9.7)$$

The last term in Eq. (9.6) then becomes

$$\int_{\Gamma} \dot{\mathbf{u}}_L \cdot d\mathbf{l} = - \int_{\Gamma} d\mathbf{l} \cdot \nabla(w + \Psi) = 0, \quad (9.8)$$

as for the other term in the last line of Eq. (9.6),

$$\sum_{\Gamma} \mathbf{u}_L \cdot \delta \mathbf{u}_L = \frac{1}{2} \sum_{\Gamma} \delta u_L^2 = 0, \quad (9.9)$$

which is a consequence of the fact that  $\Gamma$  is a closed curve, and the variation of  $u_L^2$  around it is zero. We thus conclude

$$\varphi_{\Gamma_L} = \text{constant}. \quad (9.10)$$

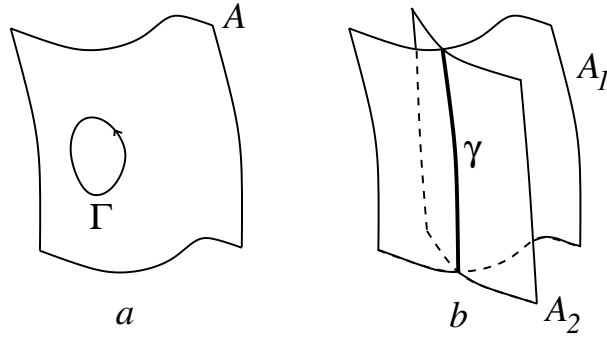


Figure 18: Representation of vortex sheets  $A$ ,  $A_1$  and  $A_2$  and of the vortex line  $\gamma$  intersection of the two vortex sheets  $A_1$  and  $A_2$ .

A consequence of Kelvin's theorem is that vortex sheets, and therefore also vortex lines are frozen in the flow. We illustrate the situation in in Fig. 18a. Suppose  $A$  is initially a vortex sheet, such as, e.g., the boundary of a vortex tube. Then, by construction, the vorticity flux  $\Phi_\Gamma$  across any contour  $\Gamma$  on  $A$  is zero. As time passes, the points on  $A$  (and on  $\Gamma$ ) are transported by the flow. By Kelvin's theorem, however, the flux  $\Phi_{\Gamma_L}$  remains equal to zero. Since  $\Gamma$  is arbitrary,  $A_L$  remains a vortex sheet.

We can verify that also vorticity lines are transported by the flow. Consider the intersection  $\gamma$  of two vortex sheets  $S_1$  and  $S_2$  shown in Fig. 18. Vortex lines passing through points on  $\gamma$  are by construction simultaneously vortex lines of  $S_1$  and  $S_2$ . However, the only line lying simultaneously in  $S_1$  and  $S_2$  is  $\gamma$ , which is therefore a vortex line.

The fact that vortex lines are frozen in the flow has important consequences on their topological properties. Since the strength of a vortex tube is constant along the tube and is conserved by the flow (if the latter is inviscid and barotropic), such a tube cannot be torn apart by the flow. Hence, it must preserve its topology: a knotted tube cannot unknot, and vice versa if it is initially unknotted.

Another consequence of vortex lines transport by the flow is the phenomenon of vortex stretching. Due to the chaotic nature of most 3D flows, the separation of fluid elements will grow exponentially with time. Points along a vortex line will undergo the same process, and the length of the vortex tube will grow exponentially with time. Now, unless the fluid is simultaneously undergoing an exponential expansion, the stretching process must be compensated by a simultaneous reduction in the section of the tubes, and since by Kelvin's theorem the strength of the tube remains constant, the vorticity in the tube must grow exponentially.

We can define the Reynolds number of a vortex tube of strength  $\varphi$  from Eq. (9.2). The equation gives us the velocity scale  $U \sim \varphi/R$ , where  $R$  is the instantaneous radius of the vortex tube. From here we we get the Reynolds number of the vortex

tube

$$\text{Re} \sim \frac{UR}{\nu} \sim \frac{\varphi}{\nu} = \text{constant}. \quad (9.11)$$

The fact that the Reynolds number remains finite would suggest that vortex stretching could continue forever without viscosity setting in and causing the breakup of the vortex tube. The statement, however, is incorrect, because as the vortex tube stretches, it densely fills the volume at its disposal, thus increasing the possibility of parts of the tube approaching other parts of that or other vortex tubes. Typically, during their interaction, the vortices roll on one another, which leads to the formation of vortex sheets where the Reynolds number becomes small. In the end, the process leads to the breakup of the flow topology and eventually to the destruction of the vortex structure.

Vortex stretching and the associated vorticity growth reflect the fact that the vorticity field is a frozen vector field whose transport properties are described by the Lie derivative defined in Eq. (9.1). Vortex stretching in the expression

$$\mathcal{L}_{\mathbf{u}}\boldsymbol{\omega} = \mathbf{u} \cdot \nabla\boldsymbol{\omega} - \boldsymbol{\omega} \cdot \nabla\mathbf{u},$$

is accounted for by the term  $-\boldsymbol{\omega} \cdot \nabla\mathbf{u}$ , while  $\mathbf{u} \cdot \nabla\boldsymbol{\omega}$  takes care of advection. In a reference frame moving locally with the fluid, we would have in fact

$$\dot{\boldsymbol{\omega}}_L = \boldsymbol{\omega} \cdot \nabla\mathbf{u}.$$

The situation is particularly transparent when  $\boldsymbol{\omega}$  and  $\mathbf{u}$  are parallel, in which case the growth of  $\boldsymbol{\omega}$  is precisely the local expansion rate of the flow.

## 9.2 Helicity conservation

The fact that the knottedness of the vortex lines in an inviscid and barotropic flow is conserved leads to the conservation of a quantity called helicity. Let us focus for simplicity on the case of an infinite fluid in which the vortex lines close on themselves. We can parameterize the knottedness of two vortex tubes  $\gamma_1$  and  $\gamma_2$  by the winding number  $\alpha_{1,2}$ , as illustrated in Fig. 19. Note that  $\alpha_{1,2} = \alpha_{2,1}$ . The helicity of the two vortex tubes is defined as

$$I_{1,2} = I_{2,1} = \alpha_{1,2}\varphi_1\varphi_2. \quad (9.12)$$

In particle physics, helicity is the spin projection onto the direction of the moment. The physical interpretation of helicity in the present fluid dynamics context is similar. Let us focus on vortex tube  $\gamma_1$  and exploit Eq. (9.2) to express both  $\varphi_1$  and  $\varphi_2$  as integrals over  $\gamma_1$ : over the section  $S_1$  in the case of  $\varphi_1$ ; over the contour  $\gamma_1$  in the case of  $\varphi_2$ :

$$\varphi_1 = \int_{A_1} d\mathbf{A} \cdot \boldsymbol{\omega}, \quad \varphi_2 = \int_{\gamma_1} d\mathbf{l} \cdot \mathbf{u}, \quad (9.13)$$

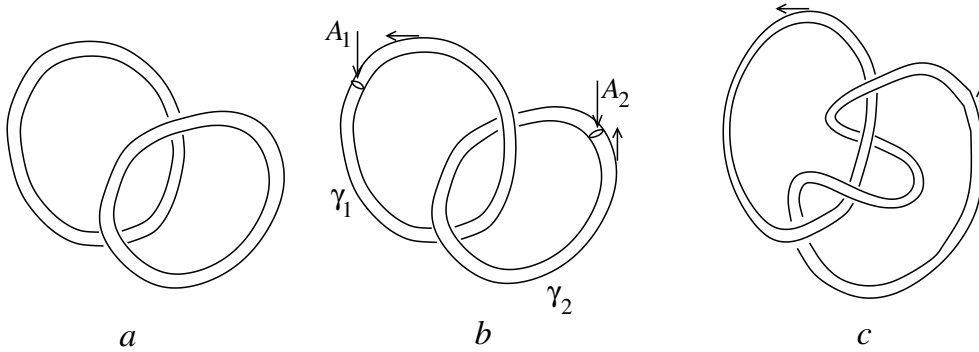


Figure 19: Degree of knottedness of vortex lines as a function of the winding number  $\alpha$ . Arrows along the tubes indicate the orientations of  $\boldsymbol{\omega}$ . Case *a*:  $\alpha = 0$ ; case *b*:  $\alpha = 1$ ; case *c*:  $\alpha = -2$ . Note that the winding number depends on the relative orientation of the vortex lines.

where, by construction,  $\boldsymbol{\omega}$  is parallel to both  $d\mathbf{A}$  and  $d\mathbf{l}$  and  $\boldsymbol{\omega} \cdot d\mathbf{l} > 0$  and  $\boldsymbol{\omega} \cdot d\mathbf{A} > 0$ . We find

$$I_{1,2} = \alpha_{1,2} \int_{A_1} d\mathbf{A} \cdot \boldsymbol{\omega} \int_{\gamma_1} d\mathbf{l} \cdot \mathbf{u} = \alpha_{1,2} \int_{V_1} d\mathbf{A} \cdot d\mathbf{l} \mathbf{u} \cdot \boldsymbol{\omega} = \alpha_{1,2} \int_{V_1} dV \mathbf{u} \cdot \boldsymbol{\omega}. \quad (9.14)$$

Since  $\varphi_1$ ,  $\varphi_2$  and  $\alpha_{1,2} = \alpha_{2,1}$  are simultaneously conserved in an inviscid fluid, the helicity of the two vortex tubes remains constant.

In the presence of more than two vortex tubes, the helicity of vortex tube  $\gamma_1$  will be

$$I_1 = \sum_{j \neq 1} I_{1,j}, \quad (9.15)$$

leading to the total helicity in the fluid

$$I = \sum_{i \neq j} I_{i,j}. \quad (9.16)$$

We can now carry out a continuum limit. We get

$$I = \int dV \mathbf{u} \cdot \boldsymbol{\omega}. \quad (9.17)$$

The velocity lines of a flow with non-zero helicity are locally helicoidal, which explains the name helicity for  $I$ .

Helicity in an inviscid fluid is a globally conserved quantity,

$$\dot{I} = 0, \quad (9.18)$$

an ideal fluid is therefore characterized by the presence of two quadratic invariants, total energy and total helicity. It turns out that helicity is also conserved in volumes

$V_L$  transported by the flow, provided  $\boldsymbol{\omega}$  is locally tangent to the boundary of  $V_L$ , which means that vortex lines neither enter nor exit  $V_L$ . We can easily verify that vortex lines lying on the surface of a vortex tube, stay on that surface. Indeed, if  $d\mathbf{A}$  is an element of  $\partial V_L$  with  $d\mathbf{A} \cdot \boldsymbol{\omega}|_{t=0} = 0$ , by Kelvin's theorem,  $d\mathbf{A} \cdot \boldsymbol{\omega}|_{t>0} = 0$  as well, and vortex lines in  $V_L$  at  $t = 0$  will remain in  $V_L$  afterward. The argument leading to helicity conservation for the vortex tubes in Eq. (9.14), thus applies to the vorticity in a volume transported by the flow, and we obtain the local conservation law

$$\dot{I}_{V_L} = 0, \quad \boldsymbol{\omega} \cdot d\mathbf{A} = 0, \quad d\mathbf{A} \in \partial V_L. \quad (9.19)$$

Note that since we cannot send  $V_L$  to zero, the helicity density  $\mathbf{u} \cdot \boldsymbol{\omega}$  is not a frozen field and therefore  $D_t(\mathbf{u} \cdot \boldsymbol{\omega}) \neq 0$ .

### 9.3 Two-dimensional flows

The vorticity dynamics of 2D flows, such as those in the atmosphere at scales much larger than the height of the troposphere, is qualitatively different from 3D. The crucial aspect is that, contrary to the 3D case, vorticity in two dimensions is by construction perpendicular to the velocity field. Thus, the vortex-stretching term  $\boldsymbol{\omega} \cdot \nabla \mathbf{u}$  is absent in the vorticity evolution equation (9.1), and the topological constraints on the structure of vortex tubes disappear. The property is reflected in the fact that the helicity of 2D flows is by construction equal to zero.

Equation (9.1) takes the form in two dimensions

$$D_t \boldsymbol{\omega} = -\nabla \times \frac{\nabla P}{\rho} + \nu \nabla^2 \boldsymbol{\omega} + \nabla \times (\mathbf{f}^{ext}/\rho), \quad (9.20)$$

where  $\boldsymbol{\omega}$  and the curls to RHS of the equation are perpendicular to the plane of the flow. If the flow is inviscid and barotropic and the external force per unit mass is curl-free,  $\boldsymbol{\omega}$  will behave like a frozen scalar,

$$D_t \omega = 0. \quad (9.21)$$

Equation (9.21) implies that the flow has a new infinite set of global invariants, namely, the integral of any function of the vorticity weighed on the fluid density is a constant of the motion,

$$I_F = \int d^2x \rho(\mathbf{x}, t) F(\omega(\mathbf{x}, t)) = \text{constant}. \quad (9.22)$$

We have indeed

$$\begin{aligned}
\dot{I}_F &= \int d^2x \left[ F \partial_t \rho + \rho F' \partial_t \omega \right] \\
&= - \int d^2x \left[ F \nabla \cdot (\rho \mathbf{u}) + \rho F' \mathbf{u} \cdot \nabla \omega \right] \\
&= - \int d^2x \left[ F \nabla \cdot (\rho \mathbf{u}) + \rho \mathbf{u} \cdot \nabla F \right] \\
&= - \int d^2x \nabla \cdot (\rho F \mathbf{u}) = 0,
\end{aligned} \tag{9.23}$$

and the property is shared by any frozen scalar, e.g., temperature, in the absence of diffusion. The quantities  $I_F$  are not conserved if the viscosity is non-zero.

The following quadratic invariant is called enstrophy, In particular we can easily derive an equation for the viscous dissipation of the quadratic invariant called enstrophy

$$\mathcal{E} = \frac{1}{2} \int d^2x \rho \omega^2. \tag{9.24}$$

We have

$$\dot{\mathcal{E}} = - \int d^2x \mu |\nabla \omega|^2. \tag{9.25}$$

We note that, contrary to helicity, enstrophy is the integral of a positive quantity, which means that enstrophy conservation cannot be satisfied by balancing contributions with different signs in the integral in Eq. (9.24). The property makes the global constraint on enstrophy more severe than the one on helicity. We shall return to the point when discussing 2D turbulence.

## 9.4 Invariance under relabeling

Conserved quantities in conservative systems are associated with the existence of symmetries, which is the content of Noether's theorem. Inviscid fluids make no exception, and we are going to show that Kelvin's theorem and the conservation laws associated with it stem from the invariance of the dynamics under relabeling of the fluid trajectories.

An inviscid fluid is essentially an ensemble of fluid elements moving under the action of pressure and external forces. The role of the variables  $q_i(t)$  in the Lagrangian of a mechanical system is taken by the Lagrangian coordinates of the fluid elements  $\mathbf{x}_L(t|\mathbf{x}_0, t_0)$ , in which the continuous label  $\mathbf{x}_0$  takes the place of the discrete index  $i$ . It is convenient to carry out the present analysis in a generic compressible case; we thus choose to deform the coordinates  $\mathbf{x}_0$  associated with the initial conditions for  $\mathbf{x}_L$ , into new coordinates  $\mathbf{y}$  such that

$$\rho(\mathbf{x}_0, t_0) d^3x_0 = d^3y = dM \tag{9.26}$$

is the fluid element mass. We can then write the density at time  $t$  in terms of the Jacobian  $J(\mathbf{y}, t)$  of the transformation  $\mathbf{y} \rightarrow \mathbf{x}_L$ ,

$$\rho(\mathbf{x}_L, t) = \left\| \frac{\partial \mathbf{x}_L}{\partial \mathbf{y}} \right\|^{-1} := J(\mathbf{y}, t). \quad (9.27)$$

The total energy of a fluid element is the sum of its kinetic energy and a potential energy term that one can identify with the volume integral of the internal energy  $\mathcal{E}$ . For simplicity, assume zero external forces and barotropic conditions,

$$\mathcal{E} = c_V P(\rho). \quad (9.28)$$

The action of the fluid takes then the form

$$\mathcal{A} = \int dt L[u_L, P; t] = \int dt \int d^3 y \left[ \frac{1}{2} u_L^2(\mathbf{y}, t) - c_V P(J(\mathbf{y}, t)) \right]. \quad (9.29)$$

A simple example of relabeling is the shift  $\mathbf{y} \rightarrow \mathbf{y}' = \mathbf{y} + \delta \mathbf{y}(\mathbf{y})$ . We require that the shift  $\mathbf{y} \rightarrow \mathbf{y}'$  still satisfies Eq. (9.26),  $d^3 y = d^3 y' = dM$ , in such a way that

$$\nabla_y \cdot \delta \mathbf{y} = 0 \Rightarrow \delta J = 0. \quad (9.30)$$

Equation (9.30) and the condition that the flow is barotropic imply that the pointwise variation of  $P$  in the shift  $\mathbf{y} \rightarrow \mathbf{y}'$  is zero. As regards the Lagrangian velocity  $\mathbf{u}_L$ , we have the change of variable

$$\mathbf{u}_L(\mathbf{y}, t) = \mathbf{u}'_L(\mathbf{y}', t) = \mathbf{u}_L(\mathbf{y}', t) + \delta \mathbf{u}(\mathbf{y}', t). \quad (9.31)$$

Invariance under relabeling of the action then takes the form

$$\delta \mathcal{A} = \frac{1}{2} \int dt \int d^3 y \delta u_L^2(t|\mathbf{y}, t_0) = \int dt \int d^3 y \mathbf{u}_L \cdot \delta \mathbf{u}_L = 0. \quad (9.32)$$

Indicate with  $\mathbf{y}_L(\mathbf{x}, t) \equiv \mathbf{y}_L(t_0|\mathbf{x}, t)$  the inverse of the mapping  $\mathbf{y} \rightarrow \mathbf{x}_L$  and define the velocity in  $\mathbf{y}$ -space

$$\mathbf{v}(\mathbf{y}, t) = \lim_{\delta t \rightarrow 0} \frac{\mathbf{y}_L(\mathbf{x}_L(\mathbf{y}, t), t) - \mathbf{y}_L(\mathbf{x}_L(\mathbf{y}, t), t - \delta t)}{\delta t}. \quad (9.33)$$

We can then evaluate the variation  $\delta \mathbf{u}_L(\mathbf{y}, t_0)$  at the current position  $\mathbf{x}_L$ , following the construction in Fig. 20,

$$\begin{aligned} \mathbf{u}_L(t|\mathbf{y}_a, t_0) &= \lim_{\delta t \rightarrow 0} \frac{\mathbf{x}_L(t|\mathbf{y}_a, t_0) - \mathbf{x}_L(t - \delta t|\mathbf{y}_a, t_0)}{\delta t} \\ &= \lim_{\delta t \rightarrow 0} \frac{\mathbf{x}_L(t|\mathbf{y}_a, t_0) - \mathbf{x}_L(t|\mathbf{y}_b, t_0)}{\delta t} \\ &= \lim_{\delta t \rightarrow 0} \frac{\mathbf{x}_L(t|\mathbf{y}_L(\mathbf{x}_c, t - \delta t), t_0) - \mathbf{x}_L(t|\mathbf{y}_L(\mathbf{x}_c, t), t_0)}{\delta t} \\ &= -\mathbf{v}(\mathbf{y}, t) \cdot \nabla_y \mathbf{x}_L(t|\mathbf{y}, t_0). \end{aligned} \quad (9.34)$$

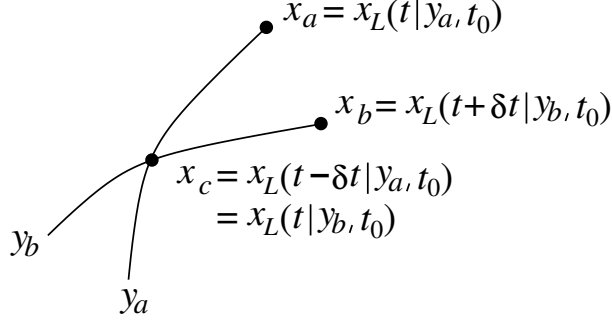


Figure 20: Lagrangian trajectories and their relative labels  $\mathbf{y}_a$  and  $\mathbf{y}_b$ .

The variation of  $\mathbf{u}_L(t|\mathbf{y}, t_0)$  then reads

$$\begin{aligned} \delta \mathbf{u}_L &= -\delta \mathbf{v}_L \cdot [\nabla_y \mathbf{x}_L + \delta \mathbf{y} \cdot \nabla_y \nabla_y \mathbf{x}_L] \\ &= -\delta \mathbf{v}_L \cdot \nabla_y \mathbf{x}_L + \delta \mathbf{y} \cdot \nabla_y \mathbf{u}_L, \end{aligned} \quad (9.35)$$

where to go to the second line of the equation, we have exploited Eqs. (9.34) and (9.30). We can substitute Eq. (9.35) into Eq. (9.32), and get

$$\begin{aligned} \delta \mathcal{A} &= \int dt \int d^3 y \left\{ -\mathbf{u}_L \cdot [\delta \mathbf{v} \cdot \nabla_y \mathbf{x}_L] + \frac{1}{2} \delta \mathbf{y} \cdot \nabla_y u_L^2 \right\} \\ &= - \int dt \int d^3 y \mathbf{A} \cdot \delta \mathbf{v}, \end{aligned} \quad (9.36)$$

where we have defined

$$\mathbf{A} = u_{L_i} \nabla_y x_{L_i}, \quad (9.37)$$

and to proceed to the second line of the Eq. (9.36), we have integrated by parts with respect to  $y$  the term  $\delta \mathbf{y} \cdot \nabla_y u_L^2$ , and then exploited Eq. (9.30). We next integrate by part with respect to  $t$  and we get

$$\delta \mathcal{A} = \int_{t_i}^{t_f} dt \int d^3 y \delta \mathbf{y} \cdot \partial_t \mathbf{A}. \quad (9.38)$$

The volume preservation condition in Eq. (9.30) implies that  $\delta \mathbf{y}$  is the curl of some vector field  $\mathbf{T}$ :

$$\delta \mathbf{y}(\mathbf{y}, t) = \nabla_y \times \mathbf{T}(\mathbf{y}, t). \quad (9.39)$$

Substituting Eq. (9.39) into Eq. (9.38) and integrating by parts with respect to  $y$  yields then the final expression

$$\delta \mathcal{A} = \int_{t_i}^{t_f} dt \int d^3 y \mathbf{T} \cdot \partial_t [\nabla_y \times \mathbf{A}]. \quad (9.40)$$

The remaining steps are straightforward. Invariance under relabeling means that the variation of  $\mathcal{A}$  with respect to  $\delta\mathbf{y}$  is zero. Since  $\mathbf{T}$  is arbitrary,  $\partial_t[\nabla_y \times \mathbf{A}] = 0$ , which implies that the circulation of  $\mathbf{A}$  around an arbitrary path  $\Gamma_y$  in  $\mathbf{y}$ -space is constant:

$$\int_{\Gamma_y} d\mathbf{y} \cdot \mathbf{A} = \text{constant}. \quad (9.41)$$

However, from Eq. (9.37),  $\mathbf{A} \cdot d\mathbf{y} = \mathbf{u}_L \cdot d\mathbf{x}$ . From Eq. (9.40) we thus recover the statement in Kelvin's theorem

$$\int_{\Gamma_L} d\mathbf{l} \cdot \mathbf{u} = \text{constant}. \quad (9.42)$$

## 9.5 Suggested reading

- J. Pedlosky, "Geophysical fluid mechanics", Chap. 7, (Springer 1987)
- R. Salmon, "Hamiltonian fluid mechanics", Annu. Rev. Fluid Mech. pp. 225 vol 20 (1988)

## 10 Compressible flows

We know how to compress a fluid by external means (say a piston in a cylinder). We know (and shall discuss extensively in the next section) that sound waves are essentially small-amplitude compression waves. We want to understand under what conditions a flow could generate the large pressure fluctuations associated with a large compression events in the fluid.

We can obtain an estimate of the ratio  $\tilde{P}/\bar{P}$  directly from the Navier-Stokes equation (5.2). Since our focus is on flow-induced compression, we neglect the term  $\mathbf{f}^{ext}$  in the equation. We obtain the estimate in terms of the characteristic length and velocity scale of the flow,  $L$  and  $U$ ,

$$\tilde{P} \sim \rho \max(U^2, \nu U/L). \quad (10.1)$$

In the case of an ideal gas, the law of state Eq. (4.8) would give us

$$\frac{\tilde{P}}{\bar{P}} \sim \frac{\max(U^2, \nu U/L)}{v_{th}^2} = \text{Ma}^2 \max(1, \text{Re}^{-1}), \quad (10.2)$$

where

$$\text{Ma} = \frac{U}{c_s} \sim \frac{U}{v_{th}}, \quad (10.3)$$

is called the Mach number, and  $c_s$  is the sound speed. By combining Eq. (10.3) with Eqs. (4.3) and (4.11), we obtain the following interesting expression connecting the Mach number with the Reynolds number and the Knudsen number,

$$\text{Re Kn} \sim \text{Ma}. \quad (10.4)$$

Substituting Eq. (10.4) into Eq. (10.2) we find

$$\frac{\tilde{P}}{\bar{P}} \sim \text{Kn}^2 \text{Re} \max(\text{Re}, 1)$$

Since by definition, in the case of a fluid,  $\text{Kn} \ll 1$ , large pressure fluctuation will only be possible for high Reynolds numbers.

We note that large density and pressure fluctuations imply large temperature fluctuations. Indeed, we can estimate from the heat transport equation (7.18),

$$D_t T \sim \frac{1}{c_V} T \nabla \cdot \rho \Rightarrow \frac{\tilde{\rho}}{\bar{\rho}} \sim \frac{\tilde{T}}{\bar{T}}. \quad (10.5)$$

Hypersonic flows can thus generate temperature perturbations much larger than the ambient temperature, which is of course relevant hypersonic aircraft design.

## 10.1 Sound waves

We can use conservation laws Eqs. (3.2), (5.2) and (7.18), together with the law of state Eq. (4.8), to obtain the dispersion relation for sound waves in a gas.

Decompose the density, pressure, and temperature into their equilibrium and fluctuation components,

$$\rho = \bar{\rho} + \tilde{\rho}, \quad T = \bar{T} + \tilde{T}, \quad P = \bar{P} + \tilde{P}. \quad (10.6)$$

We look for longitudinal waves. The problem is therefore unidimensional and we can drop indices on vectorial quantities. We make the ansatz (to be verified afterward) that viscous forces and heat transport are negligible, and assume small amplitude waves. Equations (3.2) and (5.2) then read

$$\partial_t \tilde{n} + \bar{n} \partial_x u = 0, \quad (10.7)$$

$$\bar{\rho} \partial_t \tilde{u} + \partial_x \tilde{P} = 0. \quad (10.8)$$

We next use the law of state  $P = (k_B/m)\rho T$  to write Eq. (7.34) in terms of pressure and density

$$dP = \frac{c_P P}{c_V \rho} d\rho \Rightarrow \tilde{P} = \frac{c_P k_B \bar{T}}{c_V m} \tilde{\rho}, \quad (10.9)$$

where  $c_P = 1 + c_V$  is the specific heat per molecule at constant pressure.

Solution of Eqs (10.7-10.9) yields d'Alambert's equation

$$(\partial_t^2 - c_s^2 \partial_x^2) \tilde{P} = 0, \quad (10.10)$$

where

$$c_s = \sqrt{\frac{dP}{d\rho}} = \sqrt{\frac{c_P k_B \bar{T}}{c_V m}} \sim v_{th} \quad (10.11)$$

(remember that  $P = P(\rho)$  for isentropic flows) is the sound propagation speed.

### 10.1.1 Nonlinear and non-ideal effects

The solution of Eq. (10.10) are sinusoidal waves  $\propto \exp(k(x - c_s t))$ . We evaluate the magnitude of the nonlinearity correction in the Navier-Stokes equation as

$$\frac{u \partial_x u}{\partial_t u} \sim \frac{k u^2}{\omega u} = \frac{u}{c_s} \sim \frac{u}{v_{th}}. \quad (10.12)$$

Nonlinear advection is important for  $u \sim v_{th}$ , in which case, from (10.7) and (10.8),  $\tilde{P} \sim \bar{P}$  and  $\tilde{\rho} \sim \bar{\rho}$ . Cavitation phenomena, in which  $\rho = 0$  in the troughs of the wave, thus become possible for large-amplitude waves.

Let us determine next the magnitude of the viscous correction. We find from Eq. (5.2)

$$\frac{\nu \partial_x^2 u}{\partial_t u} \sim \frac{\nu k^2}{\omega} = \frac{\nu \omega}{c_s^2}. \quad (10.13)$$

For  $\nu \simeq 0.15 \text{ cm}^2/\text{s}$  and  $c_s \simeq 340 \text{ m/s}$ , we find that in order for viscous effects to be important, we would need  $\omega \sim 10^8 \text{ Hz}$ , which is an astonishingly high frequency. Exceedingly high frequency would be required as well for diffusion to be so large to invalidate the adiabatic approximation in Eq. (10.9).

### 10.1.2 Dynamics of the loudspeaker

Let us determine the conditions for sound generation from a solid body oscillating with frequency  $\omega$ . The balance in Eq. (10.1) is replaced by

$$\tilde{P} \sim L\omega\bar{\rho}u \Rightarrow \frac{\tilde{\rho}}{\bar{\rho}} \sim \frac{u}{c_s^2}\omega L, \quad (10.14)$$

where  $L$  is the characteristic size of the body and where we have exploited Eq. (10.5). We see that for the compression contribution in the continuity equation (3.2) to be significant, we need

$$\frac{\tilde{\rho}}{\bar{\rho}} \sim \frac{u}{L\omega} \Rightarrow \frac{\omega L}{c_s} \sim 1, \quad (10.15)$$

which means that sound waves with frequency  $\omega$  must have a wavelength comparable with  $L$ . The compression, and therefore also the sound intensity, is smaller at frequencies  $\omega < c_s/L$  (that is why low frequencies require loudspeakers with large woofers).

## 10.2 The Burgers equation

The hypersonic limit  $\text{Ma} \gg 1$  corresponds to a regime in which the pressure  $P \sim \rho v_{th}^2$  is much smaller than the kinetic energy density  $(\rho/2)u^2$ . The zero-pressure version of the Navier-Stokes is called the Burgers equation, which, for negligible viscosity and in the absence of external forces takes a particularly simple form:

$$D_t \mathbf{u} = 0. \quad (10.16)$$

In a Burgers dynamics, fluid elements move at constant velocity along straight trajectories:

$$\mathbf{u}_L(t|\mathbf{x}_0, t_0) = \mathbf{u}(\mathbf{x}_0, t_0) \Rightarrow \mathbf{x}_L(t|\mathbf{x}_0, t_0) = \mathbf{x}_0 + \mathbf{u}(\mathbf{x}_0, t_0)(t - t_0). \quad (10.17)$$

The observation allows one to map the solution of the inviscid Burgers equation, which is a partial differential equation, to the solution of the ordinary differential

equation  $\dot{\mathbf{x}}_L = \mathbf{u}_L$ . The approach, called the method of characteristics, is common to other first-order partial differential equations, such as e.g. the Hamilton-Jacobi equation. The trajectories  $x_L$  in the case of the Burgers equation, and  $(p, q)$  in the case of the Hamilton-Jacobi equation, are called the characteristic curves.

The graph in  $(\mathbf{x}, t)$  of the characteristic curves of the Burgers equation is composed of straight lines, whose orientation is determined by the initial value of  $\mathbf{u}$ . Depending on the choice of the initial condition  $\mathbf{u}(\mathbf{x}_0, 0) = u_L(t|\mathbf{x}_0, 0)$ , the characteristic curves may intersect, and in this case the solution of the Burgers equation becomes multivalued. In one dimension, multivalued solutions occur for  $u\partial_x u < 1$ . The situation is illustrated in Fig. 21. Fluid parcels starting from the left with a high velocity eventually catch back slower fluid parcels starting from the right, and at  $t > 1 + |x_0|$  the fluid velocity becomes multivalued.

The finite-time break-up of the solutions of the inviscid Burgers equations is a consequence of the fact that there are no pressure forces preventing fluid parcels from compenetrating each other. A fluid description of the medium then ceases to be valid. Indeed, the intersecting characteristic curves describe a superposition of fluid jets, interpreted in a kinetic theory picture as a non-equilibrium velocity distribution (note that each jet is monochromatic, as the thermal velocity  $v_{th} \sim \sqrt{P/\rho} \rightarrow 0$  in the regime considered). Such a superposition of jets can only survive in a transition region whose width is of the order of the mean free-path  $\lambda$ , where the inviscid hypothesis for the Burgers equation ceases to be valid.

### 10.2.1 Viscous Burgers equation

A possibility to account for the presence of transition regions in a Burgers dynamics, is to add a viscous term to Eq. (10.16),

$$D_t u = \nu \partial_x^2 u. \quad (10.18)$$

It is important to note that the viscosity coefficient in Eq. (10.18) has nothing to do with the viscosity in the Navier-Stokes equation, as the condition that the

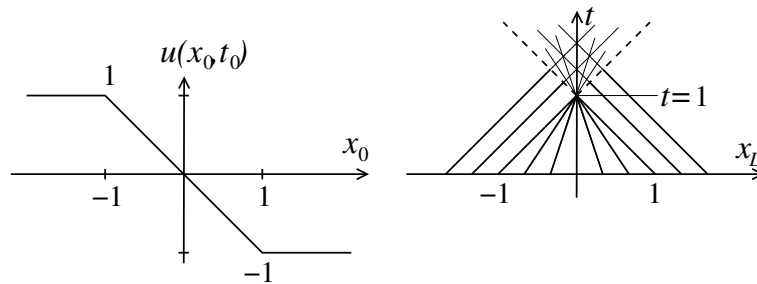


Figure 21: Characteristic lines (right) of the Burgers equation originating from a piecewise linear initial condition for  $u$  (left). The solution of the inviscid Burgers equation becomes multivalued in the space-time region above the dashed lines.

velocity differences at scale  $\lambda$  are  $\ll v_{th}$  is violated. However, we can verify that no multivalued solution are present in this case. Let us solve Eq. (10.18) with boundary conditions

$$u(\pm\infty, t) = \mp 1, \quad (10.19)$$

and initial condition as in Fig. 21. Take  $t \gg 1$  and look for stationary solutions to the problem.

Equation (10.18) reads at stationarity,

$$(1/2)\partial_x u_\nu^2 = \nu \partial_x^2 u_\nu \Rightarrow \nu \partial_x u_\nu - u_\nu^2/2 = \pm a^2, \quad (10.20)$$

where  $a$  is a constant. We solve Eq. (10.20) in the case the  $a^2$  to the RHS of the equation has a minus sign, and verify that the choice allows us to enforce the boundary conditions in Eq. (10.19) and Fig. 21. Define  $u_\nu = a\hat{u}$  and indicate derivatives with respect to  $x$  with a prime. We get

$$\frac{\hat{u}'}{\hat{u}^2 - 1} \equiv (\arctan \hat{u})' = -\frac{a}{2\nu} \Rightarrow \hat{u} = \tanh\left(b - \frac{ax}{2\nu}\right), \quad (10.21)$$

where  $b$  is another constant. The boundary condition (10.19) imposes  $a = 1$ . The initial condition in Fig. 21 requires the solution to be antisymmetric, hence  $b = 0$ . We thus obtain the result

$$u_\nu(x) = -\tanh\left(\frac{x}{2\nu}\right). \quad (10.22)$$

The limit  $\nu \rightarrow 0$  in Eq. (10.22) corresponds to a step-function solution

$$u(x) = -1 + 2\theta(x), \quad (10.23)$$

which does not coincide with the solution of Eq. (10.16) with the same boundary conditions. The limit  $\nu \rightarrow 0$  of Eq. (10.18) is thus singular and the procedure leading to Eq. (10.23) is an example of singular perturbation.

Of course, we can adapt the description to the case in which  $u(-\infty) \neq -u(+\infty)$  by a mere change of reference frame. In general we get

$$u(x) = u(-\infty) + 2U\theta(x - x_0 - Ut), \quad U = \frac{u(+\infty) - u(-\infty)}{2}, \quad (10.24)$$

where  $x_0$  is the initial position of the discontinuity.

Equation (10.24) describes a situation in which the mass of the fluid is transported to the transition region, and leads to the formation of a singularity in the mass distribution. An initially uniform mass distribution thus evolves into an ensemble of spikes, interspersed by voids, whose position and translation velocity is determined by the initial fluid velocity profile. It is easy to be convinced that in two and three dimensions, the spikes are replaced by singular mass distributions setting the boundary of two and three-dimensional voids.

### 10.2.2 The method of characteristics

A first order PDE for a field  $u = u(\mathbf{z})$  can be written in the most general form as

$$F(\mathbf{z}, u, \boldsymbol{\pi}) = 0, \quad \pi_i = \partial_{z_i} u. \quad (10.25)$$

In the case of the 1D Burgers equation,

$$F = \pi_1 + u\pi_2 = 0, \quad z_1 = t, \quad z_2 = x. \quad (10.26)$$

In the case of the Hamilton-Jacobi equation  $\dot{S} + H(\partial_q S, q, t)$ ,  $u \equiv S$  is the action and Eq. (10.25) takes the form

$$F = \pi_1 + H(\pi_2, z_2, z_1) = 0, \quad z_1 = t, \quad z_2 = q. \quad (10.27)$$

The method could be generalized to the case  $\mathbf{F}$  is a vector, and  $\mathbf{u}$  is a vector field.

The solution of Eq. (10.25) by the methods of characteristic is obtained by writing  $u = u(z_i)$  in the parametric form  $u = u(z_i(s|z_0))$ , where the  $z_i = z_i(s|z_0)$  are the characteristic curves of the equation. Suppose we have such a solution. By differentiating Eq. (10.17) along a characteristic curve, we would then obtain

$$\begin{aligned} 0 = \dot{F} &= \dot{z}_i \partial_{z_i} F + \dot{z}_i (\partial_{z_i} u) \partial_u F + \dot{\pi}_i \partial_{\pi_i} F \\ &= \dot{z}_i (\partial_{z_i} F + \pi_i \partial_u F) + \dot{\pi}_i \partial_{\pi_i} F, \end{aligned} \quad (10.28)$$

where dot indicates total derivative with respect to  $s$ . We solve Eq. (10.28) through the ansatz

$$\dot{z}_i = \lambda \partial_{\pi_i} F, \quad (10.29)$$

where  $\lambda$  is an arbitrary parameter (in general a function of  $\mathbf{z}$  and  $s$ ). By substituting Eq. (10.29) into Eq. (10.28) we get

$$\dot{\pi}_i = -\lambda (\partial_{z_i} F + \pi_i \partial_u F), \quad (10.30)$$

and by substituting Eq. (10.29) into the relation  $\dot{u} = \dot{z}_i \partial_{z_i} u = \dot{z}_i \pi_i$ ,

$$\dot{u} = \lambda \pi_i \partial_{\pi_i} F. \quad (10.31)$$

The characteristic curves are obtained by solving the system formed by Eqs. (10.29) and (10.31):

$$\dot{z}_i = \lambda \partial_{\pi_i} F, \quad \dot{u} = \lambda \pi_i \partial_{\pi_i} F, \quad (10.32)$$

in which different choices of  $\lambda$  lead to different parameterizations of the curves.

We can apply the method to the solution of the Hamilton-Jacobi equation. We verify that the choice  $\lambda = 1$ ,  $z_1 = t = s$  gives us back Hamilton's equations. From the first component of Eq. (10.29) we get the identity  $\dot{z}_1 = \partial_{\pi_1} F = 1$ , and the second component gives us

$$\dot{z}_2 \equiv \dot{q} = \partial_{\pi_2} F = \partial_p H \quad (10.33)$$

that is Hamilton's equation for  $q$ . Since  $F$  does not depend explicitly in  $S$ , Eq. (10.30) becomes  $\dot{\pi}_i = \partial_{z_i} F$ . The first component of the equation yields the identity  $\dot{S} = -\dot{H}$ , and the second component gives us Hamilton's equation for  $p$ ,

$$\dot{\pi}_2 \equiv \dot{p} = -\partial_{z_2} F = -\partial_q H. \quad (10.34)$$

### 10.3 Shock waves

Neither the inviscid Burgers equation nor the  $\nu \rightarrow 0$  limit of its viscous counterpart provide a satisfactory model of shock wave formation. The main issue in the viscous case is the unbounded growth of the mass in the shock at stationarity described by Eq. (10.23). We describe a shock as a discontinuity in the thermodynamic quantities that describe the fluid—mass, momentum, and energy—with no accumulation, which means that the flow of those quantities presents no discontinuity.

We consider the case of a normal shock, namely, an infinite planar discontinuity, which we take to be the  $x_2x_3$  plane, traveling to the left (towards smaller  $x_1$ ). We thus drop vector indices and use subscripts 1 and 2 to identify thermodynamic quantities to the left and right of the discontinuity. We expect the shock to travel at supersonic speed, which means that no perturbation can propagate to the left of the discontinuity in the quiescent fluid. Thus,  $\rho_1$  and  $P_1$  can be identified with the ambient density and pressure of the fluid, and  $-u_1$  is the speed of the shock wave; conversely,  $u_2 - u_1$  is the fluid velocity to the right of the discontinuity in the laboratory frame.

Far from the shock, the flow is uniform, and neither viscous stresses nor diffusive heat transport contribute to the dynamics. The continuity conditions for the mass, momentum, and energy flows read

$$\rho_1 u_1 = \rho_2 u_2 := J, \quad (10.35)$$

$$\rho_1 u_1^2 + P_1 = \rho_2 u_2^2 + P_2, \quad (10.36)$$

$$u_1^2/2 + w_1 = u_2^2/2 + w_2. \quad (10.37)$$

Together with an equation of state, Eqs. (10.35-10.37) allow us to determine the three thermodynamic quantities  $\rho$ ,  $u$  and  $w$  on one side of the shock from their values on the other side. However, we can obtain some information on the structure of the shock without having to solve the equations.

First, define the volume per unit mass  $v_i = \rho_i^{-1}$  and exploit Eq. (10.35) to rewrite Eq. (10.36) as

$$J^2 v_1 + P_1 = J^2 v_2 + P_2 \Rightarrow J^2 = \frac{P_2 - P_1}{v_1 - v_2}. \quad (10.38)$$

The condition  $J^2 > 0$  tells us that either  $P_2 > P_1$  and  $\rho_2 > \rho_1$  or  $P_2 < P_1$  and  $\rho_2 < \rho_1$ , but we shall verify that requiring that entropy increases in the process, selects the first option.

Next rewrite Eq. (10.37) as

$$J^2 v_1^2/2 + w_1 = J^2 v_2^2/2 + w_2, \quad (10.39)$$

and substitute in the equation the expression for  $J^2$  from Eq. (10.38). The result is

$$w_1 - w_2 + \frac{1}{2}(v_1 + v_2)(P_2 - P_1) = 0. \quad (10.40)$$

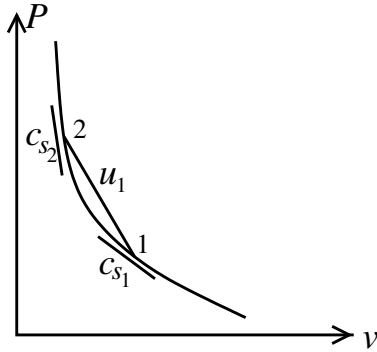


Figure 22: Rankine-Hugoniot adiabat.

Equation (10.40), called the Rankine-Hugoniot relation, allows us, given an equation of state, to determine the values of  $V$  and  $\rho$  on one side of the shock from those on the other. Values of the density and the pressure upstream of the shock determine a Rankine-Hugoniot adiabat passing through the point  $V_1, P_1$ . All points on the curve to the left of this “initial” point represent admissible values of the density and the pressure  $V_2, P_2$  downstream of the shock (see Fig. 22).

We can obtain additional information on the shock structure in the weak-shock regime. The regime corresponds to point 2 approaching the initial point 1 on the Rankine-Hugoniot adiabat. Equation (10.36) becomes in the limit, from Eq. (10.11),

$$J^2 = \rho^2 u^2 \simeq -\frac{dP}{dv} \simeq \rho^2 \frac{dP}{d\rho} = \rho^2 c_s^2, \quad (10.41)$$

where the change of entropy in going from 1 to 2 is neglected to lowest order in  $\rho_2 - \rho_1$ . We see that to lowest order in  $\rho_2 - \rho_1$ ,  $u_1 = u_2 = c_s$ , and the shock wave propagates at the speed of sound. Inspection of Fig. (22) shows actually that  $u_1 > c_s$  and  $u_2 < c_s$ : the shock is supersonic, and in the shock reference frame, the fluid goes past the discontinuity at subsonic speed  $u_2 < c_s$ . Indeed, from the fact that the chord 12 in Fig. 22 is steeper than the tangent in 1, we have

$$u_1^2 = v_1^2 J^2 > -v_1^2 \left. \frac{dP}{dv} \right|_1 = c_{s1}^2, \quad (10.42)$$

and in a similar way, from the fact that the chord 12 is less steep than the tangent in 2,

$$u_2^2 = v_2^2 J^2 < -v_2^2 \left. \frac{dP}{dv} \right|_2 = c_{s2}^2. \quad (10.43)$$

### 10.3.1 Entropy production and shock structure

We continue to focus our analysis on weak shocks for which the increments  $\delta P = P_2 - P_1$ , and therefore also  $\delta v$ ,  $\delta w$ , and  $\delta s$  can be considered small. It turns out

that we must expand Eq. (10.40) to third order in  $\delta P$  (and first order in  $\delta s$ ) to get sensible results. We rewrite Eq. (10.40) as

$$\delta w = (v + \delta v/2)\delta P, \quad (10.44)$$

and expand separately the two sides of the equation,

$$\begin{aligned} \delta w &= \frac{\partial w}{\partial s}\delta s + \frac{\partial w}{\partial P}\delta P + \frac{1}{2}\frac{\partial^2 w}{\partial P^2}(\delta P)^2 + \frac{1}{6}\frac{\partial^3 w}{\partial P^3}(\delta P)^3 \\ &= T\delta s + v\delta P + \frac{1}{2}\frac{\partial v}{\partial P}(\delta P)^2 + \frac{1}{6}\frac{\partial^2 v}{\partial P^2}(\delta P)^3, \end{aligned} \quad (10.45)$$

$$(v + \delta v/2)\delta P = \left(v + \frac{1}{2}\frac{\partial v}{\partial P}\delta P + \frac{1}{4}\frac{\partial^2 v}{\partial P^2}(\delta P)^2\right)\delta P. \quad (10.46)$$

We obtain the result

$$\delta s = \frac{1}{12T}\frac{\partial^2 v}{\partial P^2}(\delta P)^3. \quad (10.47)$$

The second derivative  $\partial_P^2 v$  is in most cases positive [that is the case for ideal gases, for which  $v(P, s) = c(s)P^{-c_v/c_p}$ ], and we confirm the hypothesis that the entropy of a fluid mass crossing the shock increases with the pressure.

Entropy production is associated with viscous dissipation within the shock. We can use Eq. (10.47) to estimate of the shock thickness  $\delta x$ . We keep considering the case of a weak shock. The total dissipation per unit mass of a fluid element crossing the shock is obtained by multiplying the viscous heat production  $\mu||\dot{\mathbf{s}}||^2 = \mu(\partial_x u)^2$  in Eq. (7.9) by the time  $\delta t \simeq \delta x/c_s$  and dividing by  $\rho$ . By equating the result with  $T\delta s$  and exploiting Eq. (10.47), we find

$$\frac{\partial^2 v}{\partial P^2}(\delta P)^3 \sim \frac{\nu\delta x}{c_s}\left(\frac{\delta u}{\delta x}\right)^2. \quad (10.48)$$

From Eqs. (10.42) and (10.43) we estimate  $\delta u \sim J\delta v \sim c_s\delta v/v \sim c_s(\delta P\partial_P v)/v$ . Substituting into Eq. (10.48), we obtain

$$\delta x \sim \frac{\nu(\partial_P v)^2 c_s}{v^2 \delta P \partial_P^2 v}. \quad (10.49)$$

The thickness of the shock diverges for  $\delta P \rightarrow 0$  (the shock ceases to be a shock). Pushing the estimate to  $\delta P \sim P$  would give, instead,

$$\delta x \sim \frac{\nu c_s}{vP} \sim \frac{\nu}{v_{th}} \sim \lambda, \quad (10.50)$$

where  $\lambda$  is the mean free path and we have exploited Eq. (4.11). We surmise that away from the weak-shock limit, the internal dynamics of the shock lies outside of the domain of fluid mechanics, and would be better described in a kinetic theory approach.

## 10.4 Suggested reading

- L.D. Landau and E.M. Lifshitz, “Fluid mechanics” Vol. 6, Secs. 10 and 82-84 (Pergamon Press 1987)

## 11 Thermal convection

Heating or cooling can lead a mass of fluid to change its volume without pressure forces contributing to the process. Buoyancy forces then enter into play, pushing the fluid element up or down depending on the density difference with the surrounding fluid. Depending on the vertical density profile of the fluid, the force on the fluid element may either go back to zero, and the motion will stop, or remain finite, and the fluid element will keep moving upward or downward—a process called convection. Convection can actually start without an external action if the vertical density profile is unstable, namely, with cold dense fluid lying on top of warm less dense fluid.

### 11.1 Stability under convection

We can apply the hydrostatic balance condition Eq. (6.1) to determine the stability properties of a stratified column of fluid. The equation takes the form

$$\partial_3 P = -g\rho, \quad (11.1)$$

Mechanical equilibrium requires  $P$  to be horizontally uniform, which implies, through Eq. (11.1) and the law of state  $P = P(\rho, T)$ , that also  $\rho$  and  $T$  are horizontally uniform. The fluid is therefore barotropic. The vertical profiles of  $P$ ,  $\rho$  and  $T$ , however, remain undetermined.

Instability occurs if the vertical displacement of a volume of air results in a density gap with the surroundings and a buoyancy lift in the direction of the displacement; conversely, the column is stable the displacement generates a buoyancy force in a direction opposite to the displacement. Instability is expected in the presence of large negative vertical temperature gradients in the column: a rising volume of hot air near the ground will find itself in regions where the air is colder and denser and will continue to rise, subjected to a positive Archimedes' forces; a volume of cold air moving downwards will find itself in hotter, lower density regions of the column and will continue to sink, subjected to a negative Archimedes' force.

Let us determine the temperature profile corresponding to marginal stability. Consider the displacement of an air parcel from height  $x_3$  to height  $x_3 + dx_3$ . Mechanical equilibrium requires that the values of the pressure in and out the parcel remain equal; the final pressure in the parcel will then be  $P_L = P(x_3 + dx_3)$ , corresponding to a variation of pressure in the displacement, from Eq. (11.1),

$$dP_L = -g\rho dx_3. \quad (11.2)$$

The displacement is supposed to take place on the time scale of the buoyancy forces, much shorter than the diffusive time scale, which means that the density and the temperature in the parcel evolve along an adiabatic. From Eq. (7.34) and the law

of state  $P = (k_B/m)\rho T$ , we get

$$dP_L = \frac{k_B\rho}{m} \left( dT_L + \frac{T_L}{\rho} d\rho_L \right) = \frac{k_B c_P}{m} dT_L, \quad (11.3)$$

where  $c_P = 1 + c_V$  is the specific heat per molecule at constant pressure. By combining Eqs. (11.3) and (11.2), we find the linear law

$$dT_L = -\frac{mg}{k_B c_P} dx_3. \quad (11.4)$$

Equation (7.34) tells us that along an adiabat the density is inversely proportional to the temperature. Thus, a situation in which  $T_L$  grows with  $x_3$  more rapidly than  $T(x_3)$  corresponds to unstable conditions.

We are thus able to conclude that marginal (neutral) stability is realized by an adiabatic temperature profile

$$\frac{dT}{dx_3} = \frac{dT_{adia}}{dx_3} = -\frac{mg}{k_B c_P}. \quad (11.5)$$

(Note that if the profile is adiabatic,  $s = \text{constant}$  and any flow in the column is automatically isentropic.) Unstable stratification corresponds to  $dT/dx_3 < dT_{adia}/dx_3$ ; stable stratification corresponds to  $dT/dx_3 > dT_{adia}/dx_3$ . In the atmosphere, isothermal conditions,  $dT/dx_3 = 0$  and so-called inversion regimes  $dT/dx_3 > 0$  are typically considered strongly stable conditions.

## 11.2 The Boussinesq approximation

We want to study convection in a range of scale  $L$  such that the variations of equilibrium quantities with height can be considered small,

$$\frac{L\partial_3\bar{\rho}}{\bar{\rho}}, \frac{L\partial_3\bar{T}}{\bar{T}} = O(\epsilon), \quad \epsilon \ll 1. \quad (11.6)$$

We use the ansatz

$$\frac{\tilde{T}}{\bar{T}} \sim \frac{\tilde{\rho}}{\bar{\rho}} \sim \epsilon, \quad (11.7)$$

and also assume that the plumes have characteristic size  $l \ll L$ , with

$$\frac{l}{L} \sim \epsilon, \quad (11.8)$$

in such a way that

$$\frac{|\nabla\tilde{\rho}|}{|\partial_3\tilde{\rho}|} \sim \frac{|\nabla\tilde{T}|}{|\partial_3\tilde{T}|} \sim 1. \quad (11.9)$$

We can estimate the magnitude of the velocity and pressure perturbation directly from the Navier-Stokes equation (5.2). At  $O(\epsilon^0)$ , of course, we get the hydrostatic balance condition  $\partial_3 \bar{P} = -g\bar{\rho}$ . To find something more interesting, we must go to  $O(\epsilon)$ ,

$$\bar{\rho} D_t \mathbf{u} + \nabla \tilde{P} = \mu[\nabla^2 \mathbf{u} + (1/3)\nabla(\nabla \cdot \mathbf{u})] - g\tilde{\rho} \mathbf{e}_3. \quad (11.10)$$

In order for convective motions to be established, the buoyancy force  $\tilde{\rho}g$  must be sufficiently strong to overcome the viscous force  $\mu\nabla^2 u$ . This leads to the dominant balance in Eq. (11.10)

$$\bar{\rho} \mathbf{u} \cdot \nabla \mathbf{u} \sim \nabla \tilde{P} \sim -g\tilde{\rho} \mathbf{e}_3 \Rightarrow U^2 \sim lg\epsilon, \quad \frac{\tilde{P}}{\bar{P}} \sim \text{Ma}^2 \sim \frac{lg\epsilon}{v_{th}^2}, \quad (11.11)$$

and the condition of negligible viscous forces is just that the Reynolds number  $\text{Re} = Ul/\nu \sim l^{3/2}(g\epsilon)^{1/2}/\nu$  is large.

We assume that the Mach number is negligible, which allows us to set, from Eq. (11.11),

$$\tilde{P}/\bar{P} = 0. \quad (11.12)$$

We thus get, from the law of state Eq. (4.8),

$$\frac{\tilde{\rho}}{\bar{\rho}} = -\frac{\tilde{T}}{\bar{T}}. \quad (11.13)$$

Substituting Eq. (11.13) into the continuity equation (3.2), allows us to estimate compression,

$$\nabla \cdot \mathbf{u} = -\left(\frac{D_t \tilde{\rho}}{\bar{\rho}} + \frac{u_3 \partial_3 \bar{\rho}}{\bar{\rho}}\right) = \frac{D_t \tilde{T}}{\bar{T}} - \frac{u_3 \partial_3 \bar{\rho}}{\bar{\rho}}, \quad (11.14)$$

where use has been made of Eq. (11.9), and we have kept terms up to  $O(\epsilon)$ . We can compare compression with the other components of the velocity gradient

$$\frac{\nabla \cdot \mathbf{u}}{\|\nabla \mathbf{u}\|} \sim \frac{u_3 \partial_3 \bar{\rho}}{\bar{\rho} \|\nabla \mathbf{u}\|} \sim \frac{l}{L} \sim \epsilon. \quad (11.15)$$

To lowest order in  $\epsilon$ , the continuity equation then coincides with the incompressibility constraint

$$\nabla \cdot \mathbf{u} = 0. \quad (11.16)$$

By substituting Eq. (11.13) into Eq. (11.10), and taking into account Eq. (11.16), we get the following approximate form of the Navier-Stokes equation

$$\bar{\rho} D_t \mathbf{u} + \nabla \tilde{P} = \mu \nabla^2 \mathbf{u} + \frac{g\bar{\rho}}{\bar{T}} \tilde{T} \mathbf{e}_3. \quad (11.17)$$

Next, we apply the ansatz in Eqs. (11.6-11.8) to the equation for heat transport (7.18). We can verify that the two terms  $D_t T$  and  $T \nabla \cdot \mathbf{u}$  in Eq. (7.18) are both  $O(\epsilon)$ . At  $O(\epsilon)$ , the transport term reads  $D_t T = D_t \tilde{T} + u_3 \partial_3 \bar{T}$ . We then substitute Eq. (11.14) into Eq. (7.18) and we get

$$c_P D_t \tilde{T} = \kappa \nabla^2 \tilde{T} + \hat{h} + u_3 \left( \frac{\bar{T}}{\bar{\rho}} \partial_3 \bar{\rho} - c_V \partial_3 \bar{T} \right), \quad (11.18)$$

where  $c_P = 1 + c_V$  and  $\hat{h}$  contains the contribution from external and viscous heating sources.

Equations (11.16-11.18) constitute the Boussinesq approximation for a stratified fluid, where the terms in brackets act as a source of temperature fluctuations.

We can linearize Eqs. (11.17) and (11.18) and carry out a normal mode analysis of the solutions. By carrying out the operation we would discover that the sign of the term in brackets in the RHS of Eq. (11.18) determines whether the solution are oscillatory or exponentially growing. Namely, positive and negative  $(\bar{T}/\bar{\rho}) \partial_3 \bar{\rho} - c_V \partial_3 \bar{T}$  correspond to unstable and stable stratification, respectively.

Equations (11.17) and (11.18) take a somewhat simpler form by expressing  $\rho$  and  $T$  in terms of the so-called potential temperature,

$$\Theta \propto T^{c_V/c_P} \rho^{-1/c_P} \propto T P^{-1/c_P}. \quad (11.19)$$

We verify that  $d\Theta = 0$  along an adiabetic. At a fixed pressure, the potential temperature is proportional to the temperature and thus allows us to identify adiabatics by their temperature at a reference pressure.

From Eq. (11.19) we find

$$\partial_3 \bar{\Theta} = -\frac{1}{c_P \bar{T}} \left( \frac{\bar{T} \partial_3 \bar{\rho}}{\bar{\rho}} - c_V \partial_3 \bar{T} \right), \quad (11.20)$$

where the term in brackets in the RHS of the equation equals the term in brackets in the RHS of Eq. (11.18). We also find

$$\tilde{\Theta} = \frac{\bar{\Theta}}{\bar{T}} \tilde{T} - \frac{\bar{\Theta}}{c_P \bar{P}} \tilde{P} \simeq \frac{\bar{\Theta}}{\bar{T}} \tilde{T} \Rightarrow D_t \tilde{\Theta} \simeq \frac{\bar{\Theta}}{\bar{T}} D_t \tilde{T}, \quad (11.21)$$

where use has been made of Eqs. (11.8) and (11.12). We substitute Eqs. (11.20) and (11.21) into Eqs. (11.17) and (11.18), and obtain the following alternative form for the momentum and heat balance equations in the Boussinesq approximation,

$$D_t \mathbf{u} + \frac{1}{\bar{\rho}} \nabla \tilde{P} = \nu \nabla^2 \mathbf{u} + \frac{g \bar{\rho}}{\bar{\Theta}} \tilde{\Theta} \mathbf{e}_3, \quad (11.22)$$

$$c_P D_t \tilde{\Theta} = \kappa \nabla^2 \tilde{\Theta} + \hat{h} - c_P u_3 \partial_3 \tilde{\Theta}. \quad (11.23)$$

## 12 Turbulence

High Reynolds number flows are usually turbulent. The interaction of the fluid with a solid obstacle leads, because of the no-slip boundary condition, to the formation of vortex sheets which are structurally unstable, roll into vortex tubes that are continuously stretched and deformed and lead to the formation of small-scale turbulent structures. A flow that is initially at spatial scale  $L$  thus breaks into a multitude of eddies at scales  $l \ll L$ . The energy of the mean flow is continuously transferred to the turbulent fluctuations, and the energy of the smallest eddies is converted to heat through viscous dissipation. This suggests us that a satisfactory description of the turbulent dynamics could be achieved by writing evolution equations for the mean velocity of the flow,  $\bar{\mathbf{u}}(\mathbf{x}, t)$ , and the turbulent kinetic energy and viscous dissipation.

Since most of the difficulties of turbulence are already present in incompressible flows, we assume incompressibility from the start. The turbulent energy and dissipation per unit mass read

$$k(\mathbf{x}, t) = \frac{1}{2} \overline{\tilde{u}^2(\mathbf{x}, t)}, \quad \epsilon(\mathbf{x}, t) = \frac{\nu}{2} \overline{\|\tilde{\mathbf{s}}(\mathbf{x}, t)\|^2}, \quad (12.1)$$

where we use tilde to identify fluctuations.

The turbulent vortices are transported by the mean flow and by turbulence. An equation for the mean flow can be obtained directly as the average of the Navier-Stokes equation (5.2):

$$\rho \bar{D}_t \bar{\mathbf{u}} + \nabla \bar{P} = \mathbf{f}^{ext} + \nabla \cdot (\mu \nabla \bar{\mathbf{u}} - \rho \overline{\tilde{\mathbf{u}} \tilde{\mathbf{u}}}), \quad (12.2)$$

where  $\bar{D}_t = \partial_t + \bar{\mathbf{u}} \cdot \nabla$ . Note the quadratic term to RHS, which contains the effect of random advection by the turbulent eddies:  $\nabla \cdot \overline{\tilde{\mathbf{u}} \tilde{\mathbf{u}}} = D_t \mathbf{u} - \bar{D}_t \bar{\mathbf{u}}$ . To solve Eq. (12.2) we need an expression for the quadratic average  $\overline{\tilde{\mathbf{u}} \tilde{\mathbf{u}}}$ . We immediately realize that since there are six independent components in  $\overline{\tilde{\mathbf{u}} \tilde{\mathbf{u}}}$ , solving an equation for  $k$  is not enough. More seriously, in the same way the equation for  $\bar{\mathbf{u}}$  contains through advection a quadratic contribution  $\overline{\tilde{\mathbf{u}} \tilde{\mathbf{u}}}$ , an equation for  $\overline{\tilde{\mathbf{u}} \tilde{\mathbf{u}}}$  will involve a cubic component  $\overline{\tilde{\mathbf{u}} \tilde{\mathbf{u}} \tilde{\mathbf{u}}}$ . A similar situation would occur if we tried to write an equation for the cubic term, and so on. The result is an infinite system of coupled equations which can realistically be solved only by assuming in some equations a specific form of the highest order correlations.

A possible strategy is to exploit the analogy between the Reynolds stress and the viscous stress, and introduce an eddy viscosity  $\mu_T$ , in which the characteristic size  $L$  of the eddies and their characteristic velocity  $\tilde{u}_L$  take the place of the mean free path  $\lambda$  and the thermal velocity  $v_{th}$  in  $\mu$  (see Eq. (4.10)). The result is

$$R_{ij} = \nu_T \overline{\dot{s}_{ij}}, \quad \nu_T = \tilde{u}_L L. \quad (12.3)$$

where

$$\tilde{u}_L \sim \sqrt{k}, \quad (12.4)$$

and  $L$  is the characteristic scale of the largest eddies in the particular region of the flow. Thus, in the same way molecular motion leads to diffusion of momentum and scalar quantities such as the temperature, one may imagine that the same effect in turbulence is produced by the individual eddies. A value of  $L$  can be estimated by assuming some sort of local equilibrium between the power delivered by the advection force by the largest eddies,  $\rho\tilde{\mathbf{u}} \cdot (\tilde{\mathbf{u}} \cdot \nabla)\tilde{\mathbf{u}} \sim \tilde{u}_L^3/L$ , and the dissipation rate  $\epsilon$ :

$$L \sim \frac{k^{3/2}}{\epsilon} \Rightarrow \nu_T \sim \frac{k^2}{\epsilon}. \quad (12.5)$$

Typically, one reabsorbs the molecular viscosity in  $\nu_T$ ,  $\nu + \nu_T \rightarrow \nu_T$  and Eq. (12.2) takes the form

$$\rho\bar{D}_t\bar{u}_i + \partial_i\bar{P} = f_i^{ext} + \partial_j(\mu_T\partial_j\bar{u}_i), \quad \mu_T = \rho\nu_T. \quad (12.6)$$

The turbulent viscosity  $\mu_T$  plays a fundamental role in the energy budget of the flow. While in the case of molecular viscosity, the energy of the flow was directly converted to heat, the eddy viscosity transfers energy from the mean flow to the turbulent fluctuations. One can get some intuitive understanding of the mechanism by referring to the concept of added mass introduced in Sec. 8.2; this is the mass of the fluid that a solid object drags along in its motion. Turbulent eddies continuously replace chunks of the moving fluid with other fluid masses that have initially zero velocity. The work required to overcome the viscous drag and keep the body in motion is then precisely the work required to accelerate those masses to the speed of the body.

We can exploit the concept of eddy viscosity to derive an effective equation for the transport of  $k$ . The structure of the equation is very similar to that of the heat transport equation (7.9), with eddy diffusion of  $k$  replacing molecular diffusion of  $T$  and turbulent energy production from the work against the turbulent stress replacing viscous heating. The result is

$$\bar{D}_t k = \nabla \cdot (\nu_T \nabla k) + 2\nu_T \|\bar{\mathbf{s}}\|^2 - \epsilon, \quad (12.7)$$

We can derive a similar equation for  $\epsilon$ :

$$\bar{D}_t \epsilon = \nabla \cdot (\nu_T^\epsilon \nabla \epsilon) + \frac{c\epsilon}{k} [2\nu_T^\epsilon \|\bar{\mathbf{s}}\|^2 - \epsilon], \quad \nu_T^\epsilon \sim \nu_T, \quad \nu_T^\epsilon \sim \nu_T, \quad c \sim 1. \quad (12.8)$$

Equations (12.6-12.8) constitute the so-called  $k - \epsilon$  model of turbulence.

Building something that goes beyond an empirical model of turbulence appears at the present state of knowledge a very difficult task. Perturbative treatment of the equation, in particular, does not work (such an approach would correspond to expand around a lowest-order  $\text{Re} \rightarrow 0$  dynamics that has no relation with turbulence). On the other hand, brute force numerical simulation of the Navier-Stokes equation is usually unfeasible (an atmospheric flow may involve eddies ranging from hundreds

of meters to the millimeter scale). There are alternative approaches in which the Navier-Stokes equation is numerically solved with a grid scale that excludes the smallest eddies in the flow (large-eddy simulations or LES). As in the case of the  $k - \epsilon$  model, the effect of the unresolved eddies is modeled by introducing an eddy viscosity  $\nu_T \sim l_{grid} \tilde{u}_{subgrid}$ , in which the large scale  $L$  and the turbulent velocity  $\tilde{u}_L$  are replaced by the scale of the grid  $l_{grid}$  and the characteristic velocity  $\tilde{u}_{subgrid}$  of the unresolved eddies; both quantities  $l_{grid}$  and  $\tilde{u}_{subgrid}$  must in some way be parameterized.

## 12.1 Homogeneous isotropic turbulence

Turbulence is spatially inhomogeneous almost by definition. The inhomogeneity scale is fixed by the geometry of the problem: in the case of a turbulent pipe flow, the diameter of the pipe; in the case of a turbulent wake downstream of a solid body, the width of the wake; in the case of a flow over a plane surface, the thickness of the boundary layer. The inhomogeneity scale itself may vary with the position (the distance downstream of the solid obstacle or along the plane surface).

Typically, the characteristic scale of the mean flow and the size  $L$  of the largest eddies are comparable:

$$L \sim \bar{u} / \partial_x \bar{u}, \quad (12.9)$$

and the statistics of the large eddies are in general neither spatially homogeneous nor isotropic. Nevertheless, if the turbulence is sufficiently strong, eddies at scales  $l \ll L$  will be present, which will see turbulence as locally homogeneous and isotropic. Furthermore, since the dynamics of smaller eddies is faster than that of larger eddies, their statistics can be assumed to be stationary.

A necessary condition for isotropy is that the strain on eddies at scale  $l \ll L$  mainly comes from eddies of comparable scale. In other words, the turbulent dynamics at a sufficiently small scale must be local in scale. We want in particular that the strain on eddies at scale  $l \ll L$  from eddies at scale  $L$  and from the mean flow (which are both anisotropic) be negligible.

We can identify in a turbulent flow three ranges of scales:

- An integral scale  $L$  of large eddies which interact directly with the mean flow and are sensitive to the geometry of the flow domain.
- An internal scale  $\eta$  of the smallest eddies, for which  $Re_\eta = \eta \tilde{u}_\eta / \nu \lesssim 1$  and the effect of viscosity is dominant.
- An intermediate “inertial” range  $L \ll l \ll \eta$  in which eddies are sufficiently small for hypotheses of homogeneity and isotropy to hold, and at the same time sufficiently large for the dynamics to be inviscid.

Kolmogorov was able, based on such simple hypotheses, to derive the energy spectrum in the inertial range of turbulence and an expression for the internal scale  $\eta$ . The simplest derivation only requires dimensional analysis, based on the hypothesis of self-similarity and independence of the inertial range dynamics on viscosity. Such hypothesis contain in a subtle way the condition that small-scale turbulent fluctuations are sufficiently random and organized small-scale structures do not create bottlenecks in the energy transfer. We can get an insight into the physics underlying the Kolmogorov theory by looking at the dynamics of a single vortex at scale  $l$ .

If vortices are distributed uniformly in the flow domain, the contribution to the turbulent energy density by eddies at scale  $l$  will be  $k_l \sim \tilde{u}_l^2$ . Vortex stretching transforms vortices at scale  $l$  into vortices at scale, say,  $l/2$  in a characteristic time  $\tau_l$ , which, if the process is dominated by vortices of comparable size, will coincide with the eddy turnover time

$$\tau_l \sim l/\tilde{u}_l. \quad (12.10)$$

We can visualize the process as a turbulent cascade in which energy is transferred from eddies at scale  $L$  to eddies at scale  $L/2$ , and from there to smaller eddies until one reaches the internal scale  $\eta$ . Now, for the process to be stationary, the energy flux from one scale to the next must be scale-independent and equal viscous dissipation:

$$\Pi_l \sim \frac{k_l}{\tau_l} \sim \frac{\tilde{u}_l^2}{\tau_l} = \Pi = \epsilon. \quad (12.11)$$

From Eqs. (12.10) and (12.11) we then get the scaling law (Kolmogorov scaling)

$$\tilde{u}_l \sim (\epsilon l)^{1/3}. \quad (12.12)$$

We can now verify that the contribution to the velocity increment  $\tilde{\mathbf{u}}(\mathbf{x} + \mathbf{l}, t) - \tilde{\mathbf{u}}(\mathbf{x}, t)$  from eddies at scale  $l$  is indeed the largest. We verify immediately that the contribution of vortices with  $l' \ll l$  is  $\tilde{u}_{l'} \sim \tilde{u}_l(l'/l)^{1/3} \ll u_l$ . On the other hand, if we imagine the eddies to be smooth objects, such that their velocity field can be Taylor expanded, the contribution to  $\Delta_{\mathbf{l}}\tilde{\mathbf{u}}(\mathbf{x}, t) = \tilde{\mathbf{u}}(\mathbf{x} + \mathbf{l}, t) - \tilde{\mathbf{u}}(\mathbf{x}, t)$  from eddies with  $l' \gg l$  will be  $\sim \tilde{u}_{l'}l/l' \sim \tilde{u}_l(l/l')^{2/3} \ll \tilde{u}_l$ . Now, stretching of vortices at scale  $l$  is produced by velocity differences at separation  $l$ ; the fact that the difference  $\Delta_{\mathbf{l}}\tilde{\mathbf{u}}(\mathbf{x}, t)$  is dominated by eddies of size  $l$  then confirms the picture of local energy transfer in scale as the result of the interaction of vortices of comparable size.

The fact that the difference  $\Delta_{\mathbf{l}}\tilde{\mathbf{u}}(\mathbf{x}, t)$  is dominated by eddies of size  $l$  allows us to write Eq. (12.12) in the equivalent form

$$|\tilde{\mathbf{u}}(\mathbf{x} + \mathbf{l}, t) - \tilde{\mathbf{u}}(\mathbf{x}, t)|^2 \sim \epsilon^{2/3} l^{2/3}, \quad (12.13)$$

which tells us that for  $\eta \rightarrow 0$  the turbulent velocity field becomes non-differentiable in space. The velocity field itself, however, remains finite and the same property is

shared by the turbulent kinetic energy:

$$k = \sum_{n=0}^{+\infty} k_n \sim \sum_{n=0}^{+\infty} \tilde{u}_{l_n}^2 / 2 < \infty, \quad l_n = 2^{-n} L. \quad (12.14)$$

We can use Eq. (12.12) to evaluate the internal scale  $\eta$ . Proceeding as in the case of the turbulent energy, the viscous dissipation  $\epsilon$  can be expressed as a sum of contributions by vortices at different scales. We see from Eq. (12.12), that the sum is dominated by eddies at scale  $\eta := L2^{n_\eta}$ :

$$\epsilon = 2\nu |\overline{\nabla \mathbf{u}}|^2 \sim \nu \sum_n \tilde{u}_{l_n}^2 l_n^2 \sim \nu \epsilon^{2/3} L^{-4/3} \sum_{n=0}^{n_\eta} 2^{4n/3} \sim \nu \epsilon^{2/3} \eta^{-4/3}. \quad (12.15)$$

From here we obtain

$$\eta \sim \nu^{3/4} \epsilon^{-1/4}, \quad (12.16)$$

which is called the Kolmogorov scale of the flow. At scales below  $\eta$  the flow is dominated by viscosity and could be described using the Stokes equation (5.10). We can then verify that for  $l < \eta$ ,  $|\overline{\tilde{\mathbf{u}}(\mathbf{x} + \mathbf{l}, t)} - \tilde{\mathbf{u}}(\mathbf{x}, t)|^2 \sim l^2$ ; in other words, the turbulent velocity field at sufficiently small scale is smooth.

From Eqs. (12.10) and (12.13) we get the scaling for the eddy turnover time

$$\tau_l \sim \epsilon^{-1/3} l^{2/3}. \quad (12.17)$$

The time required for vortex stretching from  $L$  to  $\eta$  to complete is

$$\tau_{L \rightarrow \eta} \sim \sum_n \tau_{L2^{-n}} \sim \tau_L \sum_n 2^{-2n/3} \sim \tau_L, \quad (12.18)$$

independent of  $\nu$ , which implies that the times required in the  $\nu \rightarrow 0$  limit to reduce integral scale vortices to infinitesimal smithereens remains finite.

We can take the limit  $l \rightarrow L$  in Eq. (12.13) and express the viscous dissipation in terms of properties of the large scale flow:

$$\epsilon \sim \frac{\tilde{u}_L^3}{L}. \quad (12.19)$$

We find again the result that viscous dissipation remains finite in the  $\nu \rightarrow 0$  limit; the only thing that changes is the Kolmogorov scale that goes to zero. By substituting Eq. (12.19) into Eq. (12.16) we are able to write the ratio  $L/\eta$  of the maximum and minimum scale in the turbulent flow in terms of the Reynolds number:

$$\frac{L}{\eta} \sim \left( \frac{L \tilde{u}_L}{\nu} \right)^{4/3} = \text{Re}^{4/3}, \quad (12.20)$$

which allows us to estimate the number of grid points required in a numerical simulation of a turbulent flow as  $\sim \text{Re}^4$ .

### 12.1.1 Time structure of the inertial range

The Kolmogorov law, Eq. (12.13), gives us information on the spatial structure of the turbulent flow. The temporal structure is much more intricate; this turns out to be one of the major stumbling blocks in the derivation of a theory of turbulence. The fact is that the eddy turnover time  $\tau_l$  defined in Eq. (12.10) describes the time decay of correlations in a reference frame moving with the fluid, i.e. the decay of Lagrangian time correlations. Eulerian time correlations will be affected by the transport of eddies by larger eddies and the mean flow—a phenomenon called sweep effect.

The magnitude of the sweep effect is determined by the transit time of the vortices in front of a fixed probe; in the case of vortices of size  $l$ :

$$\tau_l^E \sim l/u \sim l/\bar{u}. \quad (12.21)$$

We see from Eqs. (12.17) and (12.21) that for  $l \ll L$ ,  $\tau_l^E \ll \tau_l$ ; this tells us that vortex stretching, although crucial for the dynamics of the flow, only contributes a correction to Eulerian correlations.

The fact that the turbulent dynamics is properly described only in a Lagrangian frame, enormously complicates the derivation of a theory of turbulence based on the Navier-Stokes equation. The fact that vortices at scale  $l$  can be approximated as frozen on the time scale of  $\tau_l^E$ , however, simplifies experimental measurements. We can in fact approximate

$$\mathbf{u}(\mathbf{x}, t) - \mathbf{u}(\mathbf{x}, 0) \simeq \mathbf{u}(\mathbf{x} - \bar{\mathbf{u}}t, 0) - \mathbf{u}(\mathbf{x}, 0), \quad t \ll L/\bar{u} \sim \tau_L, \quad (12.22)$$

which is called Taylor's frozen-turbulence approximation. Equation (12.22) tells us that it is possible to reconstruct an instantaneous spatial section of a turbulent flow from the time series of the velocities measured by a fixed probe (an anemometer).

### 12.1.2 Transport of a passive scalar

The heat transport equation (7.18) is the first example of transport equation for a scalar quantity we have considered in these notes; in the case of an incompressible flow, it takes the form

$$D_t T = \kappa \nabla^2 T + h, \quad (12.23)$$

where  $h$  is a generic source term. The transport of a substance, such as e.g. a pollutant in the air, will obey an equation of identical form, with  $T$  identifying in this case the substance concentration. If there is no feedback on the flow (in the case of the temperature, this means that convection is negligible), we say that  $T$  behaves like a passive scalar.

We want to study passive scalar transport by turbulence. Suppose we have a localized heat source  $h$  that generates an inhomogeneous temperature profile in

the surroundings. An inhomogeneous time-dependent but non-turbulent flow is sufficient to generate mixing; turbulence, however, contributes to the process, with many characteristics in common with the turbulent cascade of velocity fluctuations previously discussed: large scale inhomogeneities in  $T$  are generated by the source  $h$  and converted to smaller and smaller scales fluctuations which are eventually smoothed out by diffusion. We will have an integral scale  $L_T$  where the effect of the flow geometry and the source  $h$  are substantial, followed by an inertial range where both  $h$  and  $\kappa$  play a negligible role, and an internal scale  $\eta_T$  where diffusion is dominant.

Let us focus on the inertial range. From Eq. (12.23) fluctuations at scales  $\eta_T \ll l \ll L_T$  behave like a frozen field. We have seen, when studying the dynamics of vorticity in 2D flows (see Sec. 9.3), that a frozen scalar has an infinite set of global invariant

$$\int d^3x F(T(\mathbf{x}, t)) = \text{constant}, \quad \forall F. \quad (12.24)$$

In particular, we have a quadratic invariant

$$k_T = \frac{1}{2} \int d^3x T^2(\mathbf{x}, t), \quad (12.25)$$

which behaves like a sort of energy of the temperature fluctuations. We can then repeat the same steps in the case of the velocity fluctuations and introduce a flux in scale of the temperature fluctuations

$$\Pi_l^T \sim \frac{\tilde{T}_l^2}{\tau_l} \sim \epsilon^{1/3} l^{-2/3} \tilde{T}_l^2 \sim \epsilon_T, \quad (12.26)$$

where

$$\epsilon_T = \kappa \overline{|\nabla T|^2} \sim \kappa \frac{\tilde{T}_{\eta_T}^2}{\eta_T^2} \quad (12.27)$$

is the dissipation of temperature fluctuations by diffusion. Proceeding as in the case of the velocity fluctuations we get

$$\overline{|\tilde{T}(\mathbf{x} + \mathbf{l}, t) - \tilde{T}(\mathbf{x}, t)|^2} \sim \epsilon_T \epsilon^{-1/3} l^{2/3} \quad (12.28)$$

and in the case  $\nu \sim \kappa$

$$\eta_T \sim \kappa^{3/4} \epsilon^{-1/4}. \quad (12.29)$$

Experiments and numerical simulations support Kolmogorov scaling both for the velocity and passive scalar field. There are corrections, whose existence is confirmed by mathematical analysis of Eq. (12.23). The smallness of the corrections, however,

suggests that the Kolmogorov cascade picture is correct and the role of the infinite set of conserved quantities in Eq. (12.24) is small.

A possible explanation of why higher-order invariants can be disregarded is that only  $F(T) = T^2/2$  can be decomposed as a sum of scale-dependent terms. To see why this is the case, it is necessary to work in Fourier space:

$$\tilde{T}_{\mathbf{k}}(t) = \int d^3x T(\mathbf{x}, t) e^{-i\mathbf{k}\cdot\mathbf{x}}. \quad (12.30)$$

Let us consider the case  $F$  is a simple power of  $T$  (which covers the case  $F$  is regular in  $T = 0$  and can therefore be expressed as a Taylor series in  $T$ ). We have

$$\begin{aligned} I_n &= \int d^3x \overline{\tilde{T}^n} = \int d^3x \int \prod_{j=1}^n \frac{d^3k_j}{(2\pi)^3} \overline{\tilde{T}_{\mathbf{k}_1} \dots \tilde{T}_{\mathbf{k}_n}} \exp\left(-i\mathbf{x} \cdot \sum_{j=1}^n \mathbf{k}_j\right) \\ &= (2\pi)^3 \int \prod_{j=1}^n \frac{d^3k_j}{(2\pi)^3} \overline{\tilde{T}_{\mathbf{k}_1} \dots \tilde{T}_{\mathbf{k}_n}} \delta\left(\sum_{j=1}^n \mathbf{k}_j\right). \end{aligned} \quad (12.31)$$

As claimed, only  $I_2$  is a sum of contributions dependent on a unique scale  $k^{-1}$ :

$$I_2 = \int \frac{d^3k}{(2\pi)^3} |\overline{\tilde{T}_{\mathbf{k}}}|^2. \quad (12.32)$$

In all other cases, the integrand of  $I_n$  depends on more than one wavevector, and there will be contributions in which some of the wavevectors lie out of the inertial range. For such contributions, local transfer in scale of a conserved quantity could not be invoked.

### 12.1.3 Two-dimensional turbulence

The mechanism of vortex stretching, which determines the dynamics of turbulence in three dimensions, is absent in two dimensions. Another difference with the 3D case is the presence of a second quadratic invariant, enstrophy, which leads to the question of whether energy or enstrophy determines the structure of the turbulent cascade. Also in three dimensions there is a second quadratic invariant, helicity; however, while zero enstrophy would require a flow that is globally potential (and therefore non-turbulent), in order to have zero helicity it is sufficient that the flow is globally reflection invariant. Thus, while an energy  $k_l$  at scale  $l$  implies an enstrophy content at that scale  $\mathcal{E}_l \sim k_l/l^2$ , in the case of helicity we can only state  $|I_l| \lesssim k_l/l$ .

With all the caveats put in place, let us try to understand whether a local turbulent cascade is possible in two dimensions. Let us start by considering the possibility of an enstrophy cascade and define an enstrophy flux  $\Pi_{\mathcal{E},l}$  and an enstrophy dissipation  $\epsilon_{\mathcal{E}}$ , which at stationarity are going to be equal. The same argument leading to the Kolmogorov scaling in Eq. (12.13) yields in the present case

$$\epsilon_{\mathcal{E}} \sim \frac{\mathcal{E}_l}{\tau_l} \sim \frac{\tilde{u}_l^3}{l^3} \Rightarrow \tilde{u}_l \sim \epsilon_{\mathcal{E}}^{1/3} l; \quad (12.33)$$

enstrophy dissipation equals the enstrophy injection, which is  $\sim L^{-2}$  times the energy injection; hence  $\epsilon_{\mathcal{E}} \sim \epsilon/L^2$ .

We immediately find a difficulty in the fact that the scaling  $\tilde{u}_l \propto l$  implies that the contribution to  $\Delta_{\mathbf{l}}\tilde{\mathbf{u}}(\mathbf{x}, t) = \tilde{\mathbf{u}}(\mathbf{x} + \mathbf{l}, t) - \tilde{\mathbf{u}}(\mathbf{x}, t)$  from vortices at scale  $l' \gg l$  is of the same order as that of vortices at scale  $l$ . This clearly weakens a hypothesis of local enstrophy transfer in scale. A more substantial difficulty is that energy is injected in the flow side by side with enstrophy. However, while  $\Pi_{\mathcal{E},l} = \epsilon_{\mathcal{E}}$  is constant,  $\Pi_{k,l} \equiv \Pi_l \sim \epsilon_{\mathcal{E}}l^2$  goes to zero for  $l \rightarrow 0$ . Stationarity then requires that  $\Pi_l = 0$  independent of scale. The alternative in which the dynamics is governed by energy transfer and  $\tilde{u}_l \sim (\epsilon l)^{1/3}$  as in Eq (12.12) is not viable since it would lead to  $\Pi_{\mathcal{E},l} \sim \epsilon/l^2$ , which diverges at  $l \rightarrow 0$ . The only solution is that while enstrophy is transferred from large to small scales, energy is transferred to scales larger than those of the forcing. This is indeed the situation observed in numerical simulations of 2D turbulence, with an enstrophy cascade to smaller scales and an energy cascade to larger scales simultaneously present

$$\tilde{u}_l \sim \begin{cases} (\epsilon/L^2)^{1/3}l, & l \ll L, \\ (\epsilon l)^{1/3}, & l \gg L. \end{cases} \quad (12.34)$$

The effect of helicity on the energy cascade in 3D flows is less dramatic. The fact that  $\Pi_{I,l} \lesssim \Pi_{k,l}/l = \epsilon/l$  allows to enforce simultaneously the condition that the two fluxes  $\Pi_{k,l}$  and  $\Pi_{I,l}$  are constant in scale:  $\Pi_{I,l} = \epsilon_I \sim \epsilon/L$  and  $\Pi_{k,l} = \epsilon$ . It is not necessary to invoke energy and helicity cascades going in opposite directions. The Kolmogorov scaling in Eq. (12.13) at scales  $k \ll L$  is the only one observed in experiments and numerical simulations.

## 12.2 Suggested reading

- P. Kundu, “Fluid Mechanics”, Secs. 12.1-7 (Ac. Press 2015)